A MASS SPECTROMETRIC AND THERMOGRAVIMETRIC STUDY OF THE THERMAL DECOMPOSITION OF SOME CUPRIC CARBOXYLATES

A Thesis
Presented to
The Faculty of Graduate Studies and Research
The University of Manitoba

in Partial Fulfilment
of the Requirements for the Degree

Master of Science

by

Denis C. K. Lin
December, 1969

ACKNOWLEDGEMENTS

I am deeply grateful to Dr. J. B. Westmore, my research supervisor, for his advice, helpful suggestions and enlightening discussions throughout this project.

I also wish to thank Dr. C. Reichert and Mr. D. Fung for their cooperation in the maintenance of the mass spectrometer and their interest in this study.

ABSTRACT

The thermal decomposition of twenty six cupric carboxylates were studied by mass spectrometry and thermogravimetry. The mass spectra of the decomposition products of all the cupric carboxylates are reported. Twelve cuprous carboxylates which have never been reported before (except cuprous acetate[1]), were identified among the decomposition products. Two different mass spectral fragmentation patterns are postulated according to whether the acid is an alkyl- or aryl- carboxylic acid. Some of the fragmentation steps are supported by metastable peaks.

The cuprous carboxylates are shown to be dimers. A structure similar to that of silver perfluorobutyrate[42] is proposed for the cuprous compounds. Unlike the dimeric cupric acetate[16-19], no metal-metal bond is expected between the copper atoms in the molecule.

The thermograms of the cupric carboxylates both in air and vacuum are reported. Explanations for some features of the thermograms are suggested.

TABLE OF CONTENTS

		Page
PART ONE:	INTRODUCTION	
Chapter one:	General Introduction	1
Chapter two:	Properties of Cupric Carboxylates	3
Chapter three:	Preparation of the Cupric Carboxylates	11
PART TWO:	MASS SPECTROMETRIC STUDIES	
Chapter four:	Introduction	15
Chapter five:	Principles of Mass Spectrometry	16
Chapter six:	Instrumentation	19
Chapter seven:	Experimentation and Results	22
Chapter eight:	Discussion on the Mass Spectra	50
PART THREE:	THERMOGRAVIMETRIC STUDIES	
Chapter nine:	Introduction	60
Chapter ten:	Principles and Errors in Thermogravimetric Analysis	61
Chapter eleven:	Instrumentation	66
Chapter twelve:	Experimental	68
Chapter thirteen:	Results and Discussion	71
PART FOUR:	CONCLUSION	
Chapter fourteen:	Conclusion	104
APPENDIX		105
BIBLIOGRAPHY		107

LIST OF TABLES

		Page
Table I	Magnetic Behavior of Anhydrous Cupric Carboxylates	7
Table II	Color of Cupric Carboxylate Crystals and Method of Preparation	13
Table IV	Decomposition of Copper Carboxylates for which volatile Cuprous species were not detected	24
TABLE V	Decomposition of Copper(II) Carboxylates for which Cuprous Carboxylates are among decomposition products. Non-copper containing species only.	31
TABLE VI	Mass Spectra of Cuprous Carboxylates formed as thermal decomposition products of the Cupric Carboxylates.	37
TABLE VII	Isotopic Ratios and Relative Intensities of Copper Containing Species	42
TABLE VIII	Metastable Peaks in the Cuprous Carboxylate Mass Spectra	47
TABLE IX	Conditions in T.G.A. Experiments	69

N. B. TABLE III is non-existant.

LIST OF FIGURES

		Page
FIGURE I	A schematic diagram of the structure of copper(II) acetate dihydrate	4
FIGURE II	Schematic expression of the structure of copper(II) benzoate trihydrate	5
FIGURE III	Bridging structures for the carboxylates	8
FIGURE IV	Schematic representation of Hitachi RMU-6D single-focussing mass spectrometer.	20
FIGURE V	Schematic representation of the ion source	21
FIGURE VI	Fragmentation scheme for cuprous alkylcarboxylates	51
FIGURE VII	Fragmentation scheme for cuprous arylcarboxylates	52
FIGURE VIII	A schemic diagram of the structure of silver perfluorobutyrate	53
FIGURE IX	Sketches showing the hybrid orbitals formed from a d_z^2 and a s orbital, ψ_1 and ψ_2, and the hybrids which can be formed from ψ_2 and a p_z orbital.	54
FIGURE X	Thermogram of a hypothetical sample $MX_2 \cdot 6H_2O$	61
FIGURE XI	Effect of chart speed upon the shapes of weight-loss curves	64
FIGURE XII	Schematic diagram of Cahn RG electrobalance	67
FIGURE XIII	Thermograms of cupric acetate	73
FIGURE XIV	Thermograms of cupric propionate	75
FIGURE XV	Thermograms of cupric n-butyrate	76
FIGURE XVI	Thermograms of cupric iso-butyrate	77
FIGURE XVII	Thermograms of cupric difluoroacetate	78
FIGURE XVIII	Thermograms of cupric trifluoroacetate	79
FIGURE XIX	Thermograms of cupric benzoate	81
FIGURE XX	Thermograms of cupric o-chlorobenzoate	82
FIGURE XXI	Thermograms of cupric p-chlorobenzoate	83
FIGURE XXII	Thermograms of cupric p-fluorobenzoate	84
FIGURE XXIII	Thermograms of cupric pentafluorobenzoate	86
FIGURE XXIV	Thermograms of cupric o-hydroxybenzoate	87
FIGURE XXV	Thermograms of cupric p-hydroxybenzoate	88
FIGURE XXVI	Thermograms of cupric o-methoxybenzoate	89
FIGURE XXVII	Thermograms of cupric p-ethoxybenzoate	90
FIGURE XXVIII	Thermograms of cupric o-methylbenzoate	91
FIGURE XXIX	Thermograms of cupric p-methylbenzoate	92

FIGURE XXX	Thermograms of cupric β-naphthoate	93
FIGURE XXXI	Thermograms of cupric formate	95
FIGURE XXXII	Thermograms of cupric monochloroacetate	96
FIGURE XXXIII	Thermograms of cupric dichloroacetate	97
FIGURE XXXIV	Thermograms of cupric phenylacetate	98
FIGURE XXXV	Thermograms of cupric o-nitrobenzoate	99
FIGURE XXXVI	Thermograms of cupric p-nitrobenzoate	100
FIGURE XXXVII	Thermograms of cupric o-fluorobenzoate	101

To My Parents

PART ONE

INTRODUCTION

CHAPTER ONE: GENERAL INTRODUCTION

When cupric acetate was heated in air, hydrogen or a vacuum, a white sublimate was observed and was analysed to be cuprous acetate, $Cu_2(CH_3CO_2)_2$, by A. Angel and his colleagues[1] in 1902. Thermogravimetric studies have been reported recently[2-4], however no obvious conclusions about the existence of cuprous acetate were drawn from thermogravimetric analysis. In the differential thermal analysis studies and the mass spectrometric analysis of the volatile decomposition products of cupric acetate by Hill and co-workers[5], cuprous acetate was not reported.

The thermal decomposition of other cupric carboxylates such as formate[2,6], propionate[2], n-butyrate[7], iso-butyrate[7], valerate[8], monobromoacetate[9] and various substituted benzoates[10] have been studied using thermogravimetric analysis (T.G.A.) and differential thermal analysis (D.T.A.), but there was little evidence for the existence of the appropriate cuprous carboxylates.

This study is an investigation of the thermal decomposition of a series of cupric carboxylates usingT.G.A. and mass spectrometry. The series of compounds was chosen so that: (1) there is a wide range in pK_a values of the original carboxylic acids, from 0.2 to 4.87; (2) in the case of aromatic carboxylates, steric effects can be examined. This series of compounds is listed in TABLE I. A total of twenty five compounds are included (not counting cupric trideuterated acetate).

In order to better compare the observations and results of the thermal studies on the compounds, the data obtained by mass spectrometry are presented separately from the T.G.A. data. Since the T.G.A. data can be better explained by using the results from the mass spectrometric study, the latter will be presented first, in Part Two, and the former will be presented in Part Three. Some interesting aspects that arise from this study are: (i) the identification of a new series of cuprous carboxylates; (ii) the characteristic dimeric nature of the

cuprous salts. These in turn lead to other questions such as, (i) what is the structure of the cuprous carboxylates; (ii) what stabilizes their formation and (iii) whether the presence of a metal-metal bond between the two copper atoms in the dimeric cuprous salt is feasible. As little is known about the chemistry of the cuprous carboxylates, it is hoped that this study will help to explain the nature of this series of compounds.

CHAPTER TWO: PROPERTIES OF CUPRIC CARBOXYLATES

Because of the dimeric nature and unusual magnetic behavior of some of the cupric carboxylates, these compounds have been under intense investigation for the past two decades. From X-ray data cupric acetate monohydrate is known to be a binuclear complex with bridging carboxylate groups[14] (See Figure I). In the case of cupric benzoate trihydrate, it has been shown by X-ray structural analysis that it is not a binuclear complex[12,15]. Instead it is a polymer whose chain structure can be represented schematically as in Figure II. Between the linear chains, the hydrated benzoate ions are sandwiched. X-ray structure determinations of most of the carboxylates have not been performed. However, the U.V., visible,I.R. and especially magnetic susceptibility data allow some predictions about the structural properties of these compounds. Since their structures in the solid state are usually different from those in solution and only solid cupric carboxylates were used in the experiments described here, the properites mentioned in this work relate only to the compounds in their solid state.

In the magnetic susceptibility studies of cupric alkylcarboxylates[12,16,17], it has been found that except for the formate, they all exhibit magnetic moments of approximately 1.4 B.M. at room temperature. This is very much lower than the value normally observed for "normal" cupric compounds and lower than the "spin only" value of 1.73 B.M. for one unpaired electron on the Cu(II) atom. For example, $CuSO_4.5H_2O$ has a magnetic moment of 1.91 B.M. The magnetic susceptibilities of the carboxylates do not obey the Curie-Weiss law since when the temperature is raised from 90^o to 400^o K, they pass through maxima at the region 278 ± 28^o K and then decrease. This sort of behavior is similar to that of cupric acetate and it is therefore concluded that all the alkylcarboxylates have similar structure to dimeric cupric acetate (FIG.I). A very weak, covalent,δ bond between the copper atoms has been proposed[16-19]. This magnetic behavior was interpreted by assuming that within each binuclear molecule the two copper atoms interact strongly through exchange forces, forming a lower singlet (diamagnetic) and an upper triplet (paramagnetic) electronic state. For such a situation

CUPRIC ACETATE

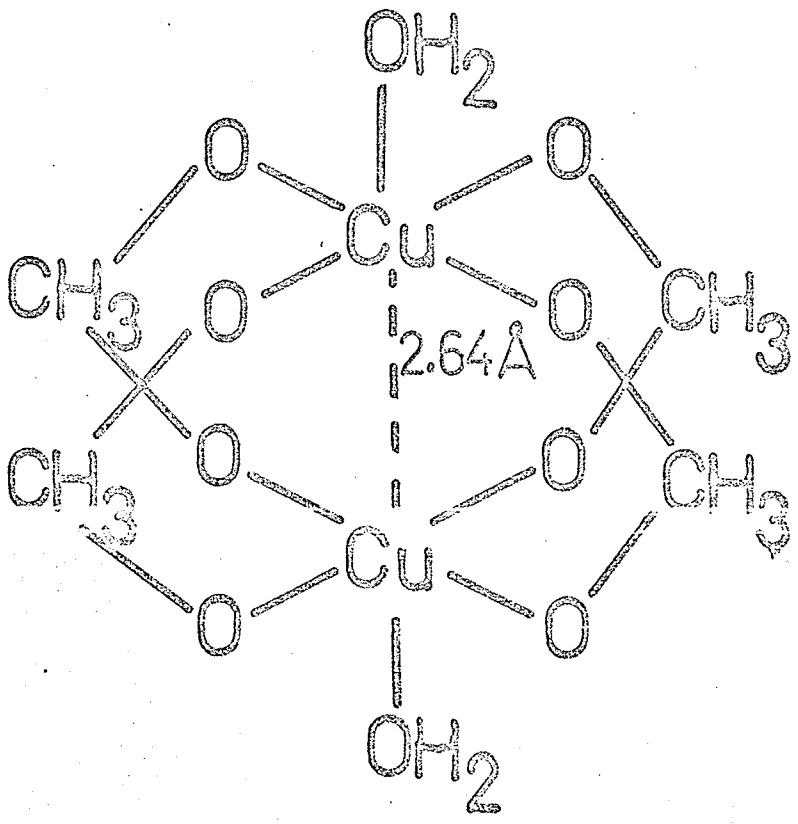

Cu-Cu (metal) = 2.556 Å

FIGURE I

A schematic diagram of the structure of copper (II) acetate dihydrate

CUPRIC ACETATE

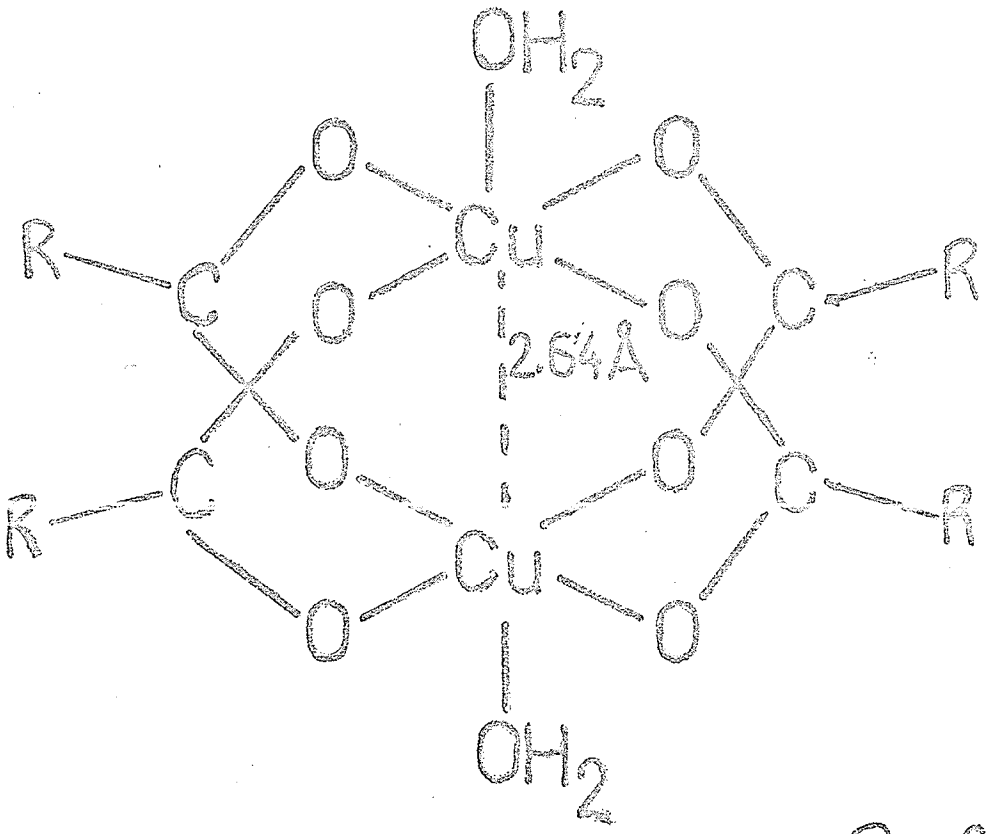

R=CH3

Cu-Cu (metal) = 2.556 Å

FIGURE I

A schematic diagram of the structure of copper (II) acetate monohydrate

x = 1.97, y = 1.91, z = 2.51 Å., Cu-Cu = 3.15 Å.; $(xy)_1$-$(xy)_2$ angle = 56°30' or 123°30'; $(xz)_1$-$(xz)_2$ angle = 31°14' or 148°46'; (COO)-$(xy)_1$ angle = 77°13' or 102°47'; (COO)-$(xy)_2$ angle = 59°15' or 120°45'.

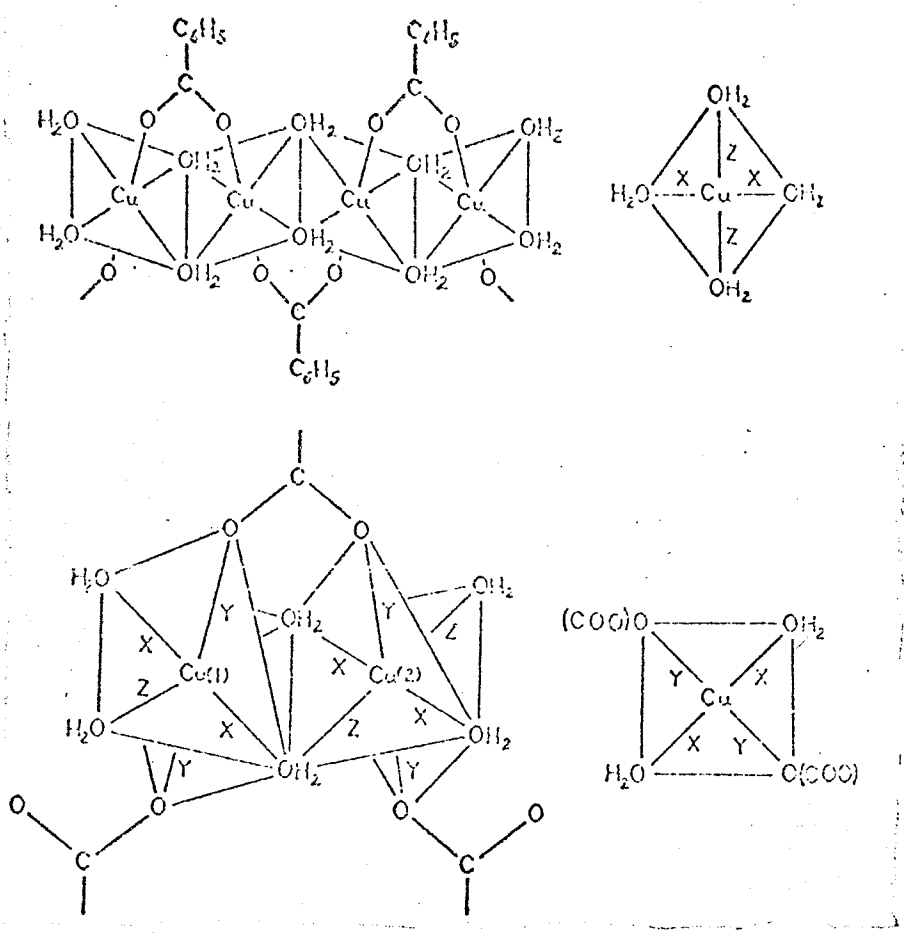

FIGURE II

Schematic expression of the structure of copper(II) benzoate trihydrate:

the molar magnetic susceptibility is given by the following equation[17,20].

$$\chi_M = \frac{g^2 N\beta^2}{3kT} \{1 + \frac{1}{3} \exp(J/kT)\}^{-1} + N\alpha \qquad \text{EQN. I}$$

where χ_M = molar magnetic susceptibility
g = Lande´ Spectroscopic splitting factor
N = Avogadro's number
β = Bohr magneton
k = Boltzmann constant
T = temperature ^oK
J = energy separation between the singlet and triplet levels (twice the exchange energy associated with the copper - copper δ bond)
$N\alpha$ = temperature-independent paramagnetic contribution {60 X 10^{-6} c.g.s., e.m.u. for Cu(II)}

It was found that the values of J lie in the narrow range 309 ± 31 $cm.^{-1}$, i.e. approximately 1 kcal. $mole^{-1}$.

Similar magnetic susceptibility studies have been made on a number of cupric arylcarboxylates[12,13,21,22]. It has been found that some have subnormal magnetic moments at room temperature and behave similarly to cupric acetate while others have higher magnetic moments and their magnetic susceptibilities obey the Curie-Weiss law. TABLE I lists all the carboxylates used in this work with the pK_a values of the original acids, their appropriate magnetic behavior and their expected structures from magnetic studies on samples dehydrated by heat and high vacuum or heat alone.

From the magnetic studies it was suggested that the carboxylate groups can have one of the three bridging configurations[21] shown in FIG. III : (a) syn-syn, (b) anti-anti or (c) anti-syn.

TABLE I

MAGNETIC BEHAVIOR OF ANHYDROUS CUPRIC CARBOXYLATES

Cupric Carboxylate	pK_a Value of Acid	Magnetic Moment @ room temp. in B.M.	Curie-Weiss Law Behavior	Expected Structure	Ref.
Formate	3.75	1.64		Polymer	12
Acetate	4.75	1.43	No	Dimer	17
Propionate	4.87	1.36	No	Dimer	17
iso-Butyrate	4.84	*		Dimer	
n-Butyrate	4.81	1.35	No	Dimer	17
Phenylacetate	4.28	1.44		Dimer	12
Monochloroacetate	2.85	1.42		Dimer	12
Dichloroacetate	1.48	1.66		Dimer	12
Difluoroacetate	1.25			Polymer	
Trifluoroacetate	0.2	1.81	Yes	Polymer	29
Benzoate	4.18	1.38	No	Dimer	22
o-CH_3-benzoate	3.92	1.41	No	Dimer	22
o-OCH_3-benzoate	4.09	*			
o-OH-benzoate	2.97	1.87		Polymer	12
o-NO_2-benzoate	3.21	1.45	No	Dimer	22
o-Cl-benzoate	2.89	1.62	No	Dimer	22
o-F-benzoate	3.27	*			
p-CH_3-benzoate	4.35	1.36	No	Mixture of Polymer & Dimer	22
p-OC_2H_5-benzoate	4.80	*			
p-OH-benzoate	4.48	*			
p-NO_2-benzoate	3.40	1.58	Yes	Polymer	22
p-Cl-benzoate	4.05	1.56	Yes	Polymer	22
p-F-benzoate	4.14	*			
pentafluoro benzoate	1.48	*			41
ß-naphthoate	4.17	1.51			12

* no literature value available

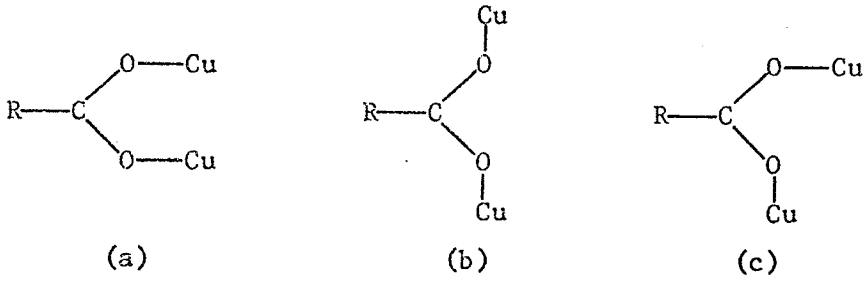

FIG. III Bridging structures for the carboxylates

Configuration (a) is to be found in dimeric cupric carboxylates and the polymeric carboxylates adopt configurations (b) or (c). Due to electrostatic repulsion, the anti-anti or anti-syn configurations are favored if a large positive residual charge remains on the copper ions after bonding with the carboxylate groups. The pK_a values of the carboxylic acids are taken as an indication of the available σ-electron density on the carboxylate oxygen atoms. Stronger acids than acetic acid have less available σ-electron density on the oxygens. Thus because the ligands are less polarizable, a greater residual positive charge is left on the copper atoms in the cupric carboxylates formed from strong acids. In these cases anti-anti or anti-syn configurations are favored. Moreover, the higher effective positive charge on the copper atoms will contract the d - orbitals. This may reduce considerably the overlap in the metal-metal bond and reduce significantly the stability of the dimeric units. Therefore it is expected that those carboxylates formed from acids with high pK_a values (weak acids) would be dimeric in structure but a structural change would occur as the pK_a value decreases. There appears to be no well-defined pK_a value at which the dimeric structure changes to an alternative structure. In fact for those acids which have pK_a values between 4.75 (acetic acid) and 3.75 (formic acid) magnetically distinct forms, or mixtures of such forms, of the same carboxylate have been prepared and observed[13, 22]. It is noted that steric factors stabilize syn-syn bonding of the ortho-substituted carboxylates, such as in the case of cupric o-methyl benzoate which is binuclear.

The electronic spectra of some cupric carboxylates have been

studied[12,22,23,24]. It was observed that they all exhibited a broad absorption band in the region 690 ± 40 mμ and, in addition, those which are believed to be binuclear show an absorption band in the region 400 mμ. For alkyl carboxylates this high-energy band occurs in a relatively narrow region about 375 mμ. However such criteria for binuclear cupric carboxylates must be used with caution because absorption bands of other origins may appear in the same region and in the cases of arylcarboxylates the band in the region of 400 mμ always occurs as a shoulder on a charge transfer band. The assignment of the band in this region for the binuclear complexes has been the subject of considerable discussion[25,26,27].

Though infra red spectrometry has not been used extensively in the investigation of cupric carboxylates, it has been shown to be useful in the structural determination of some of them[28,29,30,31]. The assignment of the bands in some cases still remains in disagreement. Where the assignments are certain, the bands caused by the C-O symmetric stretching, γ_3 and the C-O asymmetric stretching, γ_8, have been shown to be important in confirming the predictions from other methods. In binuclear cupric carboxylates γ_8 has been observed to have a higher frequency than that in the corresponding sodium salts[28,29]. In a series of salts of the same carboxylic acid with different metals, if the structures are symmetrical, bridged, binuclear complexes then both γ_3 and γ_8 are shifted in the same direction either to higher or lower frequencies than those of the sodium salt[28,30]. Thus cupric acetate and chloroacetate are shown to be binuclear while the trifluoroacetate is not. Recent I.R. study of cupric trifluoroacetate[32] showed that γ_8 was strongly split by 35 cm. $^{-1}$ and the band splitting was independent of the phase of the sample (in Nujol mull or in chloroform). It was suggested that the explanation of the splitting in terms of a vibrational coupling between two 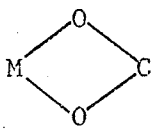 rings is favored over the possibility of bridging trifluoroacetate groups.

Currently, as a continuation of the magnetic susceptibility studies,

electron paramagnetic resonance has been employed to further examine these compounds[33]. From the EPR spectra it is possible to obtain the Spin Hamiltonian parameters of a, S = 1, triplet state. From the parameters the g value (the spectroscopic splitting factor) is obtained accurately (2.160 ± 0.004 for cupric benzoate) and thus J (singlet-triplet separation) can be estimated (EQN. I).

The thermochemistry of some of the cupric carboxylates has been investigated[2-9], and will be discussed along with the experimental data in Part Three.

CHAPTER THREE: PREPARATION OF THE CUPRIC CARBOXYLATES

The cupric carboxylates were prepared in one of the following ways:-

Method (A).From carboxylic acids which are soluble in water or exist in the liquid state at room temperature ($\sim 25^{o}C$)[11,12]:
In this group were formic, acetic, deuterated acetic, propionic, n-butyric, iso-butyric, monochloroacetic, dichloroacetic, difluoroacetic, and trifluoroacetic acids. Cupric hydroxide was freshly prepared by adding a sodium hydroxide (C.P.) solution to a cupric nitrate (C.P.) solution. The cupric hydroxide was formed as a blue gelatinous precipitate and it was filtered off and washed with distilled water. It was then added to a concentrated aqueous solution of the acid (C.P.) or the liquid acid itself. Copper hydroxide reacted with the acid to form blue or greenish blue solutions. The solutions were warmed to about $100^{o}C$ to ensure completion of the reaction. The solution was put in a dessicator containing anhydrous calcium chloride and attached to a vacuum line of about a few cm Hg pressure. Crystals of the cupric carboxylate separated out when part of the water or acid had evaporated The crystals were transferred to a vacuum system of about 3×10^{-4} mm Hg pressure to dry for about 24 hours.

Method (B). From solid carboxylic acids which are insoluble or sparingly soluble in water[12,13] :
In this group were benzoic, o-OCH_3, o-CH_3, o-F, o-OH, o-Cl, o-NO_2, p-OC_2H_5, p-CH_3, p-F, p-Cl, and p-NO_2 benzoic, phenylacetic, pentafluorobenzoic and β-naphthoic acids. A saturated solution of the sodium carboxylate was prepared by stirring for at least half an hour, a solution of aqueous sodium hydroxide (C.P.) with an excess of the solid carboxylic acid (C.P.). The excess acid was filtered off and the filtrate was added to an aqueous solution of copper nitrate (C.P.). The cupric carboxylate was precipitated and was filtered off and washed with distilled water. The carboxylates were dried under a vacuum of 3×10^{-4} mm. Hg pressure for about 24 hours.

Method (C). Forms of cupric benzoate having different magnetic susceptibilities have been prepared[12,13]. One of these forms was prepared by dissolving benzoic acid in 95% enthanol and adding this solution to an aqueous copper nitrate solution. The precipitated cupric benzoate was filtered off and dried in an oven at 90° C in the presence of air for about an hour.

TABLE II lists the color of the crystals of the cupric carboxylates and their methods of preparation.

TABLE II

COLOR OF CUPRIC CARBOXYLATE CRYSTALS

AND METHOD OF PREPARATION

Cupric Carboxylate	Method of Preparation	Color of Crystal
Formate	A	Blue
Acetate	A	Green
Deuterated acetate	A	Green
Propionate	A	Dark Green
iso-Butyrate	A	Dark Green
n-Butyrate	A	Dark Green
phenylacetate	B	Blue
Monochloroacetate	A	Yellowish Green
Dichloroacetate	A	Green Blue
Difluoroacetate	A	Sky Blue
Trifluoroacetate	A	Sky Blue
Benzoate	B&C	Blue
o-CH_3-benzoate	B	Green Blue
o-OCH_3-benzoate	B	Green Blue
o-OH-benzoate	B	Yellowish Green
o-NO_2-benzoate	B	Green
o-Cl-benzoate	B	Green
o-F-benzoate	B	Blue
p-CH_3-benzoate	B	Blue
p-OC_2H_5-benzoate	B	Light Green Blue
p-OH-benzoate	B	Dull Green
p-NO_2-benzoate	B	Blue
p-Cl-benzoate	B	Light Blue
p-F-benzoate	B	Light Blue
penta-fluorobenzoate	B	Sky Blue
β-naphthoate	B	Light Green Blue

PART TWO

MASS SPECTROMETRIC STUDIES

Although extensive studies on cupric carboxylates have been made in other fields, it is only recently that mass spectrometry has been utilized[34]. In the communication[34] (the preliminary work of this study), it was shown that on heating the cupric benzoate or acetate in the mass spectrometer decomposition occurred and the cupric carboxylates were not detected in the vapor. Instead, among the various volatile decomposition products, dimeric cuprous carboxylates were identified. Cupric acetate was the only cupric carboxylate previously reported to have the dimeric cuprous salt as one of the thermal decomposition products[1]. It is the purpose of this study to use mass spectrometry to discover whether cuprous carboxylates can be detected among the thermal decomposition products of a series of cupric salts. It is only recently that mass spectrometry has been applied to the study of metal-containing molecules and consequently information on their fragmentation behavior under electron impact is very limited. Thus, if the mass spectra of a series of related compounds can be obtained it may prove possible to make general conclusions about the spectra and to relate these to the electronic structures of the compounds.

Since J.J.Thomson's discovery[35] of neon isotopes by mass spectroscopy, a great deal of development has been taking place in this field and many books have been written on this subject[35-39].

The principles of the direct-focussing mass spectrometer, which was used in this study, are well-known and fully discussed in the above mentioned references. Basically they involve accelerating in an electric field the ions formed by electron bombardment of a sample and the subsequent separation of the accelerated ions by a variable magnetic field into ion beams, each with a specific mass to charge ratio (m/e). The ion beams are focussed and collected. The electric current produced by the ion beam is amplified and then recorded. The intensity of the ion current indicates the amount of the ion formed. A mass spectrum consists of the relative intensities of the currents at different mass to charge ratios. Generally the most intense peak in a spectrum is used as a standard (the base peak) having a relative intensity of 100.

In an electron impact process many types of ions are formed. Other than the four types that are studied in this work, there are ions formed by intermolecular processes, multiply-charged ions and negative ions. The four types are:

(A) Parent Ions

When an atomic or a molecular species is bombarded by electrons of energy between 10 and 100 ev, one of the reactions is the removal of an electron from the species forming a molecular or an atomic positive ion whose m/e ratio gives the molecular weight of the compound. The reaction may be denoted as:

$$M + e \rightarrow M^{+} + 2e$$

(B) Fragment Ions

Fragment ions are produced when various bond cleavage processes occur in the parent ion or other fragment ions. Their formation is determined by several factors, such as the Franck-Condon principle, the relative bond dissociation energies, the stability of the neutral fragment

after bond cleavage, the vibrational frequencies and the number of degrees of freedom of the parent ion. The processes can be denoted as:

$$M + e \rightarrow F_1^+ + N_1 + 2e$$

$$F_1^+ \rightarrow F_2^+ + N_2$$

Where M = parent species
e = electron
F_1^+, F_2^+ = fragment ions
N_1, N_2 = neutral fragments

(C) Rearrangement Ions

Rearrangement of atoms or groups of atoms at the moment of the unimolecular dissociation of the parent ions. Their presence cannot be accounted for by simple cleavage of the parent ions. It is known from ionization efficiency studies that it usually requires considerably more energy for the formation of rearrangement ions than for fragment ions. Rearrangement ions usually disappear from the spectra if the energy of the electron in an electron impact process is less than 20 ev. Though rearrangement ions are thermodynamically more favorable, activation energy is required. It has been observed that some fluorine-containing compounds show rather random rearrangements under electron impact.

(D) Metastable Ions

Some of the ions formed by the electron impact process may be "metastable". In general, dissociation can occur anywhere between the ion source and the collector. But if they decompose, say, from the "parent" ion, M_p, to the "daughter" ion, M_d, in the ion acceleration region of the mass spectrometer, especially if this occurs at the end of this region, characteristic peaks are recorded on the mass scale, neither at a mass corresponding to that of M_p nor to that of M_d, but rather at an effective mass, M^*. M^* can be calculated according to the following equation, EQN.II,

derived by Hipple, Fox and Condon[40]:

$$M^* = \frac{M_d^2}{M_p} \qquad \text{EQN. II}$$

This equation was developed for single-focussing sector-type mass spectrometers. The characteristics of metastable peaks are:- (1) They are of low intensity , about 0.01% to 1% of the base peak. (2) They usually are observed at non-integral masses. (3) They are broad, and may have widths extending several mass units. With the help of EQN. II metastable peaks can be very useful in the determination of the fragmentation processes of molecules under electron impact.

Identication of ions in a mass spectrum is determined from the m/e ratios and the relative intensities of the peaks produced by the ion currents. Some chemical elements have isotopes. In a mass spectrum, if a particular ion contains such elements, the ratio(s) of the intensities of the peaks due to that ion is given by the natural abundances of the isotopes of the elements. Since the natural isotopic abundance of the common elements are well known, the correct ratio of the peak intensities in a given ion indicates the presence of a particular element in that ion.

CHAPTER SIX: INSTRUMENTATION

A Hitachi RMU-6D single-focussing mass spectrometer was used for the identification of the volatile thermal decomposition products. A Honeywell 1508 visicorder recorder with four galvanometers of different sensities of the order 27, 9, 3 and 1 was used in recording the mass spectra. The solid sample (about ½ mg) was packed into a sample tube which was directly inserted into the vacuum system of the mass spectrometer via a vacuum lock. In the mass spectrometer the sample was situated inside a block heater which has a hole that opens directly into the ion source. The vacuum of the mass spectrometer under which the experiments were done was 5×10^{-6} mm Hg pressure or better. Schematic representations of the mass spectrometer and its ion source are shown in FIGS. IV and V.

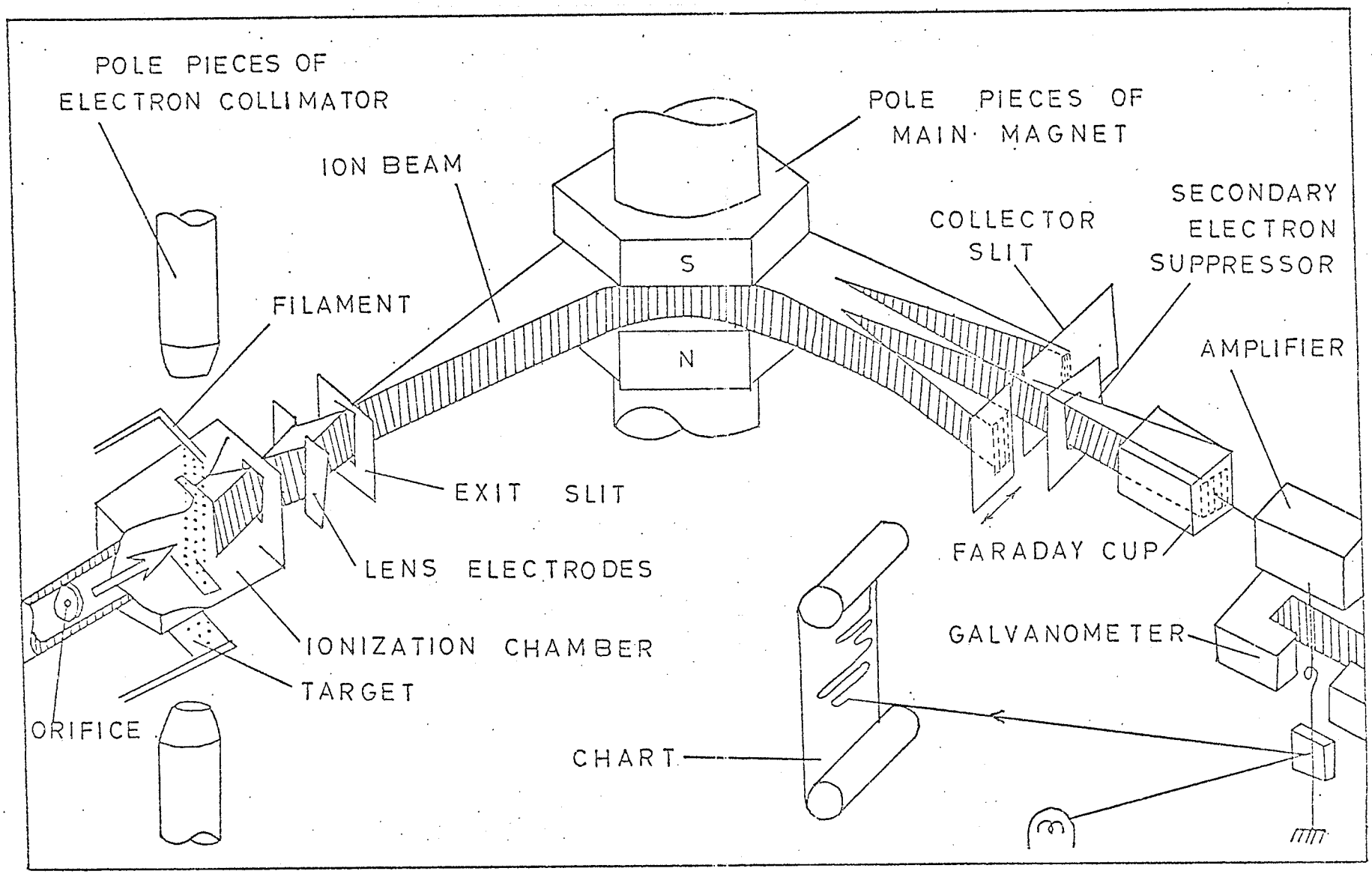

FIGURE IV

Schematic representation of Hitachi RMU-6D single- focussing mass spectrometer.

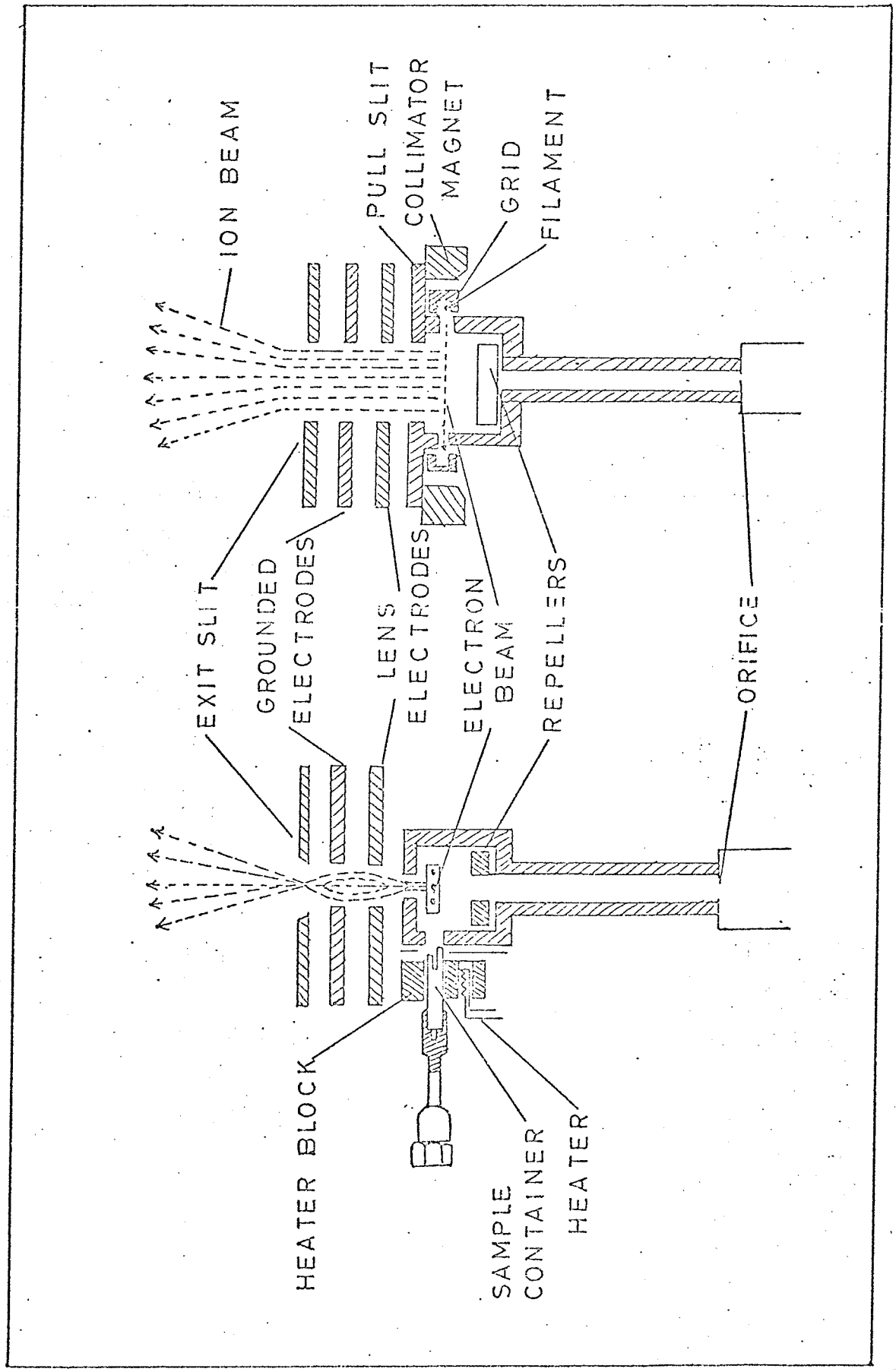

FIGURE V

Schematic representation of the ion source.

The thermal decompositions of the cupric carboxylates in the mass spectrometer were studied under a vacuum of 5×10^{-6} mm Hg pressure or better. The temperature of the ion source was at 200°C. The energy of the ionizing electrons was 50 eV.

The carboxylate was packed into the sample tube with a new wooden toothpick in such a way that the sample would not fall down when the sample tube was held upside down. About half a mg of sample was used every time. A background mass spectrum was taken. The sample was put into the block heater in the mass spectrometer previously described. When the vacuum was pumped down to the order of 1×10^{-6} mm Hg, the temperature at the block heater, i.e. the approximate temperature of the sample was noted. The mass spectra of the thermal decomposition products were recorded as follows. The temperature of the heater was slowly raised in such a way that the pressure was never more than 5×10^{-6} mm Hg at any instant. The mass spectrum of the volatile products from the heating process was recorded at convenient intervals. The maximum temperature to which samples could be heated was 300°C. During this rise of temperature, usually from 40°C to 300°C, different samples behaved differently even though the initial process is inevitably dehydration for the samples containing water of crystalization. The interesting point is that some compounds had cuprous carboxylates as volatile decomposition products while others did not.

Of all the cupric carboxylates listed in Table I, only eleven gave detectable amounts of cuprous carboxylates among the volatile decomposition products. (Trideuterated cupric acetate, $Cu(O_2CCD_3)_2$, was also studied but it is chemically the same as the acetate, and it behaved in a similar way as the acetate during the thermal decomposition process. Its mass spectrum helps to confirm the identification of the ions in the acetate spectrum, especially those which produce overlapping peaks.) The others during the heating process gave various decomposition products, but copper containing species were not detected among them. In this latter group, all of the compounds gave decomposition products containing the carboxylic acids, but in addition

some gave the acid anhydride at higher temperatures. The temperatures at which detectable decomposition started to occur were fairly sharply defined ($\pm 10^{o}$). TABLE IV lists the copper carboxylates for which no detectable cuprous species were observed, the approximate temperatures at which the acid and the acid anhydride were observed in the decomposition products, the more important ions in the spectrum, their assignment and the volatile decomposition products.

The twelve remaining cupric carboxylates (trideuterated acetate, 94.7% deuteration, included) decompose in a similar way to those in TABLE IV, in that they too give the carboxylic acid and sometimes the anhydride as decomposition products but they also have the distinctive feature that volatile copper containing species are also detected. So that the mass spectral fragmentation patterns of the cuprous carboxylates may be easily surveyed, the data for the non-copper containing decomposition products are given in a separate table, TABLE V, but one must keep in mind that this data is extracted from the same spectra in which the copper containing ions are present. TABLE VI shows the mass spectral data for the copper containing species.

TABLE IV

Decomposition of copper carboxylates for which volatile cuprous species were not detected

Cupric Carboxylate	Approx. temp. for Appearance of Acid	Approx. temp. for Appearance of Anhydride	Major ions M/e	Assignment	Major decomposition products detected
Formate	100°C	-	46	$HCOOH^+$	HCO_2H
			45	HCO_2^+	CO_2
			44	CO_2^+	H_2O
			29	HCO^+	CO?
			28	CO^+	
			18	H_2O^+	
Phenylacetate	110°C	-	136	$\phi CH_2CO_2H^+$	ϕCH_2CO_2H
			122	ϕCO_2H^+	CO_2
			106,105	ϕCO^+	H_2O
			92,91	ϕCH_2^+	ϕCO_2H?
			77	ϕ^+	CO?
			65	$C_5H_5^+$	
			44	CO_2^+	
			28	CO^+	
			18	H_2O^+	
Monochloro-acetate	95°C	-	94,96	$ClCH_2CO_2H^+$	$ClCH_2CO_2H$
			59	$CH_2CO_2H^+$	HCl
			52,50	CH_3Cl^+	CH_3Cl
			51,49	CH_2Cl^+	CO_2
			45	CO_2H^+	$(CuCl)_3$
			44	CO_2^+	$(CuCl)_4$
			42	CH_2CO^+	CO?
			38,36	HCl^+	
			37,35	Cl^+	
			28	CO^+	

TABLE IV Continued

			At about 300°C		
			392,394,396,398, 400,402,404, 406,408	$Cu_4Cl_4^+$	
			294,296,298,300, 302,304,306	$Cu_3Cl_3^+$	
			259,261,263, 265,267,269	$Cu_3Cl_2^+$	
			196,198,200, 202,204	$Cu_2Cl_2^+$	
			161,163,165, 167	Cu_2Cl^+	
			126,128,130	Cu_2^+	
Dichloro-acetate	120°C	-	115,113,111	$HCCl_2CO^+$	$HCCl_2CO_2H$
			88,86,84	$H_2CCl_2^+$	H_2CCl_2
			87,85,83	$HCCl_2^+$	CO_2
			78,76	$HCClCO^+$	HCl
			65,63	$ClCO^+$	H_2O
			51,49	H_2CCl^+	$(CuCl)_3$
			50,48	$HCCl^+$	$(CuCl)_4$
			49,47	CCl^+	
			45	CO_2H^+	
			44	CO_2^+	
			38,36	HCl^+	
			37,35	Cl^+	
			29	HCO^+	
			28	CO^+	
			18	H_2O^+	
			At about 300°C		
			408,406,404, 402,400,398, 396,394,392	$Cu_4Cl_4^+$	
			347,345,343, 341,339	$Cu_3Cl_4^+$	
			304,302,300, 298,296,294	$Cu_3Cl_3^+$	

TABLE IV Continued

			269,267,265, 263,261,259	$Cu_3Cl_2^+$	
			167,165,163, 161	Cu_2Cl^+	
o-OCH_3-benzoate	105°C	-	152	$CH_3OC_6H_4CO_2H^+$	o-$CH_3OC_6H_4CO_2H$
			135	$CH_3OC_6H_4CO^+$	CO_2
			120	$OC_6H_4CO^+$	C_2H_6
			105	ϕCO^+	H_2O
			92	$C_6H_4O^+$	HCO_2H
			77	ϕ^+	CO?
			46	HCO_2H^+	H_2CO?
			44	CO_2^+	
			30	$C_2H_6^+$, H_2CO?	
			28	CO^+	
			18	H_2O^+	
o-CH_3-benzoate	115°C	-	136	$CH_3C_6H_4CO_2H^+$	o-$H_3CC_6H_4CO_2H$
			119	$CH_3C_6H_4CO^+$	CO_2
			118	$CH_2C_6H_4CO^+$	H_2O
			105	ϕCO^+	CO
			91	$C_7H_7^+$	
			90	$CH_2C_6H_4^+$	
			77	ϕ^+	
			44	CO_2^+	
			28	CO^+	
			18	H_2O^+	
			17	OH^+	
o-F-benzoate	160°C	190°C	262	$(FC_6H_4CO)_2O^+$	$(FC_6H_4CO)_2O$
			234	$(FC_6H_4)_2CO_2^+$	o-$FC_6H_4CO_2H$
			218	$(FC_6H_4)_2CO^+$	CO_2
			140	$FC_6H_4CO_2H^+$	H_2O
			123	$FC_6H_4CO^+$	$(FC_6H_4)_2CO_2$?
			95	FC_6H_4	$(FC_6H_4)_2CO$?

		75	$C_6H_3^+$	
		69	$C_4H_2F^+$?	
		44	CO_2^+	
		28	CO^+	
		18	H_2O^+	
o-NO_2-benzoate	165°C	- 304	?	o-$NO_2C_6H_4CO_2H$
		257	$(NO_2)_3C_6H_2CO_2H^+$?	C_6H_5
		198	ϕ-C_6H_4-NO_2^+?	CO_2
		168	$(NO_2)_2C_6H_4^+$?	H_2O
		167	$NO_2C_6H_4CO_2H^+$	$NO_2C_6H_4OH$?
		150	$NO_2C_6H_4CO^+$	CO?
		139	$NO_2C_6H_4OH^+$	
		123	$NO_2C_6H_5^+$	
		93	$C_6H_5O^+$	
		77	$C_6H_5^+$	
		65	$C_5H_5^+$	
		44	CO_2^+	
		28	CO^+	
		18	H_2O^+	
		17	OH^+	
o-OH-benzoate	100°	- 138	$HOC_6H_4CO_2H^+$	o-$HOC_6H_4CO_2H$
		120	$OC_6H_4CO^+$	C_6H_5OH
		94(@220°C)	$C_6H_5OH^+$	HCO_2H
		92	$C_6H_4O^+$	CO_2
		65	$C_5H_5^+$	H_2O
		64	$C_5H_4^+$	H_2CO?
		46	HCO_2H^+	CO?
		44	CO_2^+	
		39	$C_3H_3^+$	
		30	H_2CO^+	
		28	CO^+	
		18	H_2O^+	

TABLE IV continued

p-OC_2H_5-benzoate	75°C	245°C	314	let e ≡ OC_2H_5 $(eC_6H_4CO)_2O^+$	$(eC_6H_4CO)_2O$
			286	$(eC_6H_4)_2CO_2^+$	p-$eC_6H_4CO_2H$
			270	$(eC_6H_4)_2CO^+$	CO_2
			258	$(eC_6H_4)_2O^+$	H_2O
			242	$(eC_6H_4)_2^+$	$(eC_6H_4)_2CO_2$?
			227	$(eC_6H_4)CH_2OC_6H_4^+$	$(eC_6H_4)_2CO$?
			212	$(CH_2OC_6H_4)_2^+$	$(eC_6H_4)_2O$?
			166	$eC_6H_4CO_2H^+$	$(eC_6H_4)_2$?
			138	$HOC_6H_4CO_2H^+$	
			121	$HOC_6H_4CO^+$, }? $C_6H_4CO_2H^+$	
			93	$HOC_6H_4^+$	
			77	ϕ^+	
			65	$C_5H_5^+$	
			51	$C_4H_3^+$	
			44	CO_2^+	
			28	CO^+	
			18	H_2O^+	
p-CH_3-benzoate	155°C	195°C	254	$(CH_3C_6H_4CO)_2O^+$	$(CH_3C_6H_4CO)_2O$
			226	$(CH_3C_6H_4)_2CO_2^+$	$CH_3C_6H_4COOH$
			210	$(CH_3C_6H_4)_2CO^+$	CO_2
			198	$(CH_3C_6H_4)_2O^+$	C_2H_6
			195	$(CH_3C_6H_4)C_6H_4CO^+$	H_2O
			182	$(CH_3C_6H_4)_2^+$	H_2CO?
			136	$CH_3C_6H_4CO_2H^+$	CO?
			119	$CH_3C_6H_4CO^+$	$(CH_3C_6H_4)_2CO$?
			91	$CH_3C_6H_4^+$, $C_7H_7^+$	$(CH_3C_6H_4)_2O$?
			77	$C_6H_5^+$	$(CH_3C_6H_4)_2$?
			65	$C_5H_5^+$	
			51	$C_4H_3^+$	
			44	CO_2^+	

TABLE IV continued

			30	$C_2H_6^+$, H_2CO^+?	
			28	CO^+	
			18	H_2O^+	
			17	OH^+	
$p\text{-}NO_2$-benzoate	175°C	300°C	316 (trace only)	$(NO_2C_6H_4CO)_2O^+$	$(NO_2C_6H_4CO)_2O$
			288 (trace only)	$(NO_2C_6H_4)_2CO^+$	$NO_2C_6H_4CO_2H$
			272 (trace only)	$(NO_2C_6H_4)_2CO^+$	CO_2
			167	$NO_2C_6H_4CO_2H^+$	H_2O
			150	$NO_2C_6H_4CO^+$	NO?
			137	$OC_6H_4CO_2H^+$	CO?
			121	$C_6H_4CO_2H^+$	
			104	$C_6H_4CO^+$	
			76	$C_6H_4^+$	
			65	$C_5H_5^+$	
			44	CO_2^+	
			30	NO^+	
			28	CO^+	
			18	H_2O^+	
p-OH-benzoate	90°C	-	138	$HOC_6H_4CO_2H^+$	$HOC_6H_4CO_2H$
			121	$HOC_6H_4CO^+$	CO_2
			93	$C_6H_4OH^+$	H_2O
			65	$C_5H_5^+$	
			44	CO_2^+	
			30	H_2CO^+	
			28	CO^+	
			18	H_2O^+	

TABLE IV continued

β-naphthoate	130°C	225°C	326	$(C_{10}H_7CO)_2O^+$	$(C_{10}H_7CO)_2O$
			298	$(C_{10}H_7)_2CO_2^+$	$C_{10}H_7CO_2H$
			282	$(C_{10}H_7)_2CO^+$	CO_2
			172	$C_{10}H_7CO_2H^+$	H_2O
			155	$C_{10}H_7CO^+$	$(C_{10}H_7)_2CO_2$?
			127	$C_{10}H_7^+$	CO?
			77	$C_6H_5^+$	
			44	CO_2^+	
			28	CO^+	
			18	H_2O^+	
			17	OH^+	

TABLE V

Decomposition of copper(II) carboxylates for which volatile cuprous carboxylates are among decomposition products. Non-copper containing species only.

Cupric Carboxylate	Approx. temp. for appearance of Acid	Anhydride	Major ions M/e	Assignment	Major decomposition products detected
Acetate	115°C	-	60	$CH_3CO_2H^+$	CH_3CO_2H
			45	CO_2H^+	CO_2
			44	CO_2^+	H_2O
			43	CH_3CO^+	CO?
			42	CH_2CO^+	
			41	$CHCO^+$	
			29	HCO^+	
			28	CO^+	
			18	H_2O^+	
			15	CH_3^+	
Deuterated Acetate $Cu(O_2CCD_3)_2$	115°C	-	64	$CD_3CO_2D^+$	CD_3CO_2D
			63	$CD_3CO_2H^+$	CD_3CO_2H
			46	CO_2D^+, CD_3CO^+	CO_2
			45	CO_2H^+	D_2O, DHO, H_2O
			44	CO_2^+, CD_2CO^+	CO?
			42	$CDCO^+$	
			30	DCO^+	
			28	CO^+	
			20	D_2O^+	
			19	DHO^+	
			18	H_2O^+, CD_3^+	
			17	OH^+	
			16	O^+	
Propionate	130°C	-	74	$CH_3CH_2CO_2H^+$	$C_2H_5CO_2H$
			73	$C_2H_5CO_2^+$	CO_2
			57	$C_2H_5CO^+$	C_2H_4

TABLE V continued

			45	CO_2H^+	C_2H_2?
			44	CO_2^+	CO?
			29	$C_2H_5^+$, HCO^+	
			28	$C_2H_4^+$, CO^+	
			27	$C_2H_3^+$	
			26	$C_2H_2^+$	
n-butyrate	45°C	-	88	$C_3H_7CO_2H^+$	$C_3H_7CO_2H$
			87	$C_3H_7CO_2^+$	CO_2
			73	$C_2H_4CO_2H^+$	C_3H_6
			71	$C_3H_7CO^+$	C_2H_6
			60	$CH_2CO_2H_2^+$	C_2H_4
			55	$C_2H_3CO^+$	C_2H_2
			45	CO_2H^+	CO?
			44	CO_2^+	
			43	$C_3H_7^+$	
			42	$C_3H_6^+$	
			41	$C_3H_5^+$	
			39	$C_3H_3^+$	
			30	$C_2H_6^+$	
			29	HCO^+	
			28	CO^+, $C_2H_4^+$	
			27	$C_2H_3^+$	
			26	$C_2H_2^+$	
iso-butyrate	40°C	-	88	$C_3H_7CO_2H^+$	$C_3H_7CO_2H$
			73	$C_2H_4CO_2H^+$	HCO_2H
			71	$C_3H_7CO^+$	CO_2
			55	$C_2H_3CO^+$	C_2H_6
			46	HCO_2H^+	C_2H_4
			45	CO_2H^+	C_2H_2
			44	CO_2^+	C_3H_6
			43	$C_3H_7^+$	H_2O
			42	$C_3H_6^+$	CH_4
			41	$C_3H_5^+$	CO?

TABLE V continued

			39	$C_3H_3^+$	
			30	$C_2H_6^+$	
			29	$C_2H_5^+$	
			28	CO^+, $C_2H_4^+$	
			27	$C_2H_3^+$	
			26	$C_2H_2^+$	
			18	H_2O^+	
			17	OH^+	
			16	CH_4^+, O^+	
			15	CH_3^+	
Difluoroacetate	175°C	-	96	$HCF_2CO_2H^+$	HCF_2CO_2H
			79	HCF_2CO^+	CO_2
			76	$CFCO_2H^+$	H_2CO
			67	CF_2OH^+	H_2O
			52	$H_2CF_2^+$	CO?
			51	HCF_2^+	
			50	CF_2^+	
			45	CO_2H^+	
			44	CO_2^+	
			32	HCF^+	
			30	H_2CO^+	
			28	CO^+	
			20	HF^+	
			18	H_2O^+	
			17	OH^+	
Trifluoro-acetate	135°C	-	97	CF_3CO^+	CF_3CO_2H
			95	$CF_2CO_2H^+$	CO_2
			69	CF_3^+	
			51	HCF_2^+	
			50	CF_2^+	
			45	CO_2H^+	
			44	CO_2^+	
			31	CF^+	
			28	CO^+	

TABLE V continued

Benzoate	175°C	200°C	226	$(\phi CO)_2O^+$	$(\phi CO)_2O$
			198	$\phi_2CO_2^+$	ϕCO_2H
			122	ϕCO_2H^+	CO_2
			105	ϕCO^+	ϕ_2CO_2?
			77	$C_6H_5^+$	CO?
			51	$C_4H_3^+$	
			44	CO_2^+	
			28	CO^+	
p-F-benzoate	130°C	245°C	262	$(FC_6H_4CO)_2O^+$	$(FC_6H_4CO)_2O$
			234	$(FC_6H_4)_2CO_2^+$	$FC_6H_4CO_2H$
			140	$FC_6H_4CO_2H^+$	CO_2
			123	$FC_6H_4CO^+$	H_2O
			95	$FC_6H_4^+$	CO?
			76	$C_6H_4^+$	
			75	$C_6H_3^+$	
			74	$C_6H_2^+$	
			73	C_6H^+?	
			69	$C_4H_2F^+$?	
			51	$C_4H_3^+$	
			50	$C_4H_2^+$	
			44	CO_2^+	
			39	$C_3H_3^+$	
			28	CO^+	
			20	HF^+	
			18	H_2O^+	
p-Cl-benzoate	75°C	130°C	298,296,294	$(ClC_6H_4CO)_2O^+$	$(ClC_6H_4CO)_2O$
			270,268,266	$(ClC_6H_4)_2CO_2^+$	$ClC_6H_4CO_2H$
			254,252,250	$(ClC_6H_4)_2CO^+$	CO_2
			158,156	$ClC_6H_4CO_2H^+$	H_2O
			157,155	$ClC_6H_4CO_2^+$	ClC_6H_4OH?
			141,139	$ClC_6H_4CO^+$	CO?
			130,128	$ClC_6H_4OH^+$	

			113,111	$ClC_6H_4^+$	
			75	$C_6H_3^+$	
			51	$C_4H_3^+$	
			50	$C_4H_2^+$	
			44	CO_2^+	
			38	$C_3H_2^+$	
			28	CO^+	
			18	H_2O^+	
o-Cl-benzoate	175°C	250°C	298,296,294	$(ClC_6H_4CO)_2O^+$	$(ClC_6H_4CO)_2O$
			261,259	$(ClC_6H_4CO)O(C_6H_4CO)^+$	$ClC_6H_4CO_2H$
			158,156	$ClC_6H_4CO_2H^+$	CO_2
			141,139	$ClC_6H_4CO^+$	H_2O
			113,111	$ClC_6H_4^+$	CO?
			76	$C_6H_4^+$	
			75	$C_6H_3^+$	
			51	$C_4H_3^+$	
			50	$C_4H_2^+$	
			44	CO_2^+	
			28	CO^+	
			18	H_2O^+	
Pentafluoro-benzoate	145°C	-	334	$C_{12}F_{10}^+$	$C_{12}F_{10}$
			315	$C_{12}F_9^+$	$F_5C_6CO_2H$
			296	$C_{12}F_8^+$	CO_2
			265	$C_{11}F_7^+$	H_2O
			234	$C_{10}F_6^+$	
			212	$F_5C_6CO_2H^+$	
			195	$F_5C_6CO^+$	
			168	$F_5C_6H^+$	
			167	$F_5C_6^+$	
			117	$C_5F_3^+$	
			99	$C_5F_2H^+$	
			93	C_3F_3	

69	CF_3^+
44	CO_2^+
31	CF^+
28	CO^+
18	H_2O^+

TABLE VI

Mass spectra of cuprous carboxylates formed as thermal decomposition products of the cupric carboxylates.

* N.B. The intensity is not calculated in cases where the copper containing species are observed at the same mass unit as the non-copper containing ones or other copper containing species.

TABLE VI

R	CH_3	CD_3	CH_3CH_2	$CH_3CH_2CH_2$	$(CH_3)_2CH$
Temperature	150°C	245°C	180°C	95°C	115°C
Intensity standard(100)	$Cu_2RCO_2^+$ 185	$Cu_2RCO_2^+$ 188	$Cu_2RCO_2^+$ 199	$Cu_2RCO_2^+$ 213	$Cu_2RCO_2^+$ 213
$Cu_2(RCO_2)_2^+$ in mass unit (intensity)	244(62) 246(54) 248(13)	250(73) 252(67) 254(17)	272(28) 274(25) 276(6)	300(39) 302(34) 304(8)	300(30) 302(27) 304(7)
$Cu_2(RCO_2)R^+$	-	-	-	-	-
$Cu_2(RCO_2)CO_2^+$	229(13) 231(11) 233(3)	232(9) 234(7) 236(3)	-	-	-
$Cu_2RCO_2^+$	185(100) 187(90) 189(21)	188(100) 190(86) 192(23)	199(100) 201(90) 203(21)	213(100) 215(89) 217(23)	213(100) 215(90) 217(21)
$Cu_2R_2^+$	-	-	-	-	-
Cu_2R^+	141(21) 143(21) 145(8)	144* 146* 148*	155(5) 157(4) 159(1)	169(9) 171(8) 173(3)	169(17) 171(15) 173(4)
Cu_2F^+	-	-	-	-	-
Cu_2O^+	142(14) 144(10) 146(3)	142* 144* 146*	142(7) 144(6) 146(2)	-	-
Cu_2H^+	-	-	127(11) 129(10) 131(2)	127(10) 129(9) 131(2)	127(16) 129(14) 131(3)
Cu_2^+	126(11) 128(10) 130(3)	126(8) 128(8) 130(4)	126(9) 128(8) 130(2)	126(6) 128(5) 130(1.2)	126(9) 128(8) 130(2)
$CuCO_2^+$	107(19) 109(8)	107(29) 109(14)	107(7) 109(4)	107(9) 109(3)	107(12.5) 109(6)
Cu_2^+	63(27) 65(13)	63* 65*	63(10) 65(5)	63(9)63 65(4)	63(12.5) 65(6)
Miscellaneous ions	-	-	$CuCO^+$ 91(14) 93(7)	$Cu_2(RCO_2)(RO)^+$ 272(2) 274(2) 276(1) Cu_2RO^+ 185(3) 187(3) 189(1) $Cu(RCO_2)R^+$ 193(3) 195(1.7) $HCuRCO_2^+$ 151(4) 153(2)	-

TABLE VI Continued

R	F_2CH	F_3C	C_6H_5	$p\text{-}FC_6H_4$	F_5C_6
Temperature	195°C	180°C	220°C	255°C	245°C
Intensity standard	$Cu_2RCO_2^+$ 221	$Cu_2RCO_2^+$ 239	Cu_2R^+ 203	Cu_2R^+ 221	$Cu_2(RCO_2)_2^+$ 548
$Cu_2(RCO_2)_2^+$	316(20) 318(17) 320(4)	352(13) 354(12) 356(3)	368(76) 370(68) 372(17)	404(85) 406(79) 408(19)	548(100) 550(90) 552(26)
$Cu_2(RCO_2)R^+$	-	-	324(27) 326(25) 328(6)	360(26) 362(23) 364(6)	-
$Cu_2(RCO_2)CO_2^+$	265* 267* 269*	283(8) 285(7) 287(2)	-	-	-
$Cu_2RCO_2^+$	221(100) 223(86) 225(21)	239(100) 241(89) 243(22)	247(11) 249(9) 251(3)	265(21) 267(18) 269(5)	-
$Cu_2R_2^+$	-	-	280(28) 282(25) 284(7)	316(17) 318(16) 320(5)	-
Cu_2R^+	-	-	203(100) 205(87) 207(21)	221(100) 223(89) 225(21)	-
Cu_2F^+	145(58) 147(53) 149(14)	145(65) 147(58) 149(14)	-	145(24) 147(22) 149*	-
Cu_2O^+	142(21) 144(19) 146(4)	142(21) 144(18) 146(5)	-	-	-
Cu_2H^+	-	-	127(4) 129(4) 131(1)	-	-
Cu_2^+	126(37) 128(32) 130(7)	126(27) 128(25) 130(6)	126(4) 128(4) 130(1)	126(7) 128(6) 130*	-
$CuCO_2^+$	107(9) 109(4)	107(23) 109(10)	-	-	-
Cu^+	63(93) 65(42)	63(95) 65(50)	63(52) 65(24)	63(95) 65(30)	-
Miscellaneous ions	$CuCO^+$ 91(5) 93(2)	-	CuR_2^+ 217(52) 219(25) CuR^+ 140(18) 142(9)	CuR_2^+ 253(20) 255(9)	-

TABLE VI Continued

R	o-ClC_6H_4	p-ClC_6H_4
Temperature	260°C	175°C
Intensity standard	$Cu_2(RCO_2)_2^+$ 438	Cu_2R^+ 239
$Cu_2(RCO_2)_2^+$	436(64) 438(100) 440(60) 442(20) 444(4)	436(35) 438(53) 440(31) 442(9) 444(∿1)
$Cu_2(RCO_2)R^+$	-	392(17) 394(27) 396(16) 398(4)
$Cu_2(RCO_2)CO_2^+$	-	-
$Cu_2RCO_2^+$	-	281* 283* 285* 287*
$Cu_2R_2^+$	-	348(14) 350(19) 352(12) 354(4)
Cu_2R^+	-	237(79) 239(100) 241(34) 243(9)
Cu_2F^+	-	-
Cu_2O^+	-	-
Cu_2H^+	-	-
Cu_2^+	-	126* 128* 130*
$CuCO_2^+$	-	-
Cu^+	-	63* 65*
Miscellaneous ions	-	-

The ions containing copper can be recognized by the relative intensities within a group of peaks, since copper has two isotopes of masses 63 and 65 with a natural abundance of 69.1% and 30.9% respectively. An ion containing one copper atom will appear as a doublet in the mass spectrum two mass units apart and the relative intensities of the lower mass peak to the higher one will be 0.691:0.309. An ion containing two copper atoms will be observed as a triplet of peaks in the spectrum spaced two mass units apart. For Cu_2 the relative intensities of the masses 126:128:130 are 0.477:0.427:0.096. In some of the spectra, one or two chlorine atoms are also present in the ions. For the 35:37 isotopes of chlorine the ratio is 0.758:0.242. The following ratios are calculated:-

Cu_2Cl, 161:163:165:167 = 0.362:0.439:0.176:0.013

Cu_2Cl_2, 196:198:200:202:204 = 0.274:0.421:0.235:0.060:0.005

Table VII shows the experimental ratios of peak heights of a given ion so that they may be compared with the calculated values above. Also shown are the total intensities of each ion and their intensities normalized to the base peak, which is assigned an intensity of 100.

TABLE VII

Isotopic ratios and relative intensities of copper containing species

Ions	Mass Number Ratio	Isotopic Ratio	Total Peak Height in mm.	Relative Intensity
Acetate				
$Cu_2(CH_3CO_2)_2^+$	244:246:248	0.48: 0.42: 0.10	174	61
$Cu_2(CH_3CO_2)CO_2^+$	229:231:233	0.47: 0.42: 0.11	36	13
$Cu_2(CH_3CO_2)^+$	185:187:189	0.47: 0.43: 0.10	285	100
Cu_2O^+	142:144:146	0.51: 0.38: 0.11	37	13
$Cu_2CH_3^+$	141:143:145	0.42: 0.42: 0.16	67	23.5
Cu_2^+	126:128:130	0.46: 0.42: 0.12	33	12
$CuCO_2^+$	107:109	0.70: 0.30	37	13
Cu^+	63:65	0.68: 0.32	53	19
Deuterated Acetate				
$Cu_2(CD_3CO_2)_2^+$	250:252:254	0.47: 0.42: 0.11	231	75
$Cu_2(CD_3CO_2)CO_2^+$	232:234:236	0.47: 0.36: 0.18	28	9.1
$Cu_2CD_3CO_2^+$	188:190:192	0.48: 0.41: 0.11	308	100
Cu_2^+	126:128:130	0.40: 0.40: 0.20	30	9.8
$CuCO_2^+$	107:109	0.68: 0.32	30	9.8
Propionate				
$Cu_2(C_2H_5CO_2)_2^+$	272:274:276	0.47: 0.43: 0.10	131	28
$Cu_2C_2H_5CO_2^+$	199:201:203	0.47: 0.43: 0.10	463	100
$Cu_2C_2H_5^+$	155:157:159	0.50: 0.40: 0.10	20	4.3
Cu_2O^+	142:144:146	0.48: 0.42: 0.09	33	7
Cu_2H^+	127:129:131	0.46: 0.44: 0.10	50	11
Cu_2^+	126:128:130	0.47: 0.42: 0.12	33	7
$CuCO_2^+$	107:109	0.63: 0.38	24	5
$CuCO^+$	91:93	0.67: 0.33	45	10
Cu^+	63:65	0.69: 0.31	32	7

TABLE VII continued

n-butyrate				
$Cu_2(C_3H_7CO_2)_2^+$	300:302:304	0.48: 0.42: 0.10	732	39
$Cu_2(C_3H_7CO_2)C_3H_7O^+$	272:274:276	0.50: 0.41: 0.09	44	2.3
$Cu_2C_3H_7CO_2^+$	213:215:217	0.47: 0.42: 0.11	1898	100
$Cu_2C_3H_7O^+$	185:187:189	0.46: 0.44: 0.10	59	3.1
$Cu_2C_3H_7^+$	169:171:173	0.46: 0.42: 0.12	194	10.2
Cu_2H^+	127:129:131	0.47: 0.43: 0.10	187	10
Cu_2^+	126:128:130	0.51: 0.39: 0.10	109	5.7
$Cu(C_3H_7CO_2)C_3H_7^+$	193:195	0.66: 0.34	44	2
$HCuC_3H_7CO_2^+$	151:153	0.66: 0.35	58	3
$CuCO_2^+$	107:109	0.75: 0.25	107	6
Cu^+	63:65	0.69: 0.31	102	5
iso-butyrate				
$Cu_2((CH_3)_2CHCO_2)_2^+$	300:302:304	0.48: 0.42: 0.10	147	30
$Cu_2(CH_3)_2CHCO_2^+$	213:215:217	0.47: 0.42: 0.10	489	100
$Cu_2(CH_3)_2CH^+$	169:171:173	0.46: 0.39: 0.11	84	17
Cu_2H^+	127:129:131	0.47: 0.43: 0.10	77	16
Cu_2^+	126:128:130	0.47: 0.43: 0.11	45	9
$CuCO_2^+$	107:109	0.67: 0.33	43	8
Cu^+	63:65	0.67: 0.33	43	8
Difluoroacetate				
$Cu_2(F_2CHCO_2)_2^+$	316:318:320	0.48: 0.42: 0.10	509	20
$Cu_2F_2CHCO_2^+$	221:223:225	0.48: 0.41: 0.11	2583	100
Cu_2F^+	145:147:149	0.47: 0.43: 0.11	1545	60
Cu_2O^+	142:144:146	0.48: 0.43: 0.10	547	21
Cu_2^+	126:128:130	0.48: 0.42: 0.10	954	37
$CuCO_2^+$	107:109	0.69: 0.31	162	6
$CuCO^+$	91:93	0.68: 0.32	97	4
Cu^+	63:65	0.69: 0.31	1683	65
Trifluoroacetate				
$Cu_2(F_3CCO_2)_2^+$	352:354:356	0.46: 0.43: 0.11	87	13
$Cu_2(CF_3CO_2)CO_2^+$	283:285:287	0.48: 0.42: 0.10	50	7.4

TABLE VII continued

$Cu_2CF_3CO_2^+$	239:241:243	0.48: 0.42: 0.10	674	100
Cu_2F^+	145:147:149	0.47: 0.43: 0.10	437	65
Cu_2O^+	142:144:146	0.47: 0.42: 0.11	120	18
Cu_2^+	126:128:130	0.47: 0.43: 0.10	185	27
$CuCO_2^+$	107:109	0.69: 0.31	106	16
Cu^+	63:65	0.66: 0.34	465	69
Benzoate				
$Cu_2(\phi CO_2)_2^+$	368:370:372	0.46: 0.44: 0.11	591	100
$Cu_2(\phi CO_2)C_6H_5^+$	324:326:328	0.47: 0.43: 0.10	197	33
$Cu_2(C_6H_5)_2^+$	280:282:284	0.47: 0.42: 0.11	197	33
$Cu_2\phi CO_2^+$	247:249:251	0.48: 0.41: 0.11	63	11
$Cu_2C_6H_5^+$	203:205:207	0.47: 0.44: 0.10	554	94
Cu_2H^+	127:129:131	0.49: 0.41: 0.10	22	3.7
Cu_2^+	126:128:130	0.49: 0.41: 0.10	22	3.7
$Cu(C_6H_5)_2^+$	217:219	0.67: 0.33	228	39
$CuC_6H_5^+$	140:142	0.66: 0.34	73	12
Cu^+	63:65	0.69: 0.31	144	24
p-F-benzoate				
$Cu_2(FC_6H_4CO_2)_2^+$	404:406:408	0.46: 0.43: 0.10	563	88
$Cu_2(FC_6H_4CO_2)FC_6H_4^+$	360:362:364	0.48: 0.41: 0.11	169	26
$Cu_2(FC_6H_4)_2^+$	316:318:320	0.45: 0.42: 0.13	115	18
$Cu_2FC_6H_4CO_2^+$	265:267:269	0.48: 0.42: 0.11	132	21
$Cu_2FC_6H_4^+$	221:223:225	0.48: 0.43: 0.10	643	100
Cu_2F^+	145:147:149	1.00: 0.89: ?	140	22
Cu_2^+	126:128:130	1.00: 0.77: ?	39	6
$Cu(FC_6H_4)_2^+$	253:255	0.69: 0.31	90	14
Cu^+	63:65	0.76: 0.24	384	60
Pentafluorobenzoate				
$Cu_2(F_5C_6CO_2)_2^+$	548:550:552	0.46: 0.42: 0.12	108	-
o-Cl-benzoate				
$Cu_2(ClC_6H_4CO_2)_2^+$	436:438:440: 442:444	0.26: 0.40: 0.24: 0.08: 0.02	62	-

TABLE VII continued

p-Cl-benzoate				
$Cu_2(ClC_6H_4CO_2)_2^+$	436:438:440:442:444	0.27: 0.42: 0.24: 0.07: 0.01	654	58
$Cu_2(ClC_6H_4CO_2)ClC_6H_4^+$	392:394:396:398	0.27: 0.42: 0.24: 0.06	332	29.5
$Cu_2(ClC_6H_4)_2^+$	348:350:352:354	0.27: 0.39: 0.26: 0.07	245	21.8
$Cu_2ClC_6H_4^+$	237:239:241:243	0.36: 0.45: 0.16: 0.04	1125	100

Metastable peaks were observed in some of the cuprous carboxylate spectra. They are listed in Table VIII. As explained in Chapter Five EQN. II, a metastable peak appears in a mass spectrum at a mass given by

$$M^* = \frac{Md^2}{Mp}$$

where Mp is the mass of the parent ion in mass units
Md is the mass of the daughter ion in mass units

Since both the parent ion and daughter ion are present in the mass spectrum it is possible to calculate the expected position of the metastable peak for every possible transition. All the possible combinations in forming the metastable peaks were computed with the aid of a IBM 360 computer using FORTRAN IV language. The program is in the APPENDIX. The computer prints out the calculated metastable peaks in numerical order. When the experimental value is compared with the calculated values the parent and daughter ion for each metastable transition can readily be discovered. Since metastable peaks are broad, the experimental values listed in TABLE VIII give the range of the diffuse peaks and the approximate mass where the maximum intensity was observed.

TABLE VIII

Metastable Peaks in the Cuprous Carboxylate Mass Spectra

Metastable ion observed (in mass units)	Metastable ion calculated (in mass units)	Parent	Daughter	Fragmentation
n-butyrate				
246→251	250.58	304	276	$Cu_2(C_3H_7CO_2)_2^+$
	248.59	302	274	
Max ∿247	246.61	300	272	↓-CO
				$Cu_2(C_3H_7CO_2)C_3H_7O^+$
150→155	154.89	304	217	$Cu_2(C_3H_7CO_2)_2^+$
	153.06	302	215	
Max ∿152	151.23	300	213	↓-$C_3H_7CO_2$
				$Cu_2C_3H_7CO_2^+$
∿60	60.56	88	73	$C_3H_7CO_2H^+ \xrightarrow{-CH_3} C_2H_4CO_2H^+$
iso-butyrate				
60.5	60.56	88	73	$(CH_3)_2CHCO_2H^+ \xrightarrow{-CH_3} CH_3CHCO_2H^+$
39	39.09	43	41	$(CH_3)_2CH^+ \xrightarrow{-CH_2} CH_3CHCH^+$
Difluoroacetate				
93→98	98.67	225	149	$Cu_2F_2CHCO_2^+$
	96.60	223	147	
Max ∿96	95.13	221	145	↓-$FCHCO_2$
				Cu_2F^+
Benzoate				
285→290	289.20	372	328	$Cu_2(\phi CO_2)_2^+$
	287.23	370	326	
Max ∿287	285.26	368	324	↓-CO_2
				$Cu_2(\phi CO_2)C_6H_5^+$
240→247	245.90	328	284	$Cu_2(\phi CO_2)C_6H_5^+$
	243.94	326	282	
Max ∿243	241.98	324	280	↓-CO_2
				$Cu_2(C_6H_5)_2^+$

TABLE VIII continued

185→172	169.36	372	251	$Cu_2(\phi CO_2)_2^+$
	167.57	370	249	↓ $-\phi CO_2$
Max ∿168	165.79	368	247	$Cu_2\phi CO_2^+$
other possibilities for this range				
	170.71	251	207	$Cu_2\phi CO_2^+$
	168.78	249	205	↓ $-CO_2$
	166.83	247	203	$Cu_2C_6H_5^+$
	170.07	282	219	$Cu_2(C_6H_5)_2^+$
	168.88	284	219	↓ $-Cu$
	168.17	280	217	
	166.98	282	217	$Cu(C_6H_5)_2^+$
90.5	92.07	219	142	$Cu(C_6H_5)_2^+$
	90.32	217	140	↓ $-C_6H_5$
				$CuC_6H_5^+$
56.5	57.40	106	78	ϕCO^+
	56.47	105	77	↓ $-CO$
				$C_6H_5^+$
p-F-benzoate				
318→325	324.74	408	364	$Cu_2(FC_6H_4CO_2)_2^+$
	322.77	406	362	↓ $-CO_2$
Max ∿321	320.79	404	360	$Cu_2(FC_6H_4CO_2)FC_6H_4^+$
275→283	281.32	364	320	$Cu_2(FC_6H_4CO_2)FC_6H_4^+$
	279.35	362	318	↓ $-CO_2$
Max ∿278	277.38	360	316	$Cu_2(FC_6H_4)_2^+$
206→213	209.98	263	235	$(FC_6H_4CO)_2O^+$
	208.99	262	234	↓ $-CO$
Max ∿209				$(FC_6H_4)_2CO_2^+$
182→190	188.20	269	225	$Cu_2FC_6H_4CO_2^+$
	186.25	267	223	↓ $-CO_2$
Max ∿186	184.31	265	221	$Cu_2FC_6H_4^+$

TABLE VIII continued

108	108.06	140	123	$FC_6H_4CO_2H^+$
				↓ -OH
				$F\phi CO^+$
73.5	73.37	123	95	$FC_6H_4CO^+$
				↓ -CO
				$F\phi^+$
59	59.21	95	75	$FC_6H_4^+$
				↓ -HF
				$C_6H_3^+$
p-Cl-benzoate				
350→359	358.38	442	398	$Cu_2(ClC_6H_4CO_2)_2^+$
	356.40	440	396	
Max ∿354	354.41	438	394	↓ $-CO_2$
	352.44	436	392	$Cu_2(ClC_6H_4CO_2)ClC_6H_4^+$
308→316	314.86	398	354	$Cu_2(ClC_6H_4CO_2)ClC_6H_4^+$
	312.89	396	352	
Max ∿311	310.91	394	350	↓ $-CO_2$
	308.94	392	348	$Cu_2(ClC_6H_4)_2^+$
238→247	244.63	298	270	$(ClC_6H_4CO)_2O^+$
	242.65	296	268	
	240.67	294	266	↓ -CO
				$(ClC_6H_4)_2CO_2^+$
123→127	124.65	155	139	$ClC_6H_4CO_2^+$
	126.63	157	141	
Max ∿124				↓ -O
				$ClC_6H_4CO^+$
88.8	88.64	139	111	$ClC_6H_4CO^+$
	90.5	141	113	
				↓ -CO
				$ClC_6H_4^+$
50.8	50.67	111	75	$ClC_6H_4^+$
	50.22	112	75	
	49.77	113	75	↓ -HCl
				$C_6H_3^+$
33	33.00	128	65	$ClC_6H_4OH^+$
				↓ -ClCO?
				$C_5H_5^+$

From the results in Chapter Seven, it is possible to devise two types of fragmentation scheme for the new series of cuprous carboxylates depending upon whether the ligand is the anion of an aliphatic or aromatic carboxylic acid. FIGURES VI and VII show the patterns of the two types of fragmentation scheme. Although a complete fragmentation scheme cannot be postulated without ambiguity, some rationalization of the spectra seems possible. It appears to be more convenient to use the concept of molecular orbitals than the valence bond structures in an attempt to rationalize the spectra.

The mass spectra indicate that cuprous carboxylates are dimers. Though their structures have not been experimentally determined, an analogy can be drawn from the structure of dimeric silver perfluorobutyrate[42] which is shown in FIGURE VIII. Thus a probable structure for the cuprous carboxylates is

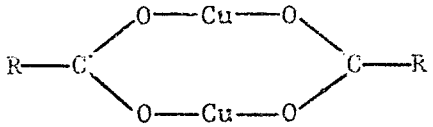

in which R represents an alkyl or aryl group. In the silver perfluorobutyrate, the distance between the silver atoms is 2.90 Å which is almost the same distance between the silver atoms in metallic silver (2.889 Å). If cuprous carboxylate behaves similarly the copper-copper distance will be about 2.56 Å. If the O-O separation is about 2.08 Å as for the silver complex, then the OCuO bond angle will be slightly $<180^{\circ}$. The OAgO angle is about 160°. It has been suggested[43,44] for Cu^{I} and Ag^{I} complexes in which 2-fold coordination occurs, that due to a relatively small energy difference between the filled 3d orbitals and the unfilled 4s and 4p orbitals extensive hybridization is permitted among them (FIGURE IX). The electron pair initially in the d_{z^2} orbital occupies ψ_1 giving a circular region of relatively high electron density from which ligands are somewhat repelled and regions above and below this ring in which the electron density is relatively low. Ligands are attracted to these regions. By further mixing of ψ_2 with the p_z orbital, two hybrid orbitals Φ_1 and Φ_2, suitable for forming a pair of

FIGURE VI

Fragmentation Scheme for Cuprous Alkylcarboxylates

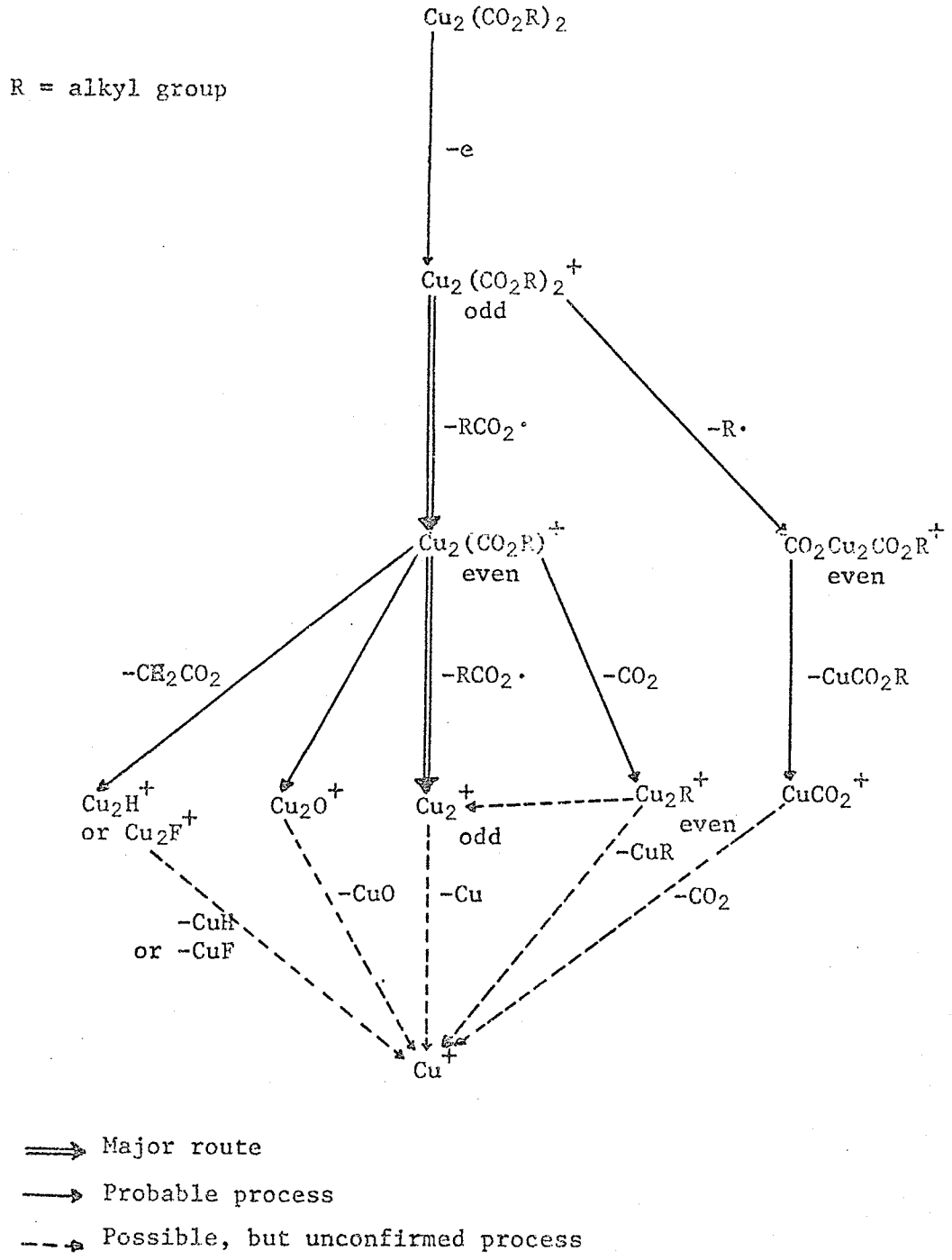

FIGURE VII

Fragmentation Scheme for Cuprous Arylcarboxylates

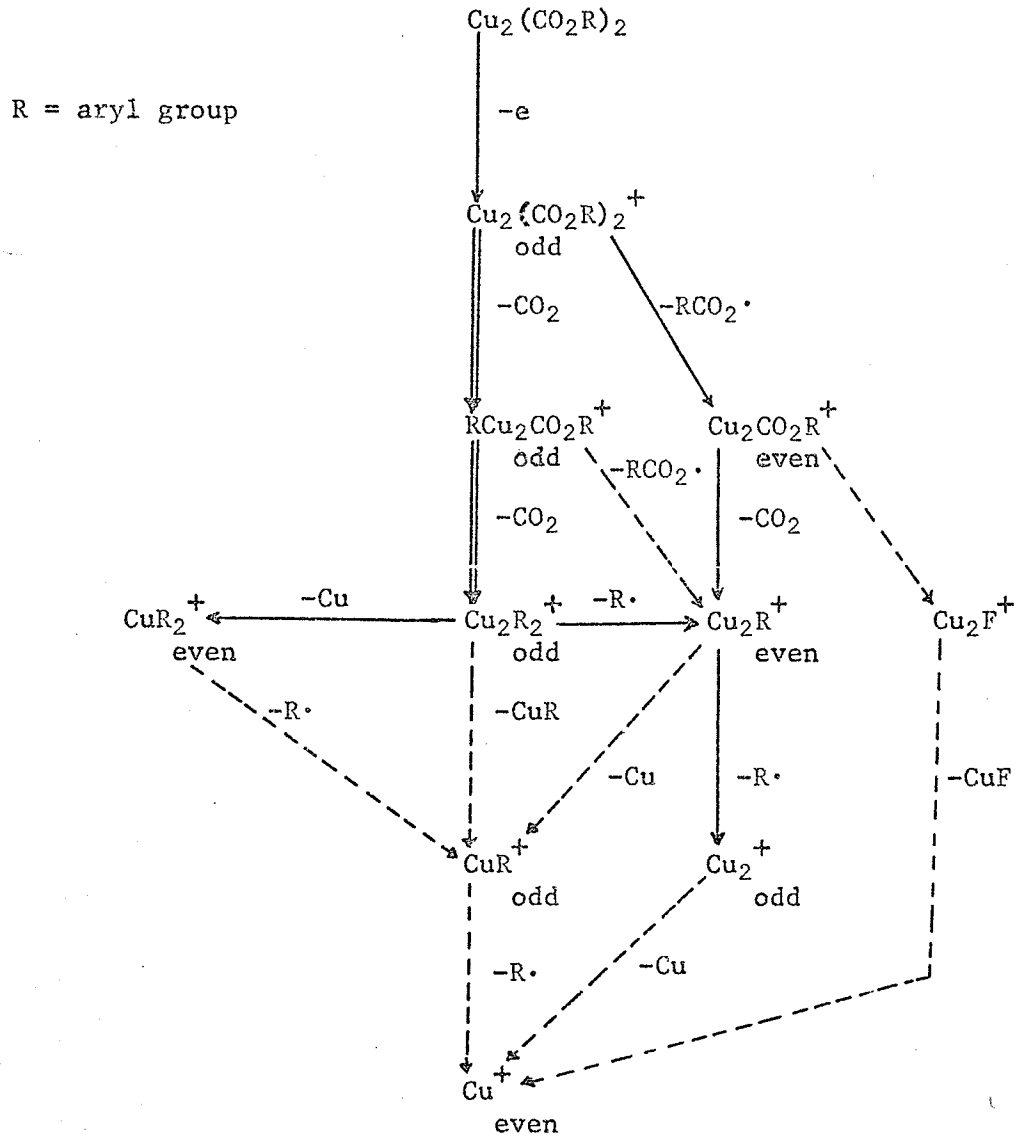

SILVER PERFLUORO-BUTYRATE

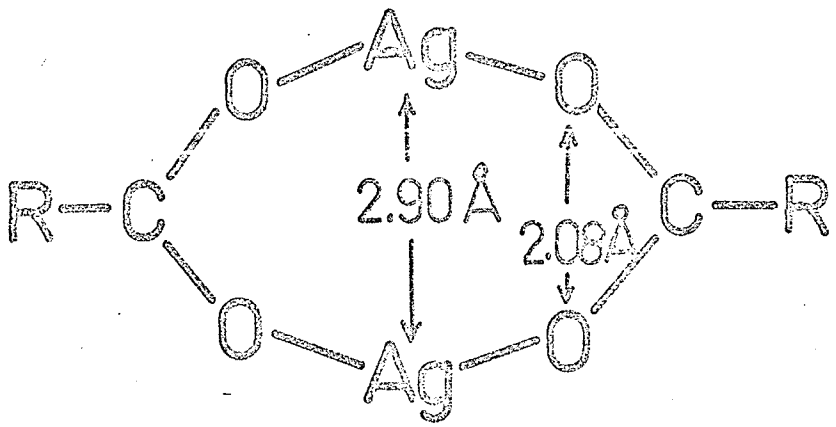

R = $CF_2CF_2CF_3$

Ag–Ag (metal) = 2.889 Å

FIGURE VIII

A schematic diagram of the structure of silver perfluorobutyrate

FIGURE IX

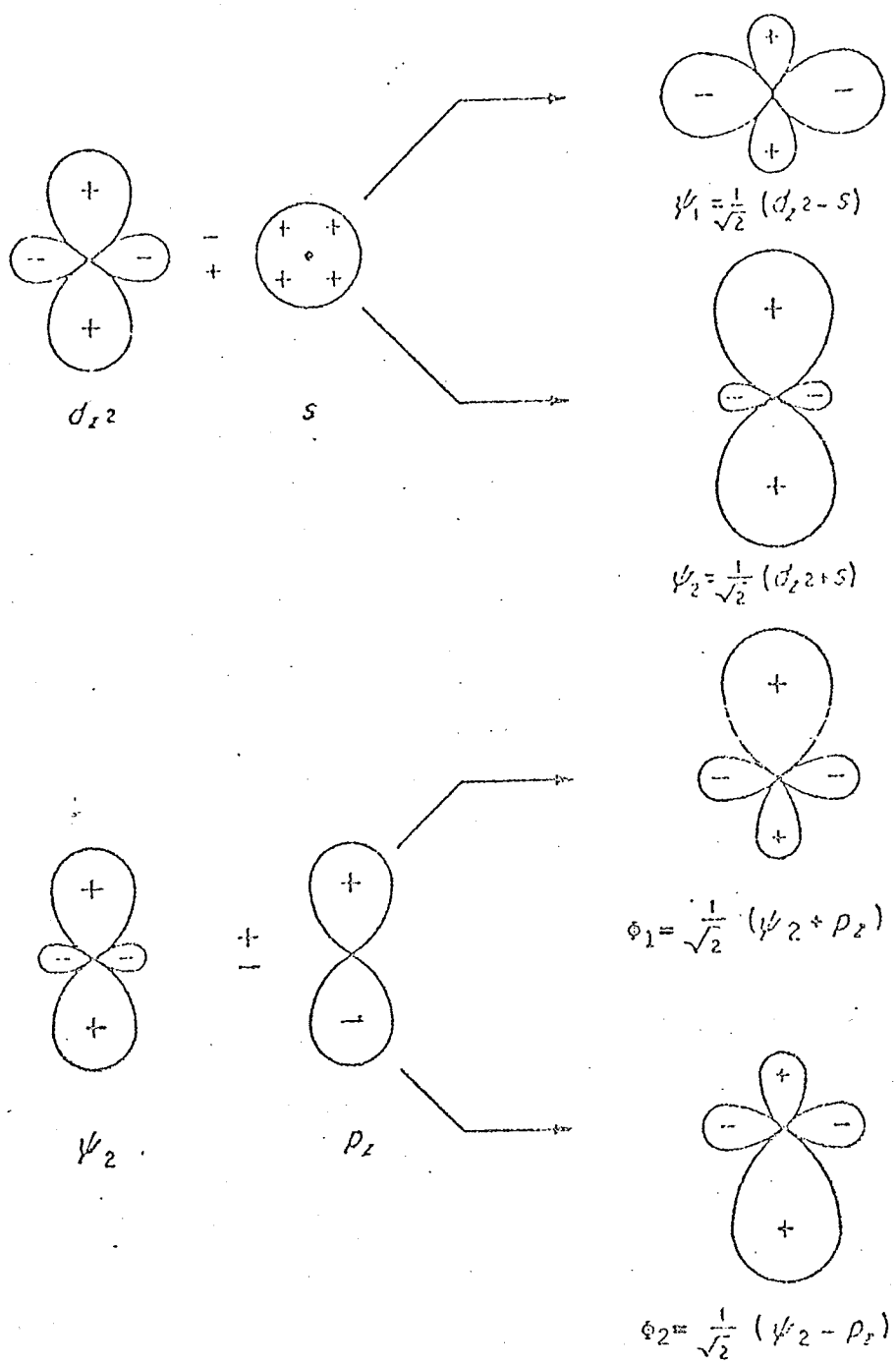

Sketches showing the hybrid orbitals formed from a d_z^2 and a s orbital, ψ_1 and ψ_2, and the hybrids which can be formed from ψ_2 and a p_z orbital. In each sketch the z axis is vertical and the actual orbital is the figure generated by rotating the sketch about the z axis.

linear covalent bonds can be formed. Thus in cuprous carboxylate the the hybrid orbitals Φ_1 and Φ_2 of the copper atoms are used as acceptors for the lone pair of oxygen electrons. The copper-copper distance indicates that there may be some sort of interaction between the two metal atoms. In the case of the silver complex, the diamagnetism of the crystal shows that the bridging structure does not involve unpairing of electrons in the silver core[42]. As stated the electron density is high in a circular region around the copper atom. Since these high electron density regions tend to repel each other, no bonding is expected between the copper atoms in the dimeric cuprous carboxylate molecule. Little electron delocalization is to be expected between the copper atoms and the rest of the molecule because oxygen does not have any vacant low lying acceptor orbitals. In the silver complex the C-O bond lengths are all equal and normal for a carboxyl group indicating delocalization of electrons over the carbon and two oxygen atoms. The same situation probably holds for the cuprous carboxylate dimers.

Two possibilities seem most likely for the formation of the molecular ion, viz. the electron can be removed from a molecular orbital having mainly metal character, i.e. a non-bonding d orbital, or the electron can be removed from a molecular orbital having mainly ligand character, i.e. the π orbital of the carboxyl group. The first possibility would place most of the positive charge on one of the copper atoms but this can be reduced (by partial delocalization of the π electrons from the carboxyl group onto the copper atom). The second possibility would place the positive charge on the carboxyl group. Thus, the molecular ion could be represented by either (a) or (b).

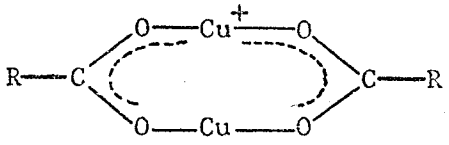

(a)

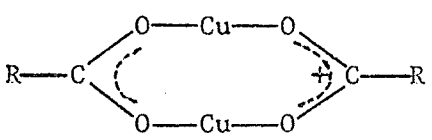

(b)

It has been possible to obtain a sufficient number of cuprous

carboxylate dimers to study the influence of the R group on the mass spectra. It is to be expected that electron withdrawing substituents would destabilize the molecular ion, and electron releasing substituents would stabilize the molecular ion. Aryl substituents should be particularly effective in this respect. Thus, the relative intensity of the molecular ion is lowest for R = CF_3 and CHF_2 and highest for R = Phenyl.

A dominant feature of mass spectra in general is the tendency towards formation of even-electron ions, i.e. ions in which there are no unpaired electrons. Since most neutral molecules are even-electron species it follows that their molecular ions will be odd-electron species. Even electron ions can be formed by elimination from these ions of odd-electron neutral species (radicals). Exceptions to this generalization occur when very stable even-electron neutral molecules, such as H_2O, CO, CO_2 can be eliminated.

Elimination of R· or RCO_2· from the molecular ion leads to species which may be designated as (c) and (d) respectively.

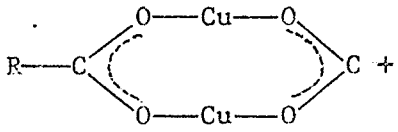

(c)

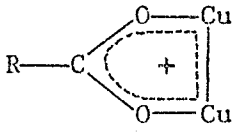

(d)

Formation of (c) occurs much less readily than (d). (c) was observed (at low relative intensity) in only three spectra. (d) is the most abundant ion in the spectrum when R is an alkyl group, suggesting that it is a stable species. The structure shown involves interaction between the copper atoms. Such interaction would probably stablize the ion. This interaction between the two copper atoms in the ion can be rationalized in the following manner. The $3d_{z^2}$, empty 4s and $4p_y$ orbitals of each copper atom can form the following normalized orthogonal hybrid orbitals:

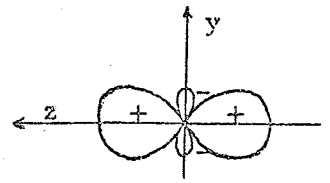

$$\Phi_a = \frac{1}{\sqrt{12}}(2s + 2\sqrt{2}\, d_z^2)$$

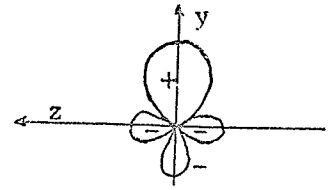

$$\Phi_b = \frac{1}{\sqrt{12}}(2s - \sqrt{2}d_z^2 + \sqrt{6}p_y)$$

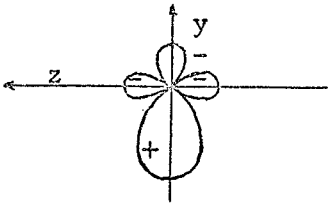

$$\Phi_c = \frac{1}{\sqrt{12}}(2s - \sqrt{2}d_z^2 - \sqrt{6}p_y)$$

The directions of the axes are indicated as follows,

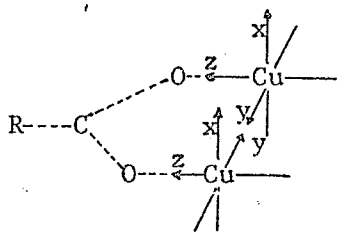

The z axis lies along the CuO bond and the y axis lies in the Cu-Cu direction. A non-bonding pair of electrons occupies Φ_c which points away from the other copper atom. Φ_a acts as the acceptor for the donor pair of electrons from the oxygen atom. The Φ_b orbitals of the copper atoms overlap with each other and form a covalent bond if electron promotion from a 3d orbital occurs. The d_{xz} orbitals can be used to form a δ bond between the copper atoms. Furthermore the d_{xz} orbitals have the same symmetry with respect to reflection in the molecular plane (i.e. antisymmetric) as the pπ system of the carboxylate group. The excess electronic charge on the copper atoms can be transferred back to the carboxylate group via the d_{xz} orbital and the pπ system. Such interaction would tend to stabilize the species. This ion is probably formed by the departure of $RCO_2^{\cdot}$ radical from the parent molecular ion. The positive charge thus left is most likely shared by the

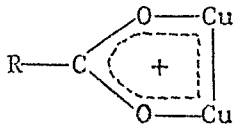

ring. Support for bond formation between the copper atoms is given by the presence of other ions containing two copper atoms

in the spectra, and in which copper-copper bond formation cannot be denied. Furthermore, the relative intensities of species containing a single copper atom is low. Further fragmentation of (d) is not extensive, except when R = CF_3 or CHF_2. This may be because the electronegative substituent has a destabilizing effect, as noted above, and because ions can be formed in which there are strong copper-fluorine bonds formed by migration of fluorine from the ligand to the copper-atom. The migration of fluorine in fluorine containing compounds has been mentioned earlier (Chapter Five). Cu_2F^+ ions were observed in both cases for R = CF_3 and CHF_2. When R is an aryl group the most important fragmentations of the molecular ion involve successive losses of CO_2, a stable even-electron molecule, and migration of the aryl group to one of the copper atoms. This leads to ions which are formally odd-electron species. Apparently the aryl group is able to give sufficient stabilization to these ions by virtue of its delocallized π system. The odd-electron species $Cu_2R_2^+$ can eliminate either a copper atom or the aryl radical (the first process is supported by the presence of a metastable peak in the spectrum of cuprous benzoate) to give the even-electron ions Cu_2R^+ and CuR_2^+. The former species forms the base peak in these spectra.

PART THREE

THERMOGRAVIMETRIC STUDIES

In Part Two eleven cuprous carboxylates have been identified from the mass spectra. Since it was not possible to heat the cupric carboxylates above 300°C in the mass spectrometer, the thermal decomposition processes above this temperature were left unexamined. It is the purpose of this part of the study to investigate the thermal decomposition of cupric carboxylates thermogravimetrically up to a temperature of 500°C or higher. It is hoped that the existence of cuprous carboxylates other than the eleven mentioned in Part Two can be deduced from the thermogravimetric analysis results. If cuprous carboxylate is an intermediate stable species in the process of thermal decomposition of the cupric salt then one would expect to be able to observe a plateau in the thermograms. Charbonnier and his co-workers[10] interpreted their T.G.A. for cupric fluorobenzoates and p-chlorobenzoate by suggesting that the cuprous salts might be the stable species which caused the appearence of inflexion in the graphs. If such evidence can be observed in the T.G.A. studies, it will help to determine the more accurate temperatures at which cuprous carboxylates are formed under the conditions of the T.G.A. experiments. The T.G.A. of some of the cupric carboxylates, including some of those that are known to have cuprous salts as decomposition products from the mass spectrometric study in Part Two, have been examined by other workers[2,6-10] but only in the cases of cupric acetate[2], fluorobenzoates and p-chlorobenzoate[10] specific mention of the cuprous salts were made. A T.G.A. study of the series of cupric carboxylates listed in TABLE I will help to evaluate the T.G.A. method of investigation.

The thermogravimetric method of analysis (T.G.A.) was started by Honda[45] in about 1915. Only since about 1947 has this technique been widely accepted after the application of the Chevenard thermobalance to problems in analytical chemistry by Duval[46]. Basically thermogravimetry is a technique whereby a sample is continuously weighed as it is heated at a constant, preferably linear rate of temperature increase. The resulting weight change against temperature curve, or thermogram, so obtained gives information concerning the thermal stability and composition of the original sample, its intermediate compounds and the composition of the residue.

To illustrate the principle of T.G.A., consider the thermogram of a hypothetical compound, $MX_2 \cdot 6H_2O$ as given in FIG. X[47]. It is assumed that the sample is heated in an air atmosphere at a reasonable heating rate of $5^{o}C$ / min. From A to B on the curve, the sample is stable in

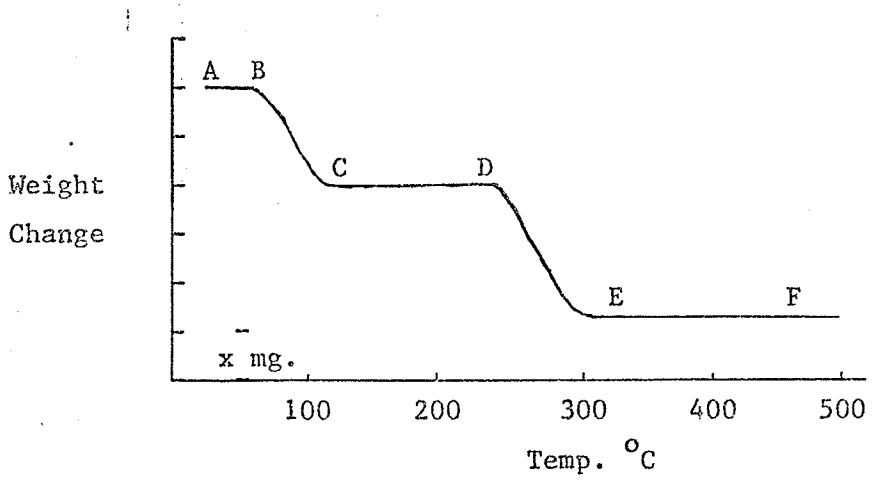

FIGURE X THERMOGRAM OF A HYPOTHETICAL SAMPLE $MX_2 \cdot 6H_2O$

that there is no change in weight. At B, the sample begins to lose weight, the process being completed at C. The first weight loss, it is assumed, is due to the evolution of the six moles of water per mole of sample, thus giving the anhydrous compound, MX_2. In actual practice, however, either the gaseous evolved product would have to be identified

by analysis or the sample removed at C and subjected to analysis. Most interpretations of the curve are subjective in that if the weight change, BC, corresponds to that expected for the loss of the water molecules, then this is the reaction that is assigned to the transition. The latter method is more rapid, but also subject to false interpretation. From C to D, the compound MX_2 is stable and gives a horizontal plateau in the curve. At D, the sample decomposes further, giving another plateau from E to F which, it is assumed, has the composition of the oxide, MO. In an air atmosphere, MO could easily be formed. Again, distance DE would correspond to the weight loss expected for the decomposition reaction. The curve is quantitative in that the compound stoichiometry can be calculated at any temperature. The utility of the technique lies in the simplicity of the method and the information obtained from a single measurement. However it is not unusual to use complimentary techniques such as, X-ray diffraction, infrared absorption spectroscopy, differential thermal analysis, gas chromatography and mass spectrometry to interpret the thermogram.

There are a number of factors that affect the thermogram of a sample. Some of them have been studied and discussed by several authors[47-51]. The factors fall into two categories:-

1. Instrumental factors
   - (a) Furnace heating rate
   - (b) Recording or chart speed
   - (c) Furnace atmosphere
   - (d) Geometry of sample holder and furnace
   - (e) Sensitivity of recording mechanism
   - (f) Composition of sample container
2. Sample characteristics
   - (a) Amount of sample
   - (b) Solubility of evolved gases in sample
   - (c) Particle size
   - (d) Heat of reaction
   - (e) Sample packing
   - (f) Nature of the sample
   - (g) Thermal conductivity

Many of the above factors such as sample holder geometry, recording speed, balance sensitivity and sample container air buoyancy are fixed with any given thermobalance. Other factors such as sample particle size, packing, the solubility of evolved gases in the sample, furnace convection currents and electrostatic effects are variable and difficult to reproduce. Some of the more general factors will be discussed.

1.(a) Heating rate. The apparent decomposition temperatures on a thermogram decrease with a decrease in heating rate. But a decrease in heating rate does not affect a sample that undergoes a fast irreversible reaction. The detection of intermediate compoundes is also dependent on the heating rate employed. At fast heating rates, the curves may not reveal intermediate curve breaks.

1.(b)Recording or Chart speed. The effect of chart speed on the recording of the curves of various reaction is quite pronounced. In Figure XI[47] (a), for a slow thermal decomposition reaction a fast chart speed flattens the curve. In Fig. XI (b), for a slow reaction followed by a rapid one, a fast chart speed shows more resolution. A similar effect occurs in Fig. XI (c) for a fast reaction followed by a slow one.

1.(c) Effect of furnace atmosphere. Variations in atmosphere are particularly important because the sample under investigation evolves a gas or reacts with a gas from the atmosphere surrounding it. In the former case, for an increase in concentration of the ambient gas the rate of decomposition will decrease. In the latter case, a change of furnace atmosphere may change the course of decomposition entirely.

2.(a) Amount of sample. Heat for the thermal decomposition has to be transfered through the sample. Thus thermograms of different shapes may be obtained for different amounts of the same sample especially when there is a big difference in the amount.

2.(c) Particle size. In general, a decrease in particle size of the sample lowers the temperature at which thermal decomposition reactions are completed.

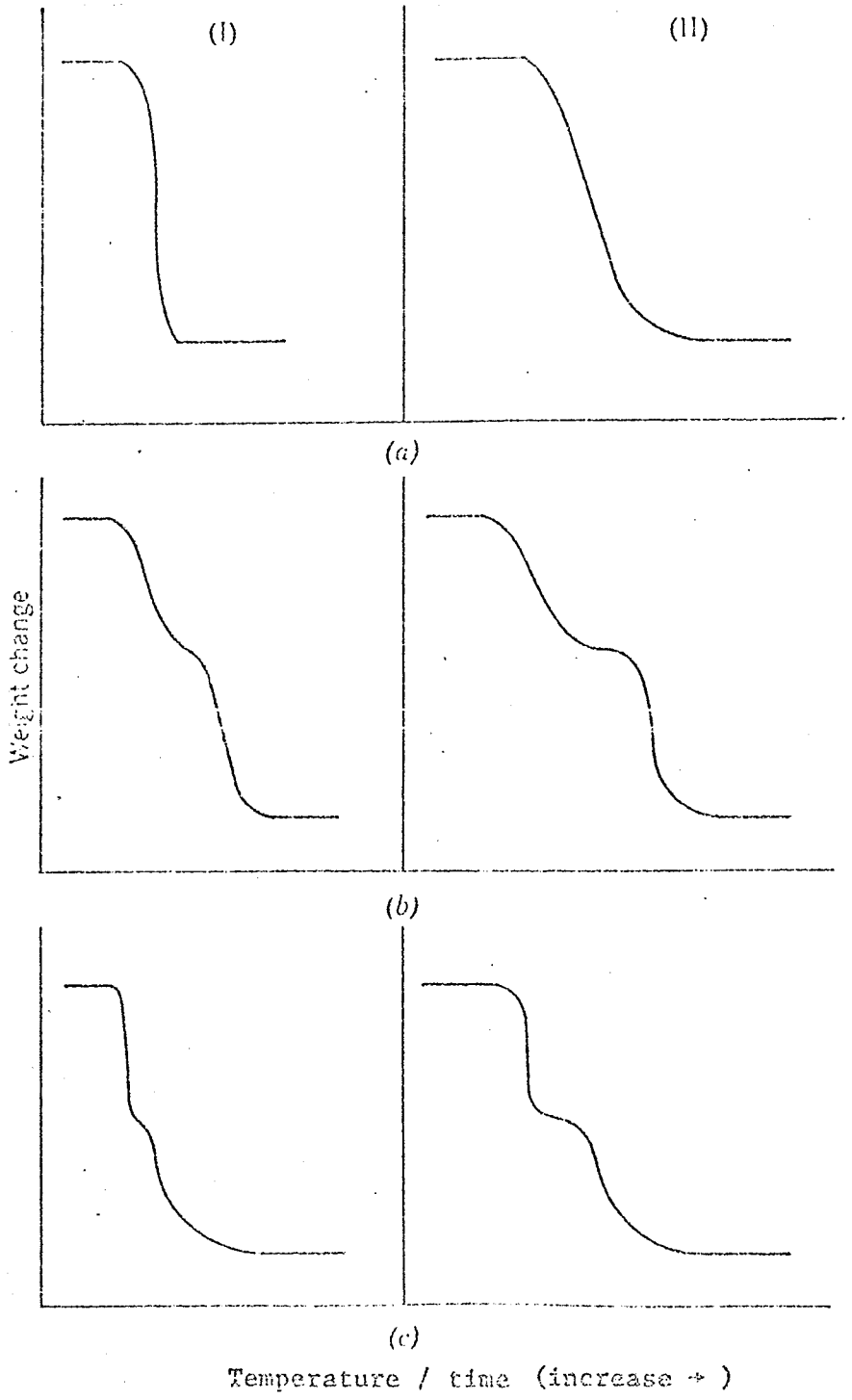

FIGURE XI

Effect of chart speed upon the shapes of weight-loss curves; (I) slow chart speed; (II) fast chart speed.

2.(d) The Heat of Reaction. The heat of reaction will affect the difference between the sample temperature and furnace temperature, causing the sample temperature to lead or lag the furnace temperature depending on whether the heat effect is exothermic or endothermic.

There are a number of possible sources of error that lead to inaccuracies in the thermograms. They are:

(1) Sample container air buoyancy
(2) Furnace convection currents and turbulence
(3) Random fluctuations in the recording mechanism and balance
(4) Furnace induction effects
(5) Electrostatic effects on balance mechanism
(6) Environment of the thermobalance
(7) Condensation on sample support
(8) Temperature measurement and calibration
(9) Weight calibration of recording balance
(10) Chart paper rulings
(11) Reaction of the sample with sample container

Accurate thermograms require that corrections be made for these errors. Many of these errors are interrelated and cannot be considered separately. Some of them can be eliminated by proper thermobalance design, construction and location in the laboratory. Others, such as air buoyancy and convection currents are different for each particular instrument. The effect of air buoyancy is a function of heating rate, load and temperature whereas in the case of furnace convection currents and turbulence their effect is largely dependent on the size and shape of the sample container. Corrections to these factors can probably be estimated by calibrations. One major source of error is in the temperature of the sample which is usually taken as the temperature measured by a thermocouple above or below the sample container. Though calibration helps to correct the sample temperature, the accurate temperature measurement is further complicated by the nature of the decomposition reaction (exothermic or endothermic) and the sample conductivity.

A thermobalance is used in T.G.A. Basically it consists of a recording balance, a furnace, a furnace programmer and a recorder. The instrument used in this study was a Perkin-Elmer TGS-1 thermobalance 219-0161-60Hz. The Cahn R G electrobalance is a part of the Perkin-Elmer instrument. The recorder used was Texas Instrument Inc. Servo/Riter I Model WD, S/N 2195.

The Cahn balance is a null-point instrument in which a light source photocell is the detector and an electromagnetic D'Arsonval movement supplies the restoring force. A schematic diagram of the balance is shown in FIGURE XII. Loop A has a range from 0 to 200 mg.; loop B from 5 to 1000 mg.; and loop C is used to tare the other loops. Any weight change causes the balance beam to move. This motion is detected by the change in photocell voltage caused by the movement of the shutter attached to the beam which interrupts the light source. The photocell voltage is amplified and then applied to the coil attached to the beam. The coil is in a magnetic field and current passing through it exerts a movement on the beam, instantaneously restoring it to the null position. The coil current is thus a measure of sample weight. The Cahn balance is mounted in a vacuum bottle. The lowest pressure permissible is 10 mm. Hg.

The furnace consists of a platinum resistance wire in a hollow ceramic cylinder, which heats the sample according to the temperature program selected. The furnace acts as both heater and temperature sensor. When in use, it is supported from below inside a hangdown tube on the vacuum bottle.

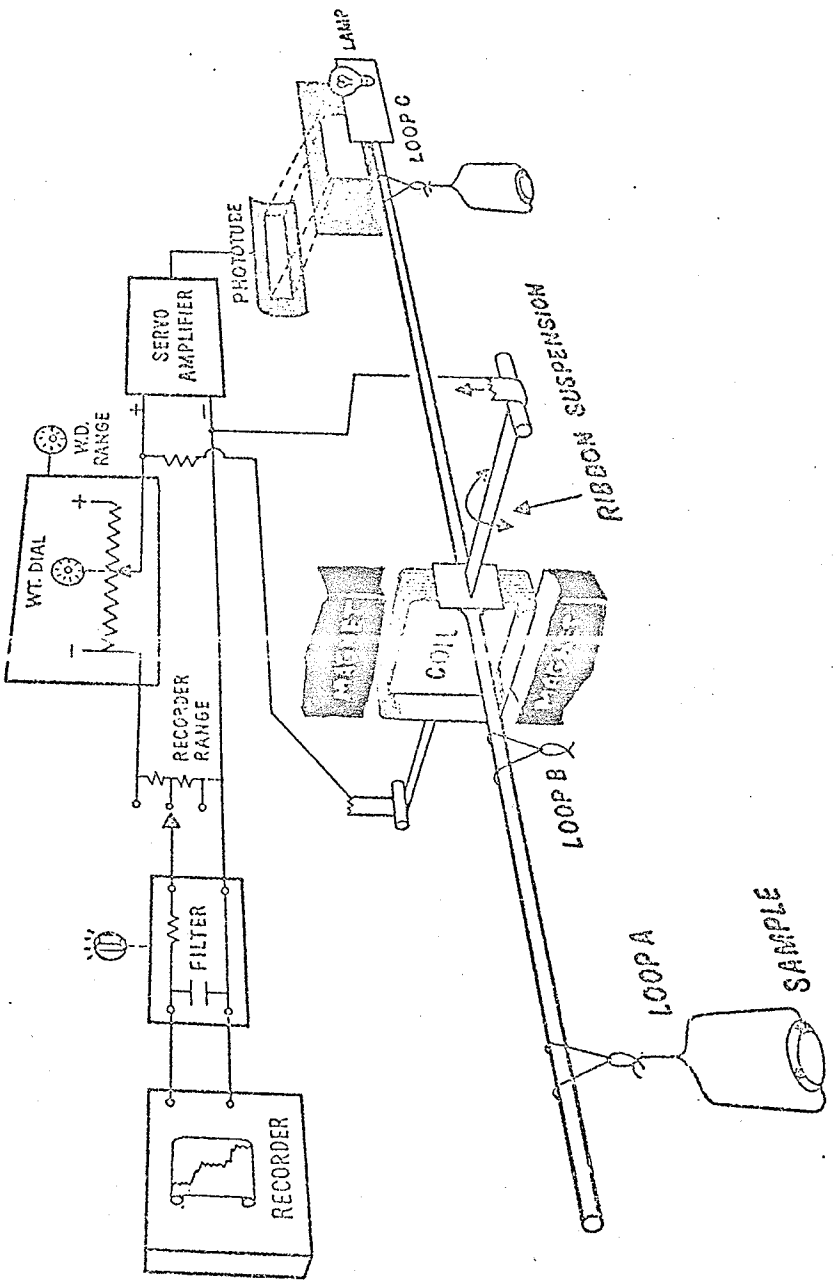

FIGURE XII

Schematic diagram of Calr. RG electrobalance

The T.G.A. study of the cupric carboxylates was done in vacuum as well as in air. Due to the number of factors and possible sources of error (discussed earlier in Chapter Ten) that affects a thermogram, the following procedures were used in an attempt to obtain accurate thermograms:

(1) Sample Handling. In order to compare the thermograms, about the same amount of sample was used, about 1 mg. for every sample. The thermograms are reported as percentage weight loss so that the amount of samples used did not have to be exactly 1 mg. To minimise the difference in sample particle size, the samples were ground in a mortar with a pestle until they were in a powder form with no visible difference between them, except in the case of the hygroscopic cupric trifluoroacetate which could not be handled in air. Uniformity in packing the sample was attempted by gently pressing the powder sample in the sample pan with a spatula. The samples were spread out as evenly as possible in the sample pan. The same size and shape of sample pans were used. They were made of platinum to avoid possible reaction of the sample with the sample pan and the pan with the furnace atmosphere.

(2) Weighing the samples. The Cahn electrobalance was calibrated according to the manual so that during the course of the experiments a full scale deflection on the recorder represented a weight of 1 mg. of sample. In order to account for the weight loss or gain due to air buoyancy and other various factors on the sample pan, a thermogram of the sample pan alone was obtained before every sample run and under the same conditions as the sample run (heating rate, pressure, atmosphere etc.). The thermogram should be a straight line, that is no weight gain or loss should be apparent on the chart record. Thus any deviation of the chart record from the base line for the dummy run was added to or subtracted from the chart record of the sample run to obtain the thermogram of the sample.

(3) Temperature Calibration. In general, in T.G.A. it is difficult to know the true temperature of the sample because the temperature

measuring device is not in contact with the sample. In order to obtain as accurate a temperature as possible a temperature calibration utilizing the Curie points of a number of metals and alloys was done according to the manual under the same conditions as the sample runs. Basically, a sharp change in apparent weight occurs when certain metals or alloys are heated in a magnetic field as their temperature passes through their Curie temperatures, which are known accurately. The thermogram obtained in such a manner was used for the temperature correction of the thermogram of the samples. However one must realize that even after such a procedure the temperature of the sample was assumed to be the same as that of the metals or alloys during the course of heating.

(4) General Procedure. The preceding three procedures are descriptions of individual parts of the experiments. The experiments were performed according to the following sequences. The conditions under which the experiments were done are listed in TABLE IX.

Atmosphere	Air	Vacuum
Heating Rate	10°C/min.	10°C/min.
Chart Rate	12 in./hr.	12 in./hr.
Pressure	Atmosphere	10 mm.Hg

TABLE IX

CONDITIONS IN T.G.A. EXPERIMENTS

First, the thermogram of the sample pan was obtained under the appropriate conditions with the base line set at the center of the chart paper so that both weight gain or loss could be detected. Then the temperature calibration was made with the following metal and alloys in nitrogen (oxidation of the metal or alloys may take place in air at high temperature); Alumel (Curie pt. 158°C), Mumetal (390°C), Nicroseal (445°C), Perkalloy (598°C) and Iron (786°C); and in vacuum the following were used:Alumel (158°C), Nickel (350°C), Nicroseal (445°C) and Perkalloy (598°C).

The chart recorder was then zeroed with no sample in the sample pan. The sample was next loaded into the sample pan until there was a full scale deflection (1 mg.) or an almost full scale deflection of the recorder. Precaution was taken to make sure that the sample pan hung freely. As soon as the recording pen for weighing traced a level, straight line indicating that the sample pan with the sample was in equilibrium with its surroundings, the furnace was switched on. Another recording pen was used to mark the temperature simultaneously. The sample was heated to the desired temperature. Corrections were made to the thermogram thus obtained using the temperature calibration thermogram and the sample pan thermogram. Then the weight loss was converted into percentages.

The thermograms of the twenty five cupric carboxylates are presented in FIGURES XIII to XXXVII. The eleven cupric carboxylates which have been confirmed by mass spectrometry to decompose thermally giving cuprous carboxylates (under 300°C) among the products, are presented first in FIGURES XIII to XXIII. The thermograms obtained in air and vacuum for a compound are both placed in the same figure.

The thermograms of some of the cupric carboxylates have been reported in literature[2,6-10]. In general, the thermograms obtained in this study agree with them. However higher decomposition temperatures are recorded in this work; this most likely is due to the faster heating rate employed in our experiments. One common feature in all the thermograms is that the curve obtained in vacuum (10 mm.Hg) indicates that the decomposition temperatures are lower than those in air. This trend may be caused by evacuation of volatile decomposition products. The same reasoning can be applied to explain the lower decomposition temperatures obtained in the mass spectrometric study which was done in a much better vacuum (10^{-6}mm. Hg). Therefore it must be emphasized that the temperatures shown on the thermograms are only applicable to T.G.A. studies performed under similar conditions.

The residues remaining after the thermal decompositions were usually a mixture of cupric oxide and some carbonaceous material when the decomposition took place in air, and metallic copper or a mixture of cuprous oxide and carbonaceous material when the decomposition took place in vacuum. The carbonaceous material was noted by Angel[1] and his co-workers in the thermal decomposition of cupric acetate. They proposed a formula of $C_{11}H_4O_4$ for the carbonaceous material from the results of their analysis. This carbonaceous substance can be distinguished from the rest as the material insoluble in concentrated nitric acid. The copper oxide residues were estimated from the percentage weight loss in the thermogram. It is not unusual that the weight loss should differ from the theoretical value for a residue of copper oxide because of the presence of a minute quantity of carbonaceous substance (less than 10% of the residue in cupric acetate) and the loss of copper through volatile copper

containing decomposition product (2 to 4% in the case of cupric acetate[1]). In some cases, such as chloroacetate, there is very little residue left; this is due to the formation of volatile cuprous chloride as a major decomposition product. Cupric bromoacetate has been observed to behave in a similar manner[9].

During the course of heating there is usually no well-defined plateau observed except when dehydration of the original sample occurs. This seems to be the case even when the cuprous carboxylate does exist; it is usually not a stable transient species or it may be a species produced by one of two or more competing processes that may occur during the course of decomposition. However in some cases, an inflexion on the curve was observed; as reported in the literature[10], suggesting the possible formation of a cuprous carboxylate. There are other cases where several inflexions were observed on a thermogram indicating a complicated decomposition.

Figure XIII shows the thermograms of cupric acetate. The thermogram obtained in air assumes the same shape as the one obtained by Le Van My et al[2]. The plateau B → C indicates the formation of the anhydrous salt after the removal of water of crystalization from the hydrated salt which takes place in the 90°C to 140°C temperature range. The decomposition of anhydrous cupric acetate into the residue starts to occur at about 200°C. There is no indication of the formation of any cuprous acetate. However from the mass spectrometric data some cuprous salt does form. One can only assume that the cuprous carboxylate is one of the products of the decomposition. Suggestions have been made that the decomposition proceeds according to the following equations[4]:

$$Cu_2(CH_3CO_2)_4 \cdot 2H_2O \rightarrow Cu_2(CH_3CO_2)_4 + 2H_2O$$

$$Cu_2(CH_3CO_2)_4 \rightarrow 2CuO + 2CH_3COCH_3 + 2CO_2$$

But these do not account for the formation of cuprous acetate. Therefore, there must be some competing reation occurring simultaneously with cuprous carboxylate as a reaction product. The thermogram obtained in

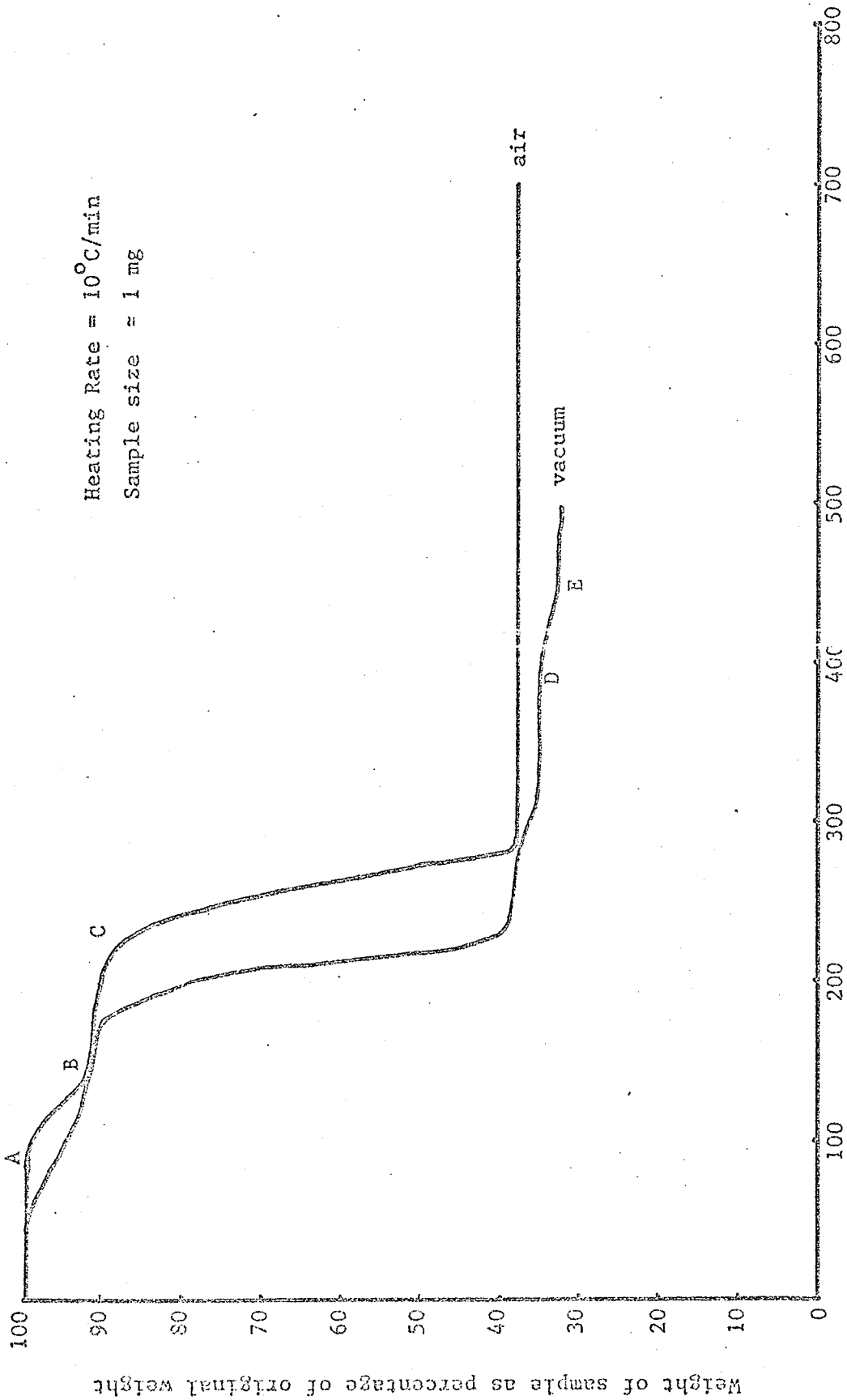

FIGURE XIII Thermograms of Cupric Acetate

vacuum differs from the one obtained in air in the sense that the temperatures of dehydration and decomposition are lower and the weight of the residue is smaller. The smaller residue is probably caused by the formation of cuprous oxide and copper instead of cupric oxide in the in the case of the thermogram obtained in air. Another reason can be that the formation of the volatile cuprous salt is more favorable in vacuum, which results in a higher weight loss. This is supported by the high intensity of ions due to the cuprous salt relative to other species in the mass spectrum. The slight loss in weight D→E on the thermogram after the decomposition of anhydrous cupric acetate could be due to further decomposition of cupric oxide into cuprous oxide and copper, or decomposition of organic by-products.

Figure XIV shows the thermograms of cupric propionate. It appears that the propionate as used, was mostly anhydrous, since only a small initial weight loss occurs. The rest of the thermogram seems similar to that of cupric acetate. The thermogram obtained by Le Van My et al[2] appears to be that of the hydrated salt. An inflexion is observed in the vacuum thermogram at about 195°C. The percentage weight loss corresponds to that required for the formation of the cuprous salt.

Figures XV and XVI show the thermograms of cupric n-butyrate and iso-butyrate respectively. They are in good agreement with those in the literature[7]. The sharp drops at about 280°C in the air thermograms indicate the presence of more than one process in the decomposition reactions. The thermograms obtained in vacuum seem to follow a similar pattern to the cupric acetate

Figures XVII and XVIII show the thermograms of cupric difluoroacetate and trifluoroacetate respectively. No indication of the formation of cuprous carboxylates can be observed. In the air thermogram of the trifluoroacetate the hygroscopic property of the salt is shown by the gain of weight of the sample at the early stage of heating. The thermograms show the same type of behavior as cupric acetate.

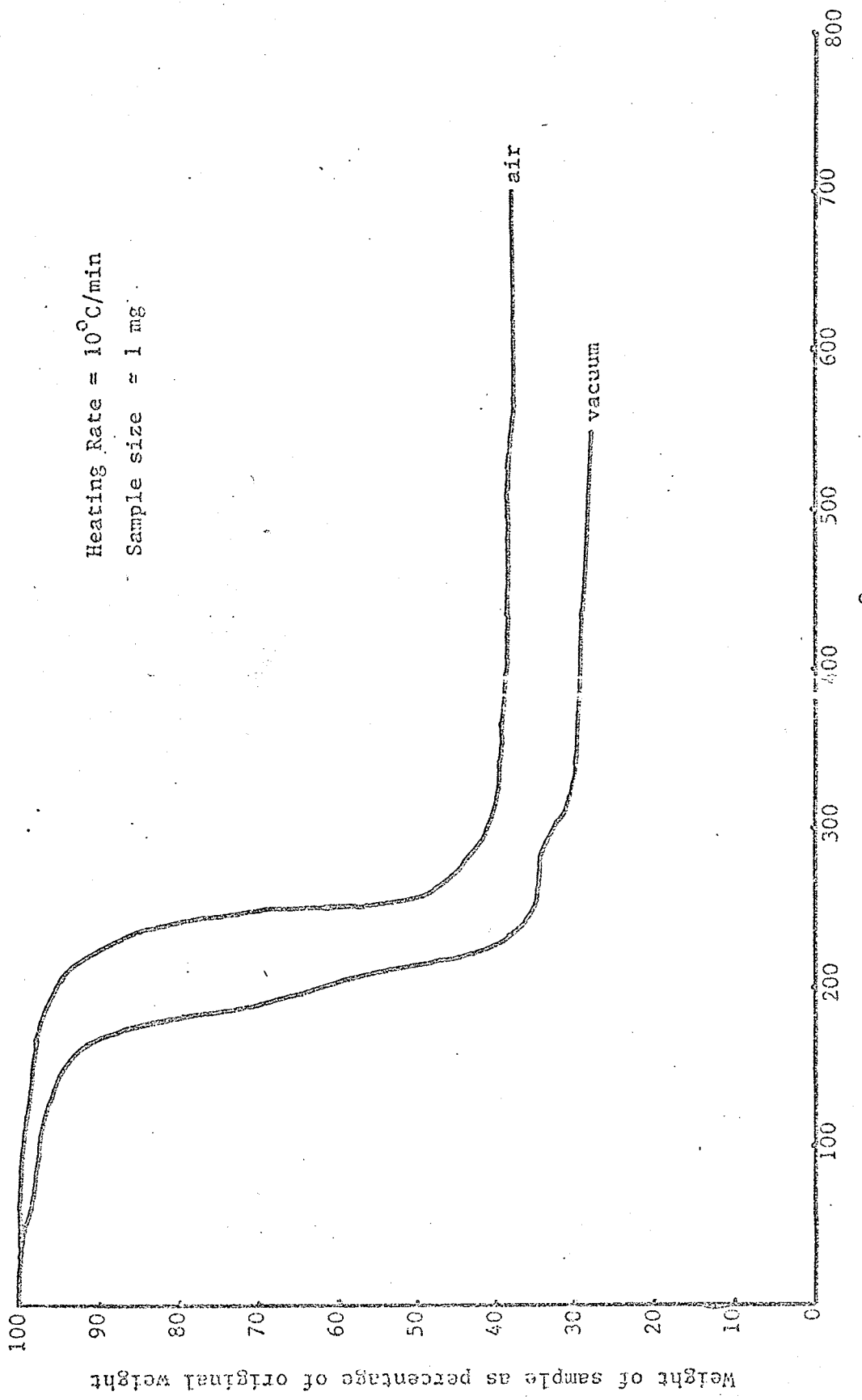

FIGURE XIV Thermograms of Cupric Propionate

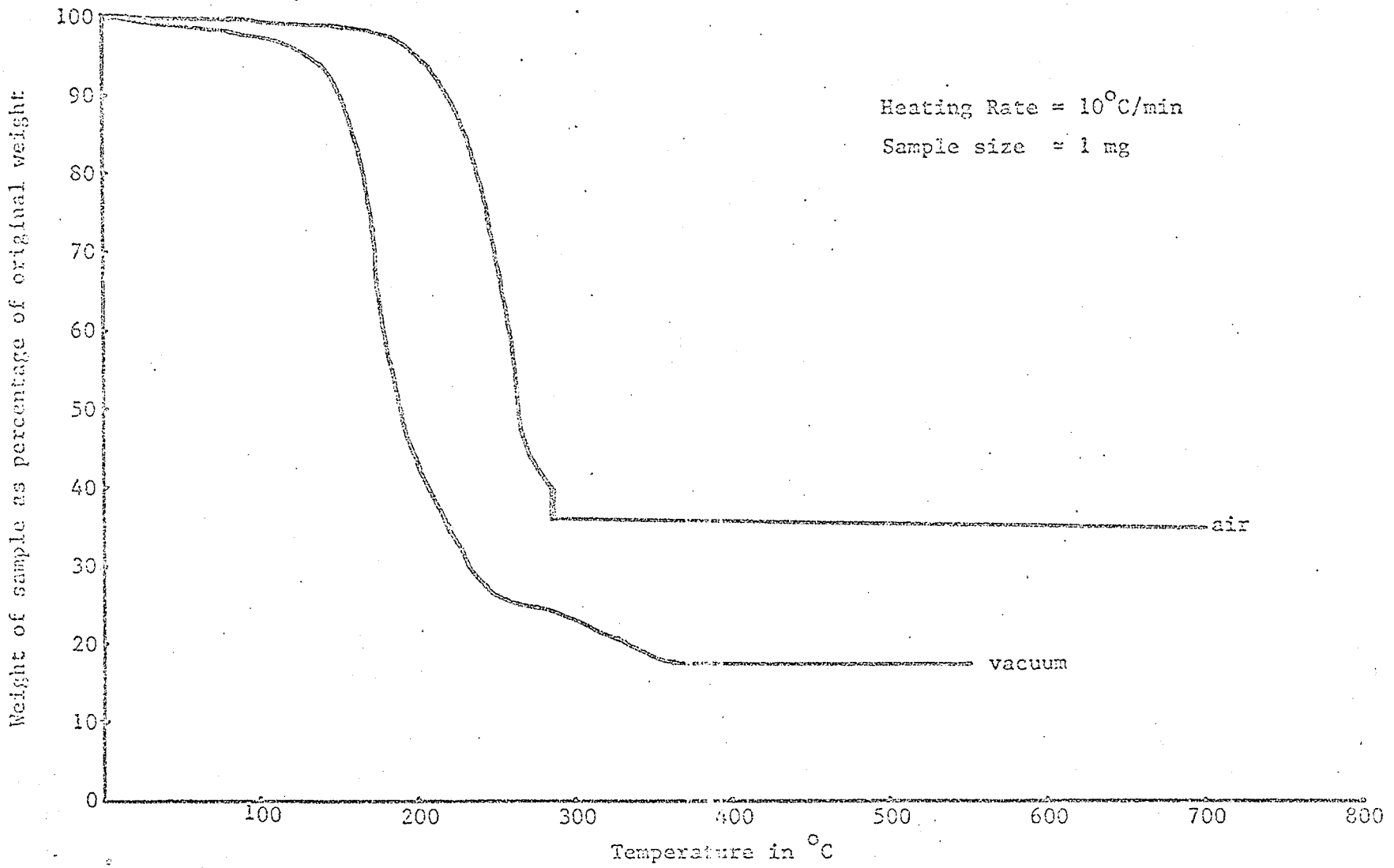

FIGURE XV Thermograms of Cupric n-Butyrate

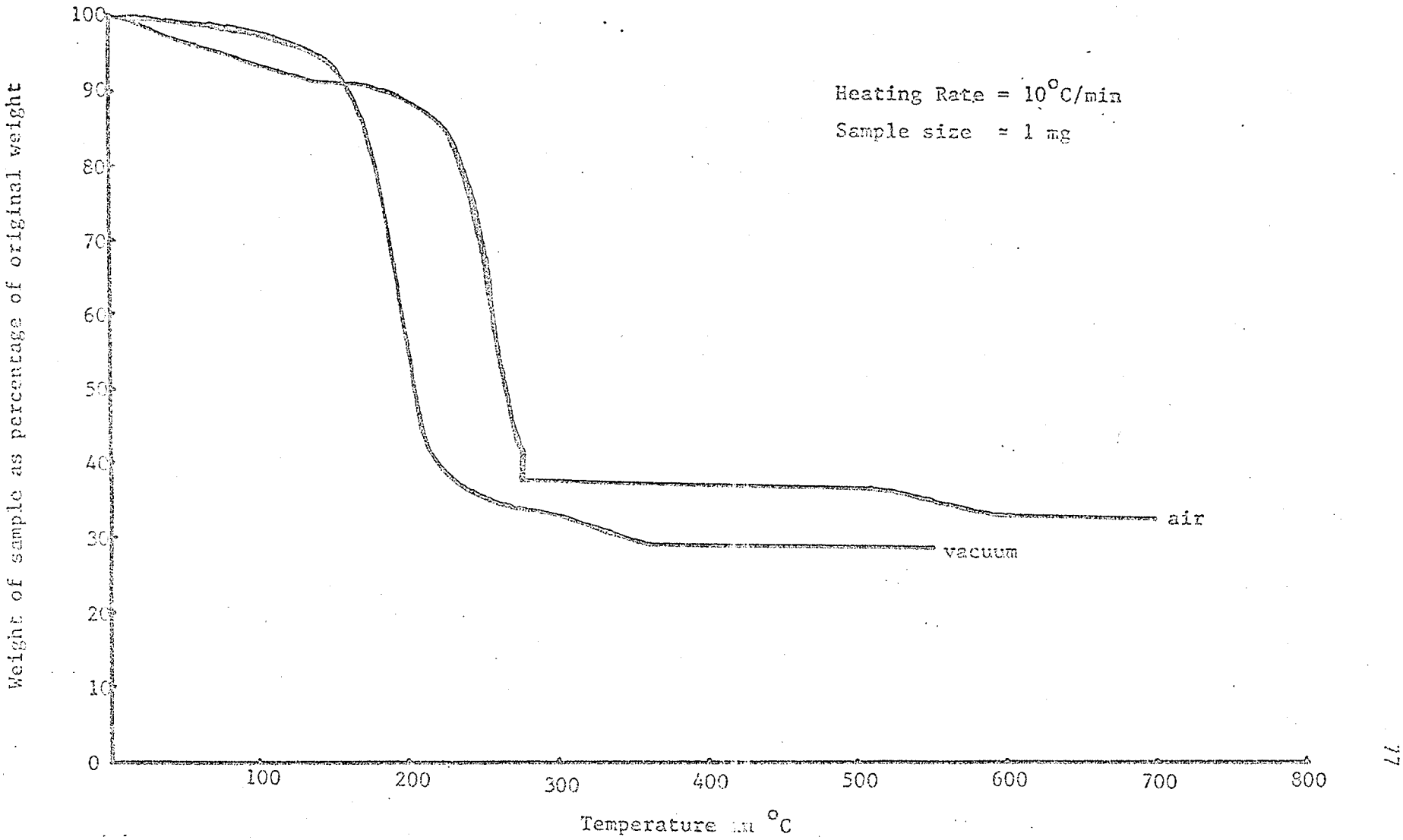

FIGURE XVI Thermograms of Cupric iso-Butyrate

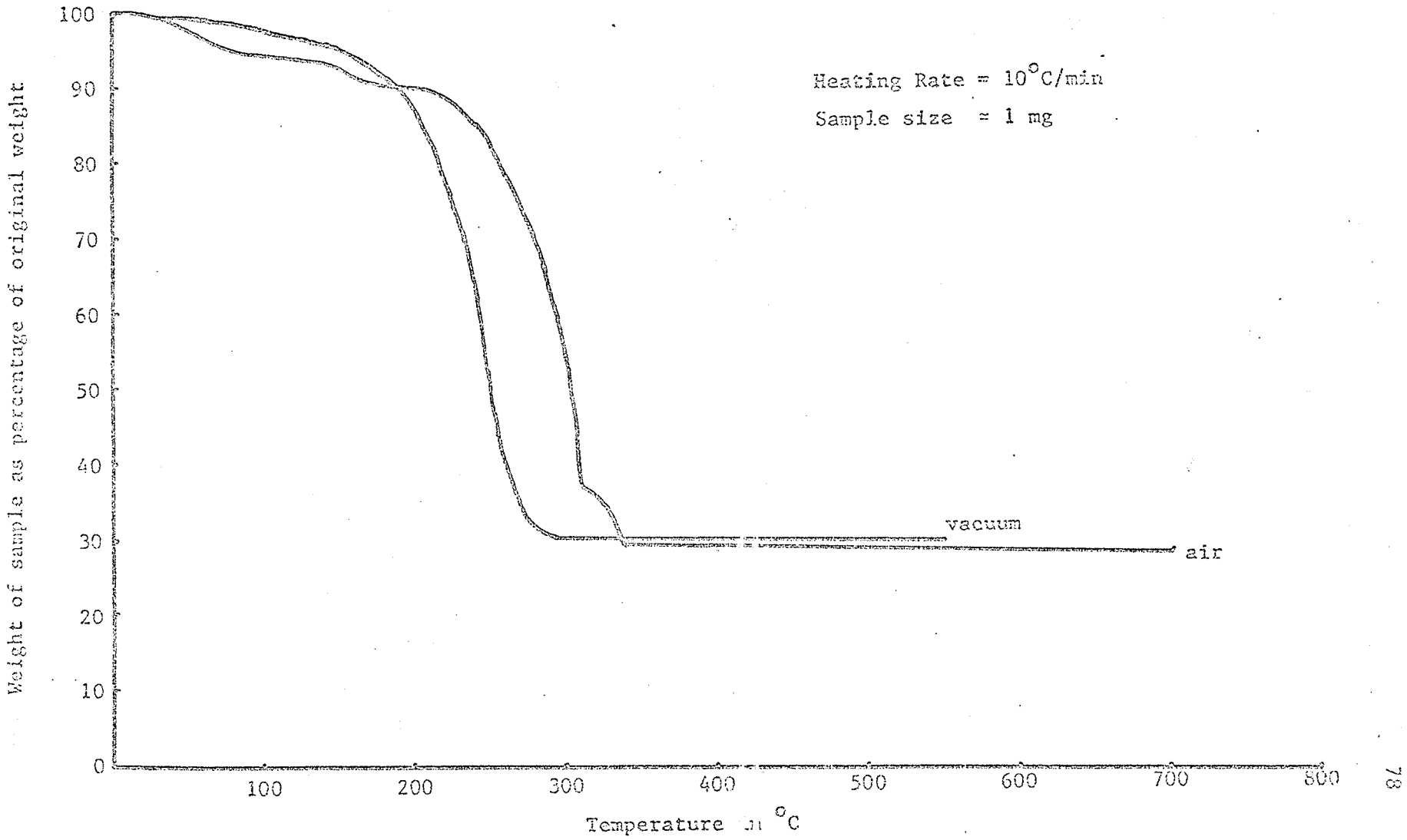

FIGURE XVII Thermograms of Cupric Difluoroacetate

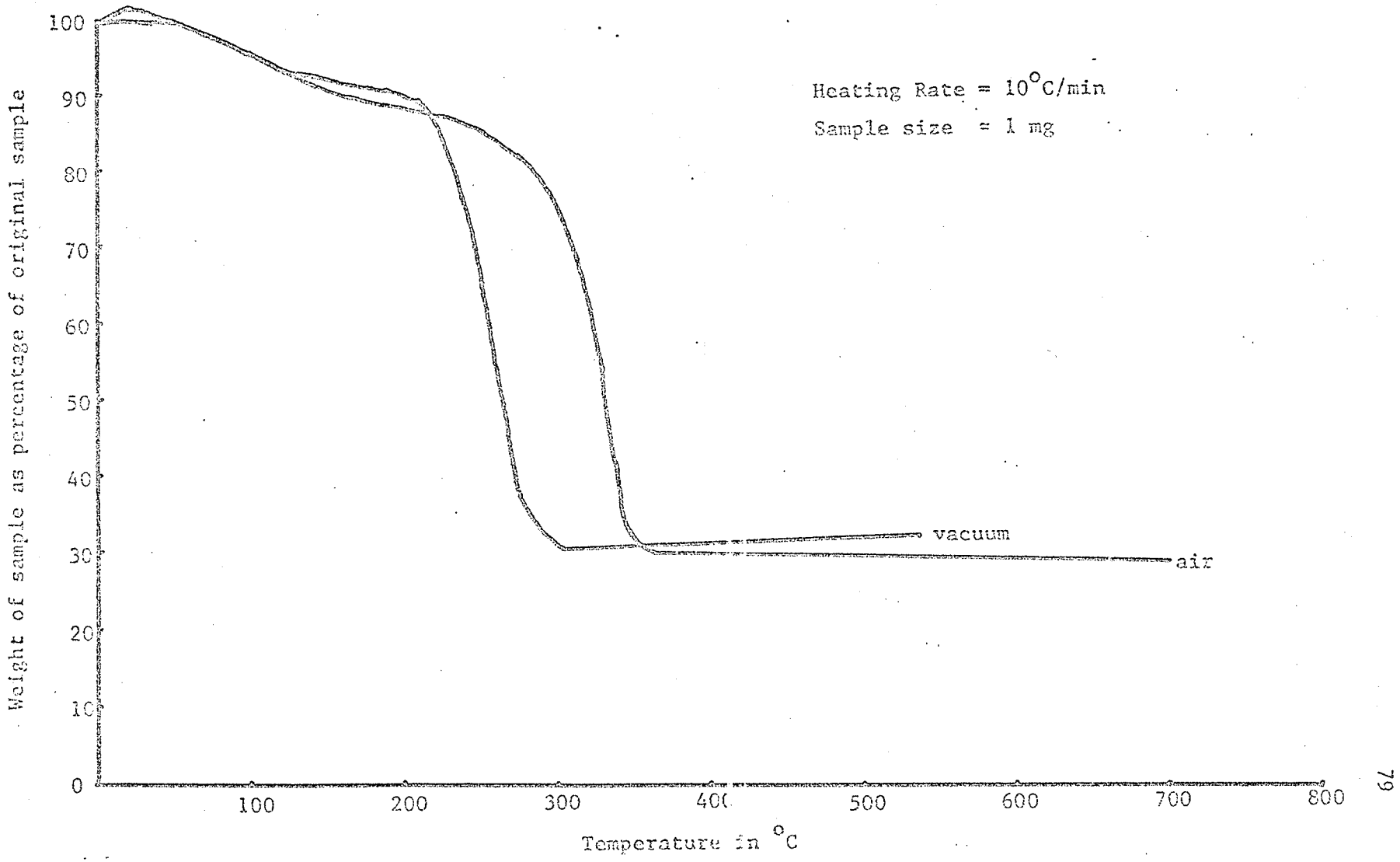

FIGURE XVIII Thermograms of Cupric Trifluoroacetate

Figure XIX shows the thermogram of largely anhydrous dimeric cupric benzoate. The first decomposition in the air thermogram upon heating can be explained from the mass spectra as mainly the loss of benzoic acid. The distinct inflexion may signify the presence of stable cuprous benzoate (by percentage weight loss). Further decomposition occurs at 365°C giving benzoic anhydride as the major decomposition product. The thermogram obtained in vacuum shows a definite change in the shape of the curve. The inflexion that apparently separates the two stages of decomposition when the sample is heated in air, becomes much less obvious. This implies that the rates of different reactions change as the atmosphere is evacuated. A mechanism for the thermal decomposition has been proposed[52], but the cuprous benzoate was unaccounted for.

Figure XX is the thermogram of cupric o-chlorobenzoate. The sample appears to be monohydrated. The anhydrous salt starts to decompose at about 260°C in air. The major decomposition products identified in the mass spectra are the anhydride, the acid and some cuprous salt. However the thermogram shows that there are probably other processes occurring when heated to over 300°C since only a minute quantity of residue is left behind. These processes probably involve the formation of volatile copper chlorides. The thermogram in vacuum seems to take a different course in decomposition above 300°C which results in a larger amount of residue.

Figures XXI and XXII are the thermograms of hydrated cupric p-chloro and p-fluorobenzoates respectively. The thermograms in air have the same shape reported by Charbonnier et al[10]. The inflexions in the decompositions of the anhydrous salts approximately correspond to the cuprous salts by percentage weight. These inflexions appear as plateaus in the thermograms obtained in vacuum, an indication of the possibility of stable cuprous carboxylate in vacuum. This explains the high intensity of ions due to cuprous carboxylates in the mass spectra.

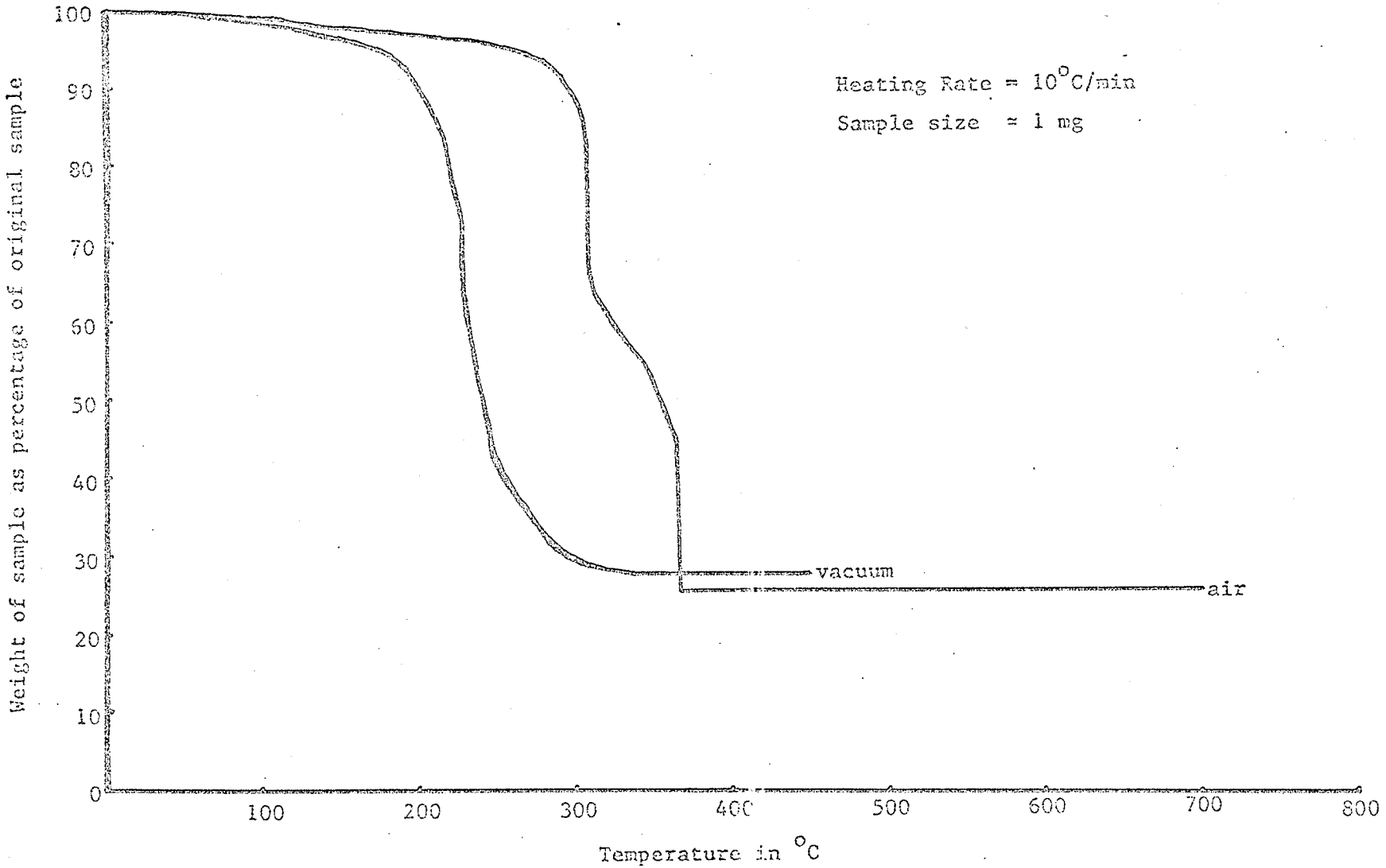

FIGURE XIX Thermograms of Cupric Benzoate

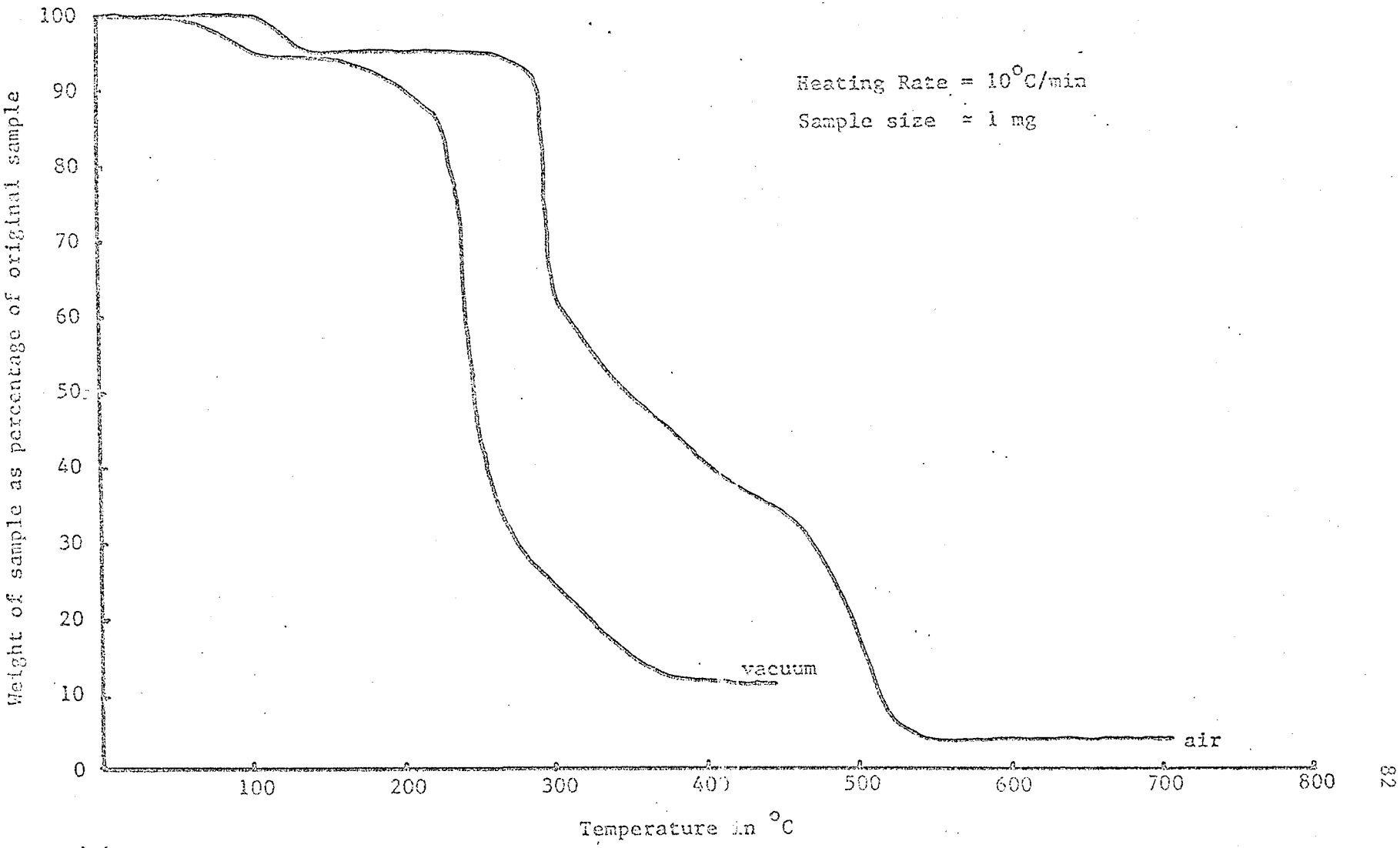

FIGURE XX Thermograms of Cupric o-Chlorobenzoate

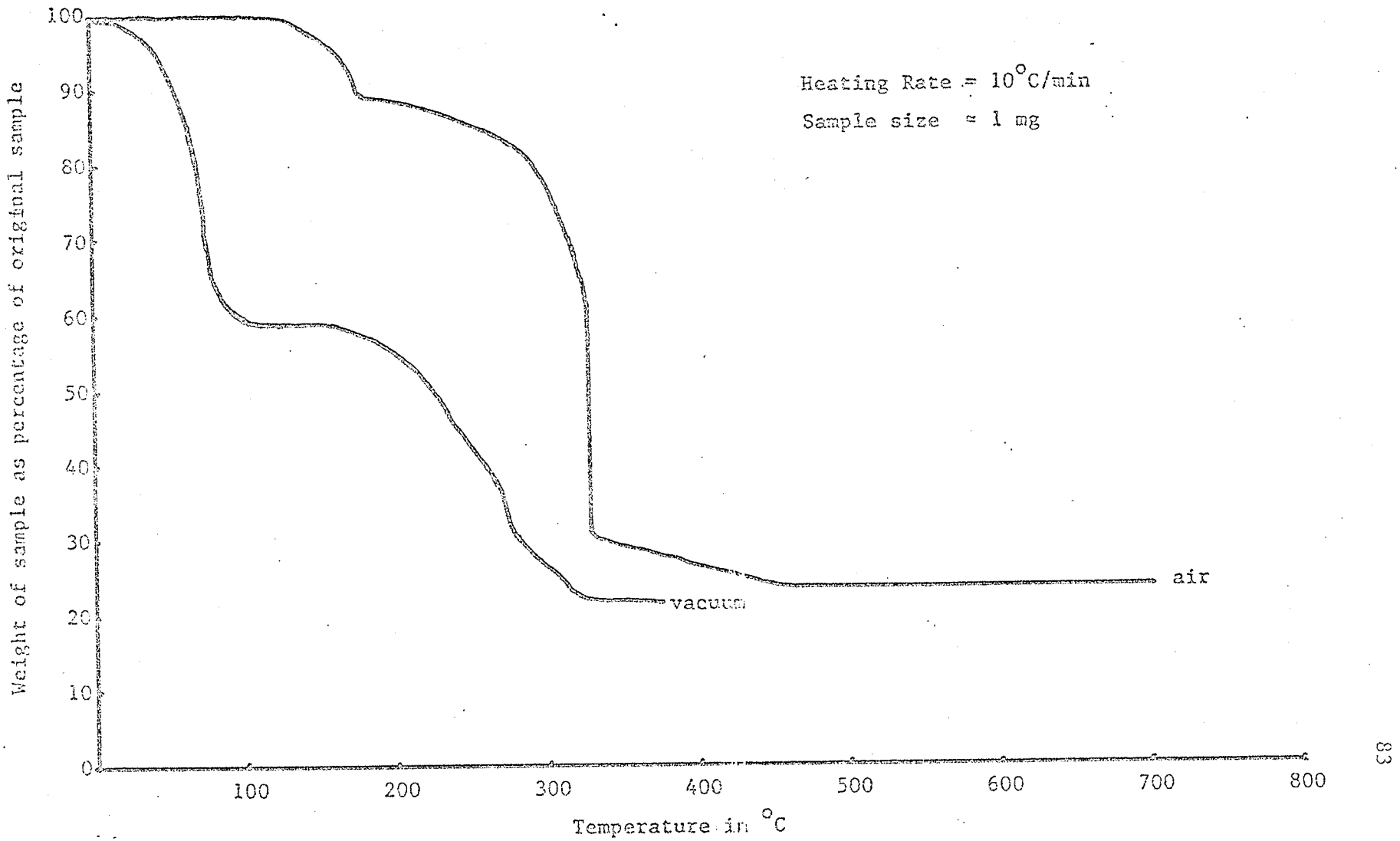

FIGURE XXI Thermograms of Cupric p-Chlorobenzoate

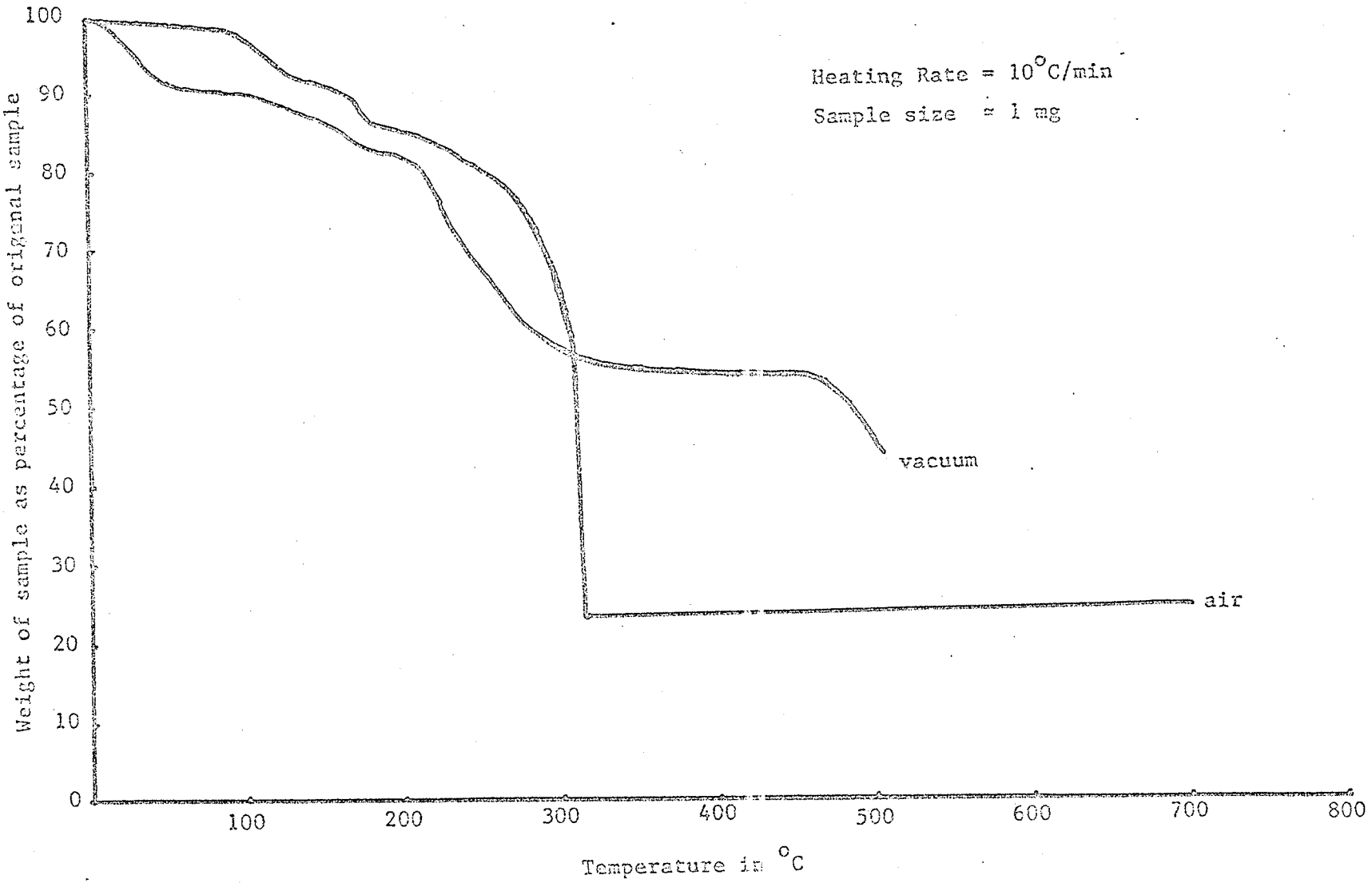

FIGURE XXII Thermograms of Cupric p-Fluorobenzoate

Figure XXIII shows the thermograms of anhydrous cupric pentafluorobenzoate. Little information can be extracted from the thermogram obtained in air. However the difference between the thermograms in vacuum and in air shows that the sample seems to decompose in a different manner in each case. In the mass spectra, $C_{12}F_{10}$ and pentafluorobenzoic acid had been identified as major decomposition products with formation of a trace of the cuprous salt. The plateau in the thermogram in vacuum after the first decomposition stage may be, but not necessarily, an indication of the formation of a stable cuprous salt, although by percentage weight loss it is a little low in weight. It decomposes further at about 380°C.

It was hoped at the beginning of this study that a generalized pattern of the thermograms could be established for all the cupric carboxylates which are known from the mass spectra to decompose into cuprous salts. Such a pattern, if it exists, might be applied to predict the possibility of the existence of other cuprous carboxylates from thermal decomposition of other cupric salts. Though reasonable descriptions for the eleven cupric carboxylates discussed so far can be formulated individually with the aid of the mass spectrometric data, no well defined pattern was discovered among the thermograms.

Figures XXIV to XXXVII are the thermograms of the fourteen cupric carboxylates which do not show any evidence of decomposition into the cuprous salt in the mass spectra. These too do not seem to have a general pattern of decomposition among them. Some of the thermograms can be explained reasonably but some show signs of complications which defy rationalization with the mass spectral data gathered. The carboxylates that belong to the latter group are cupric o-OH, p-OH, o-OCH_3, p-OC_2H_5, o-CH_3, p-CH_3 benzoates and ß-naphthoate (Figures XXIV to XXX respectively). The only clear indications from these thermograms are the dehydration steps. In many of the aromatic carboxylates the residue is too heavy for CuO alone. The many inflexions on the decomposition curve

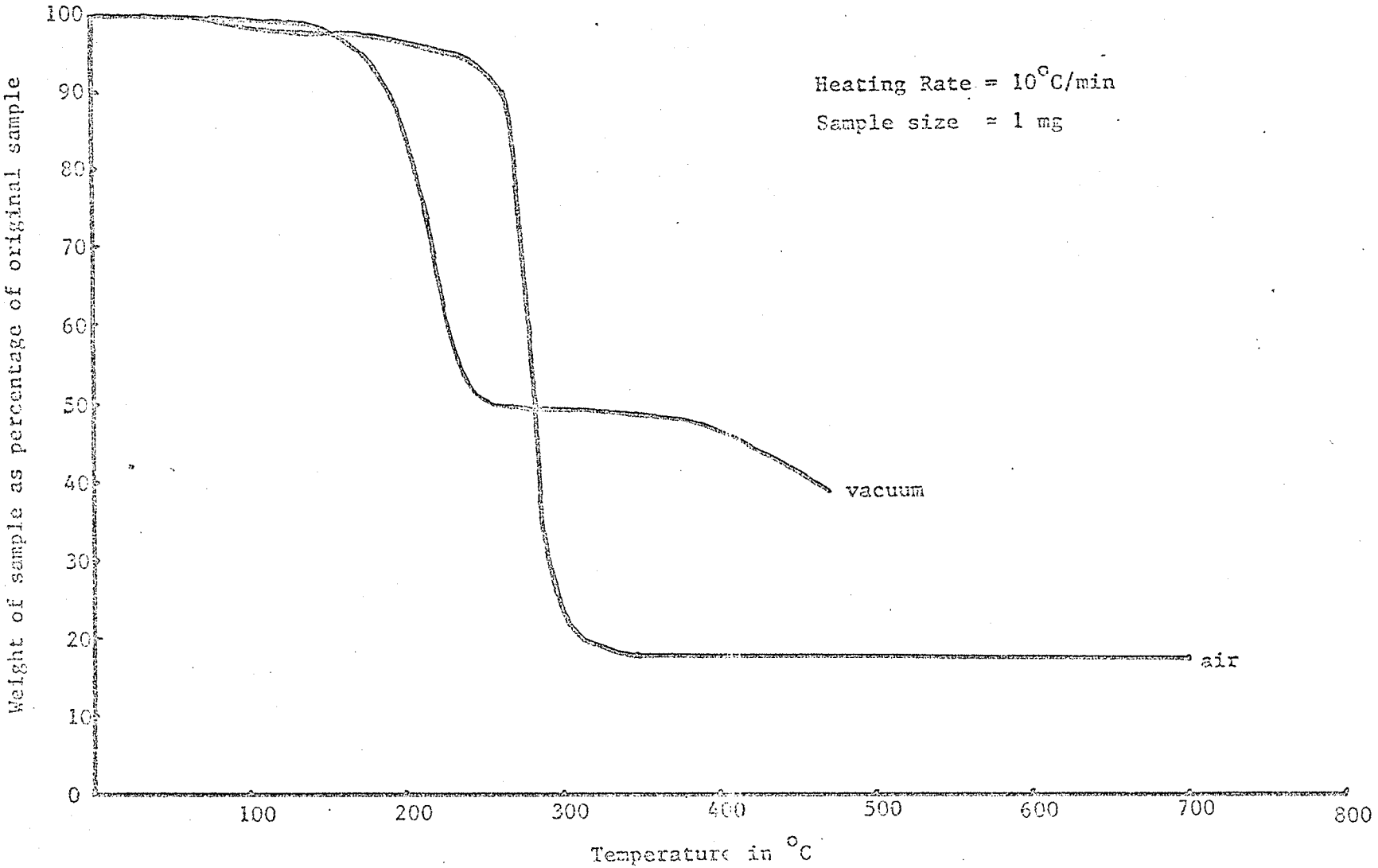

FIGURE XXIII Thermograms of Cupric Pentafluorobenzoate

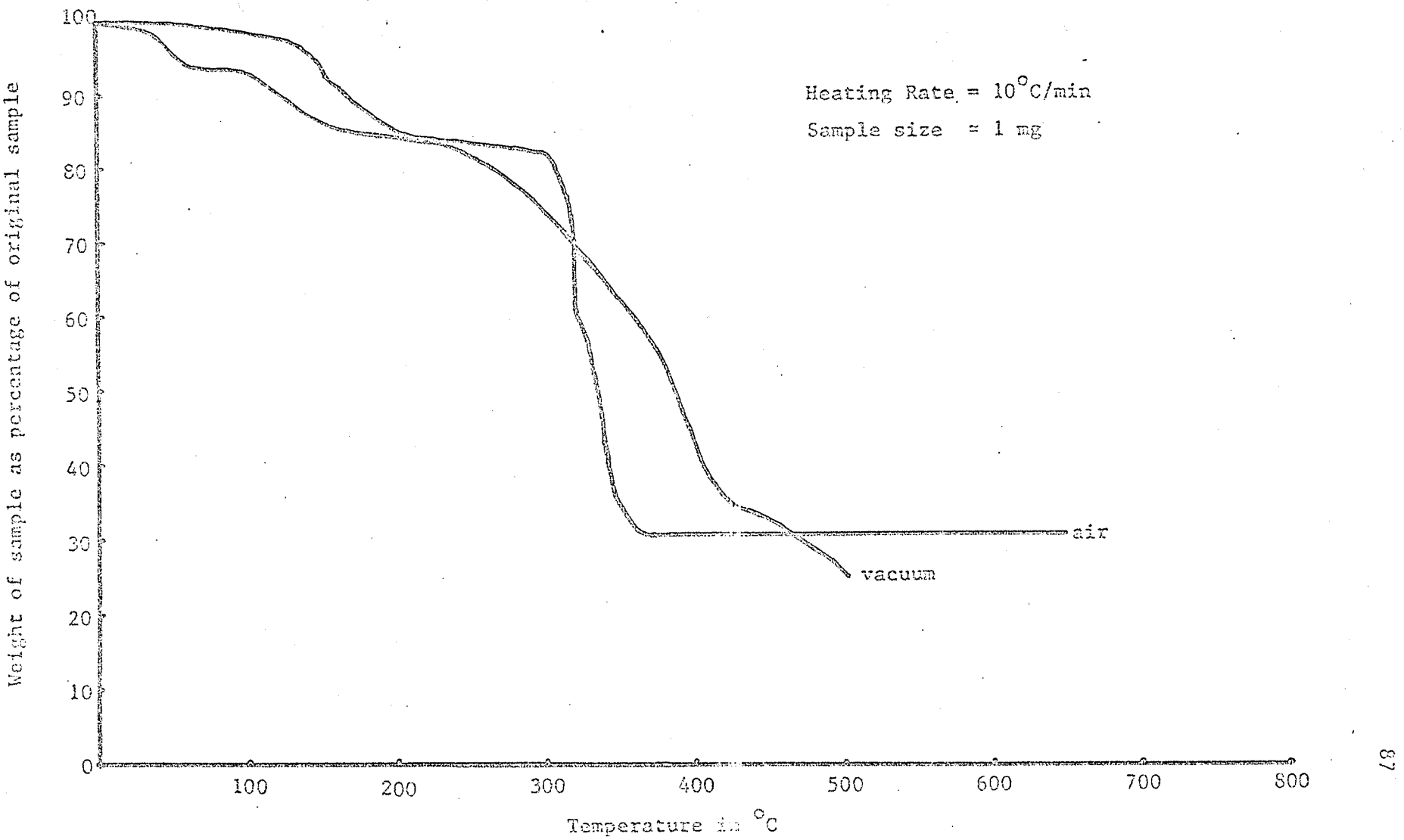

FIGURE XXIV Thermograms of Cupric o-Hydroxybenzoate

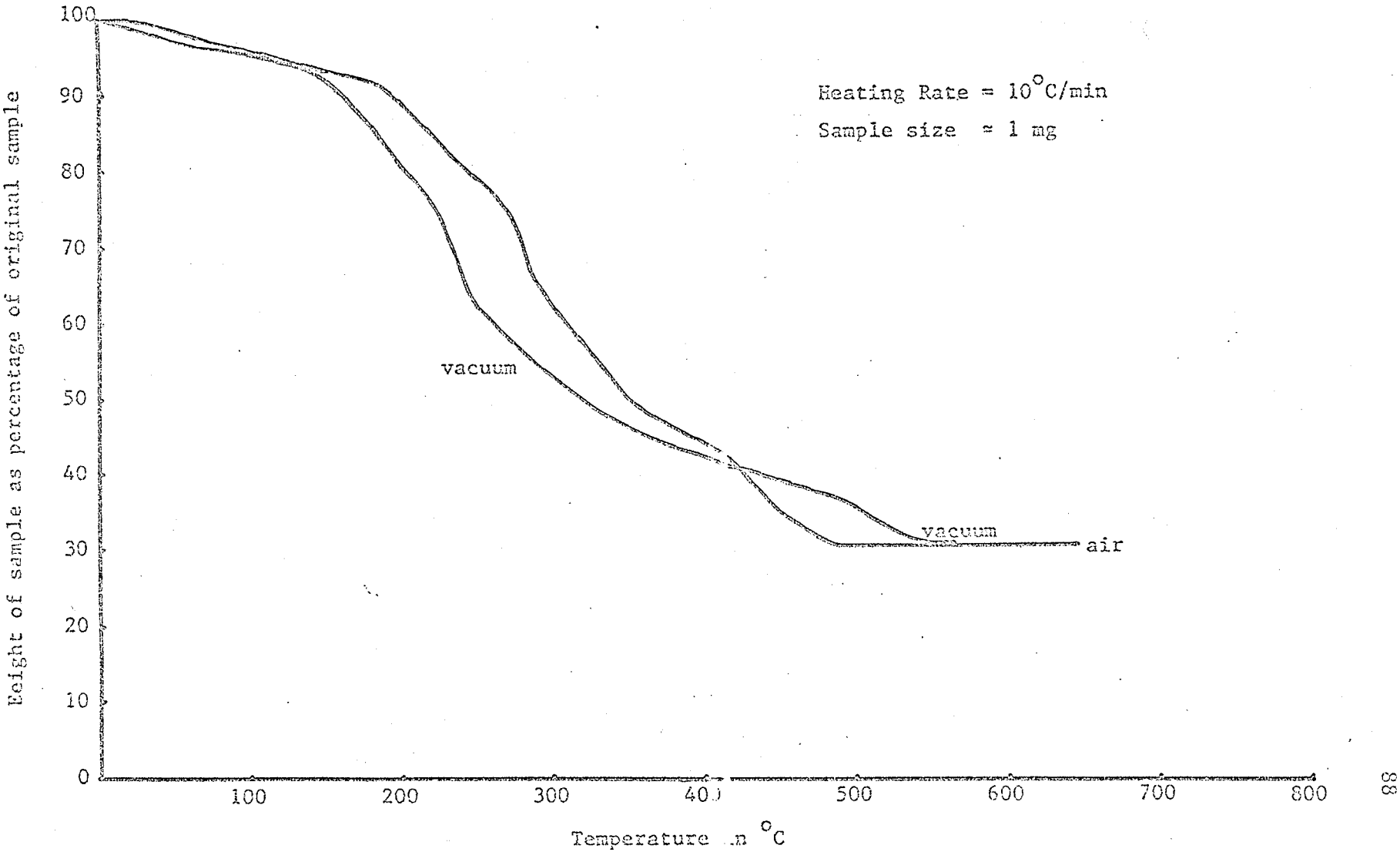

FIGURE XXV Thermograms of Cupric p-Hydroxybenzoate

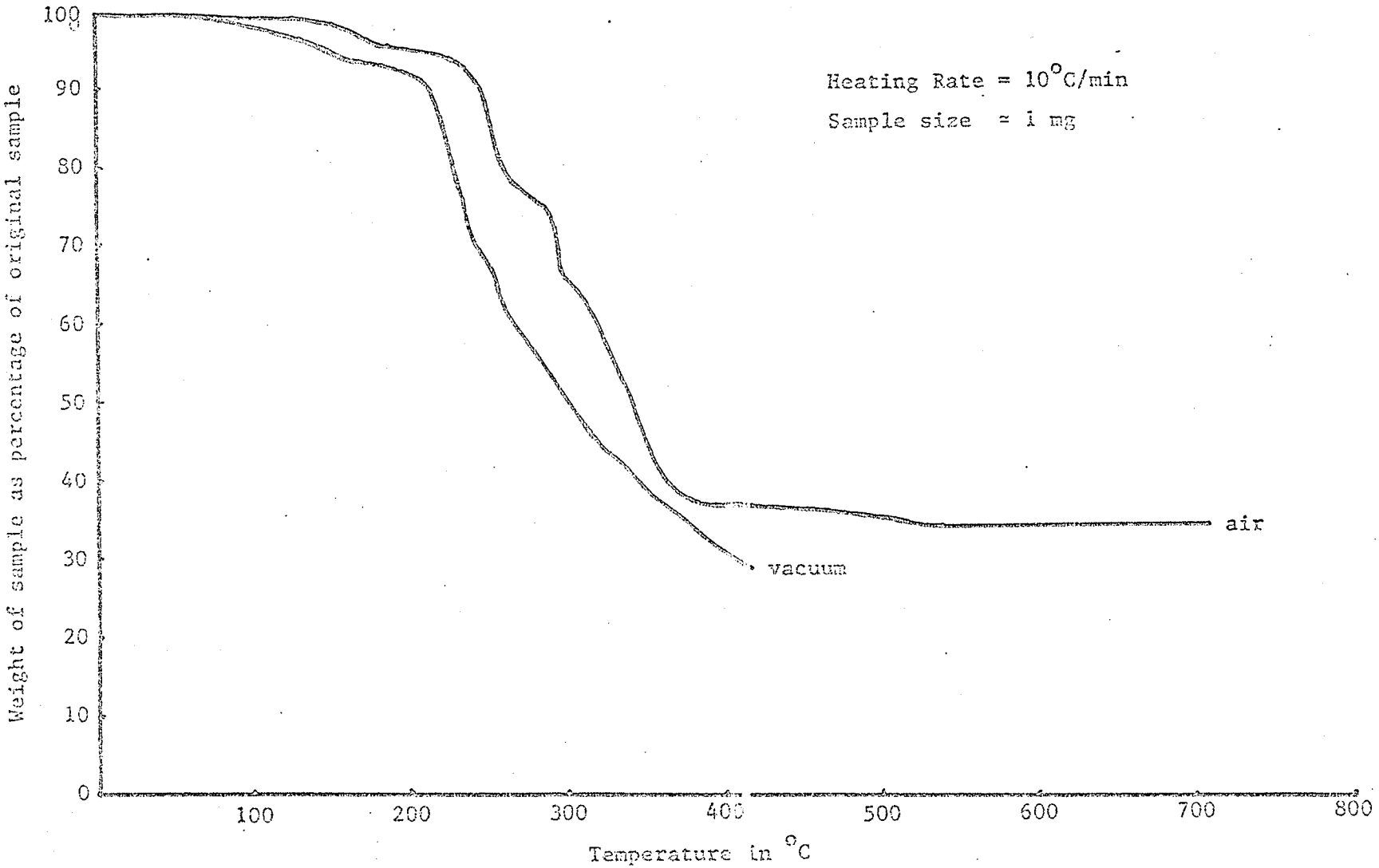

FIGURE XXVI Thermograms of Cupric o-Methoxybenzoate

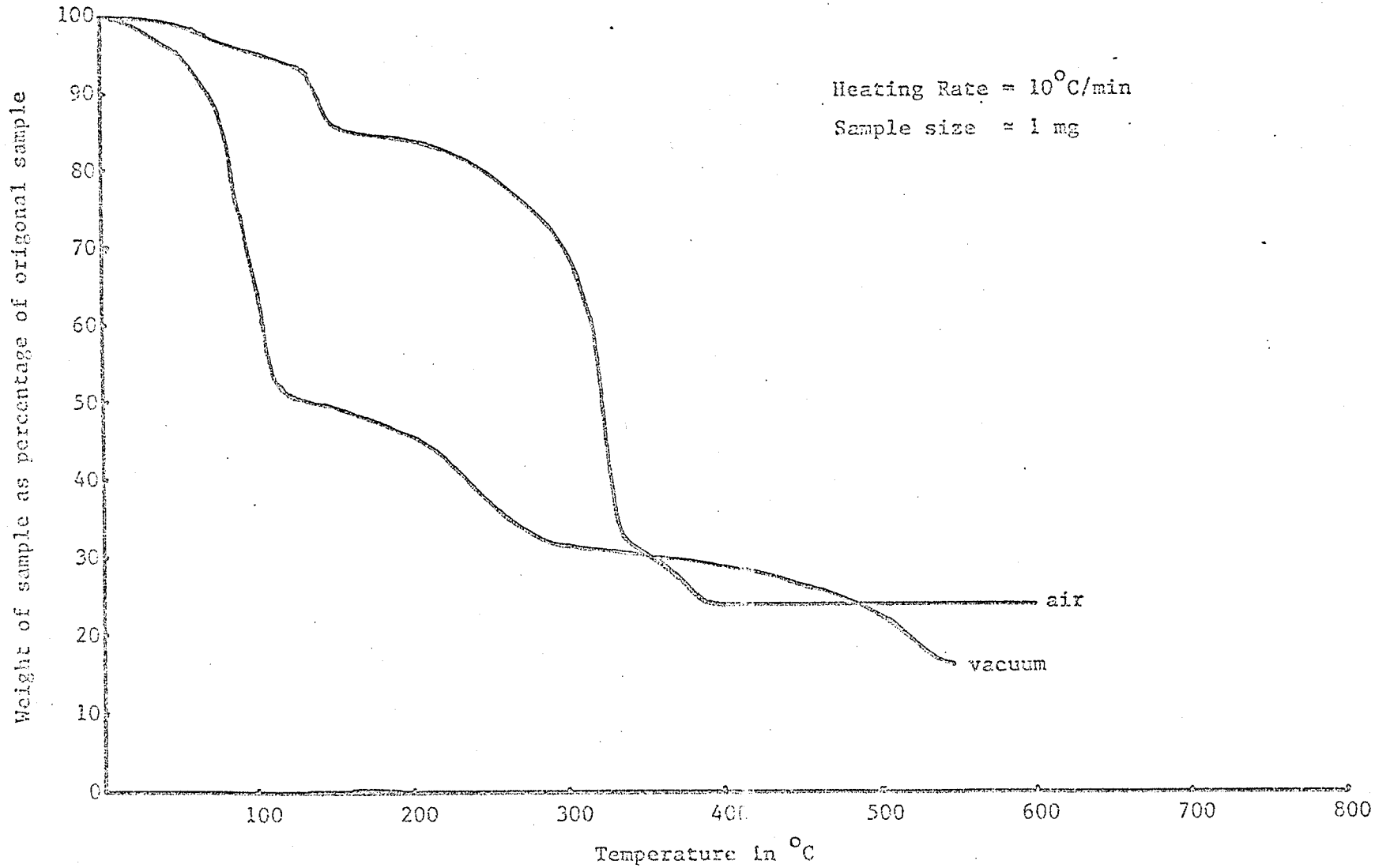

FIGURE XXVII Thermograms of Cupric p-Ethoxybenzoate

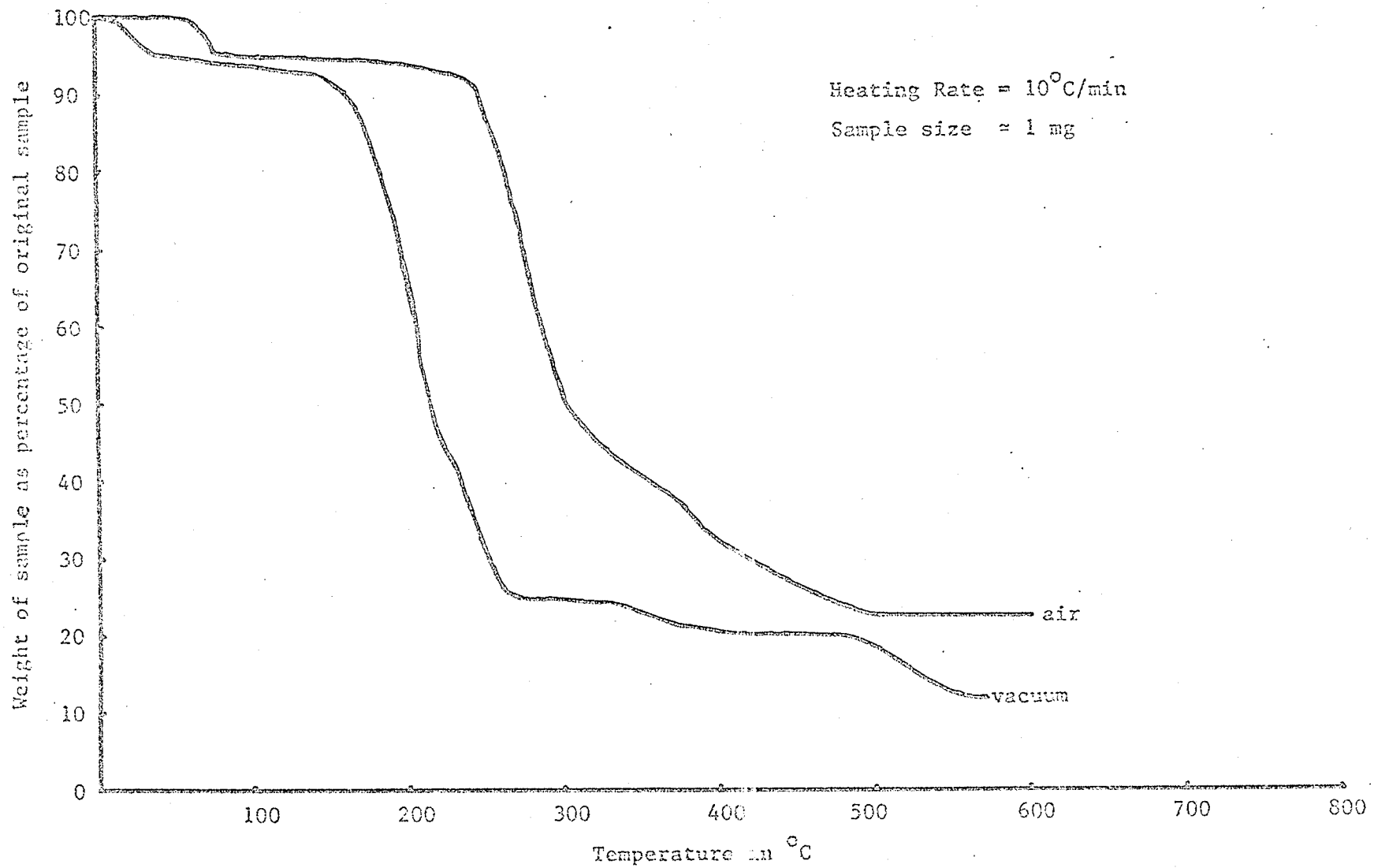

FIGURE XXVIII Thermograms of Cupric o-Methylbenzoate

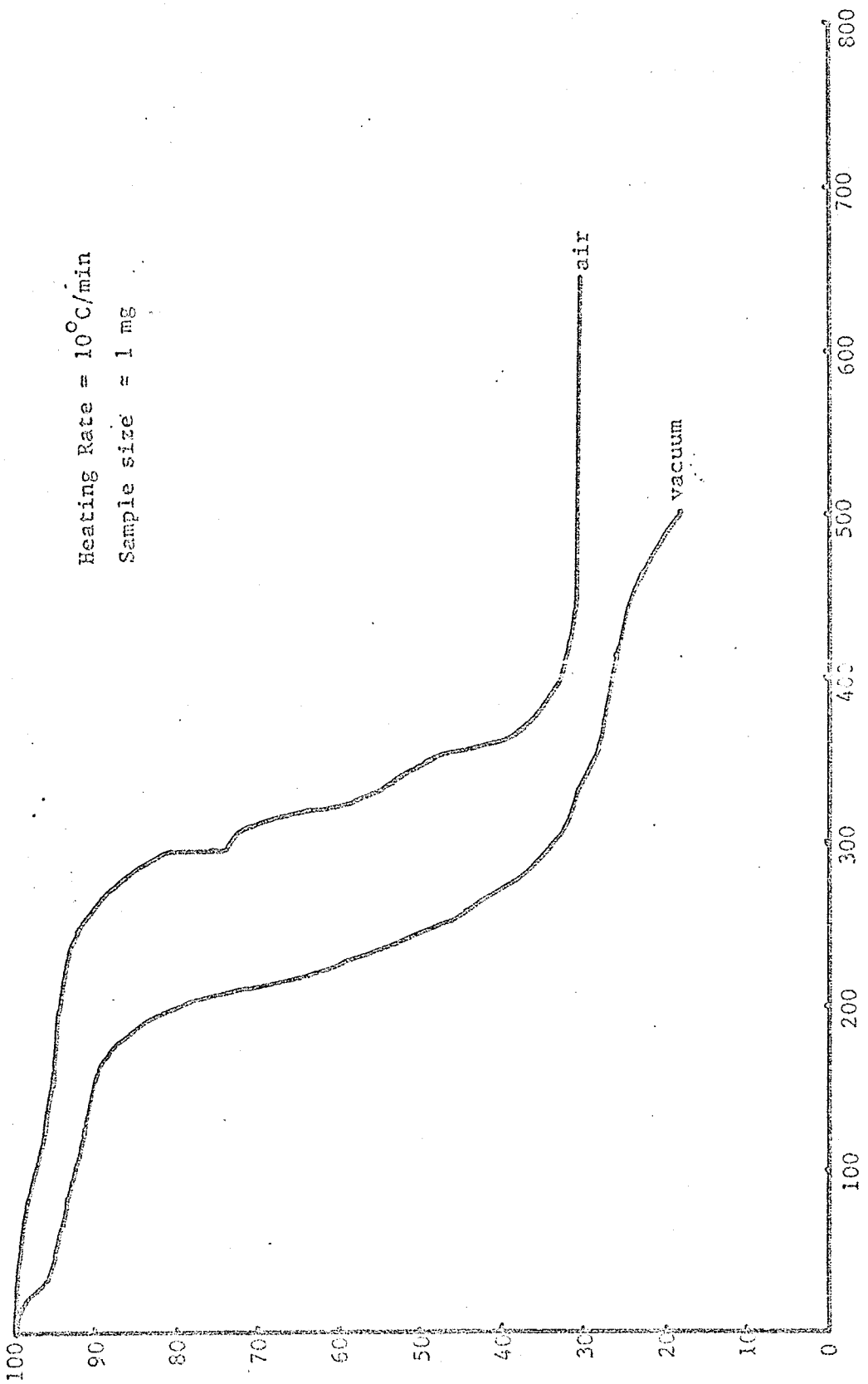

FIGURE XXIX Thermograms of Cupric p-Methylbenzoate

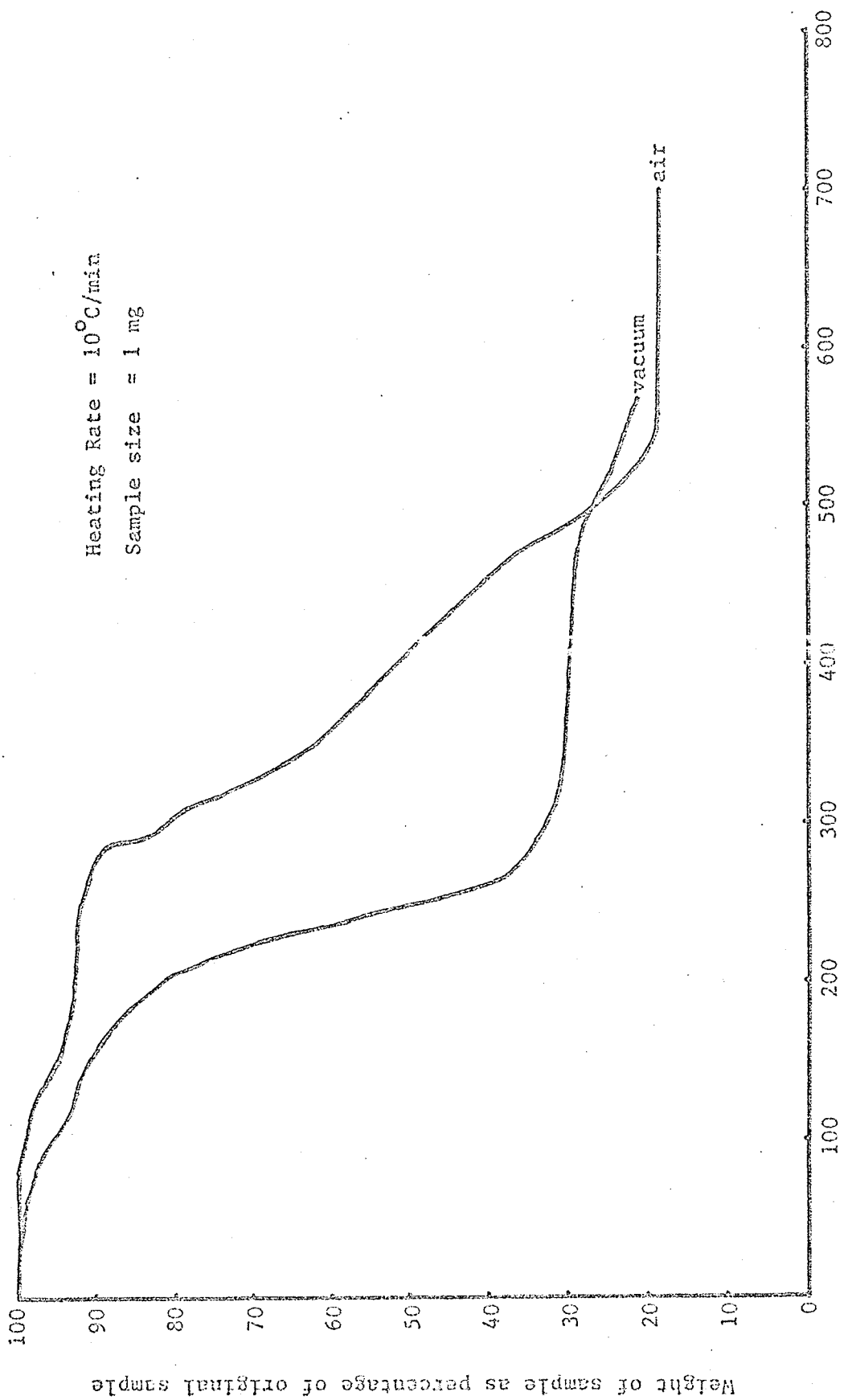

FIGURE XXX Thermograms of Cupric β-naphthoate

after the initial dehydration process suggest the possibility that many decomposition processes are taking place.

Figure XXXI is the thermogram of cupric formate. The sample seems to be partially dehydrated. The thermograms of the dihydrate and tetrahydrate salt have been examined before[2], and apart from the dehydration part of the thermograms they appear to be similar to Figure XXXI. The weight gain after the deconposition in air is probably an indication of the oxidation of some of the metallic copper to cupric oxide. The decomposition in vacuum results in the formation of metallic copper.

Figures XXXII and XXXIII are the thermograms of the cupric monochloroacetate and dichloroacetate respectively. The formation of volatile cuprous chloride in the mass spectrometer is very prominent. This explains why the thermograms in vacuum do not show the presence of a residue after decomposition. When compared with the mass spectral data the curve at lower temperatures (below 250°C) seems to be the result of the formation of other volatile organic compounds such as CH_3Cl and $ClCH_2CO_2H$ in the monochloroacetate and CH_2Cl_2 and Cl_2HCCO_2H in the dichloroacetate. The thermograms in air show similar trends in the decompositions. However, the formation of copper chlorides competes with the formation of copper oxides. This results in the presence of some residue after decomposition.

Figure XXXIV shows the thermograms of cupric phenylacetate. The thermogram in air indicates the sample was hydrated whereas in vacuum the sample was partially dehydrated. The evacuation of the thermobalance probably caused the loss of water before the sample was heated. From the mass spectrometric data the decomposition seems to be quite simple; only phenylacetic acid was detected as a major product. However, after the first steep descent a second decomposition stage is observed before the final plateau is reached and this indicates the occurrence of other decomposition processes.

Figures XXXV and XXXVI are the thermograms of cupric o-NO_2 and p-NO_2 benzoates respectively. They both indicate straight forward

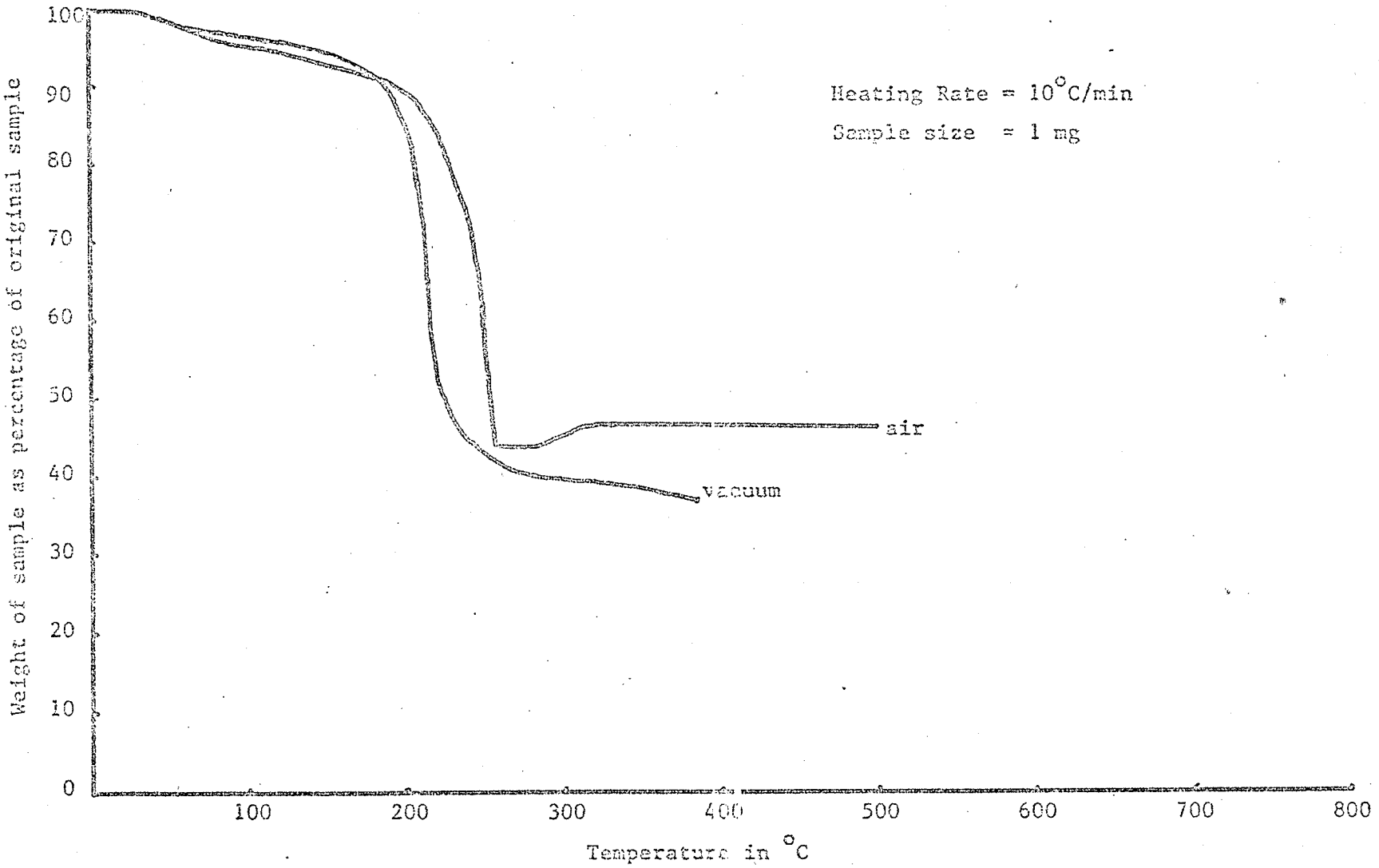

FIGURE XXXI Thermograms of Cupric Formate

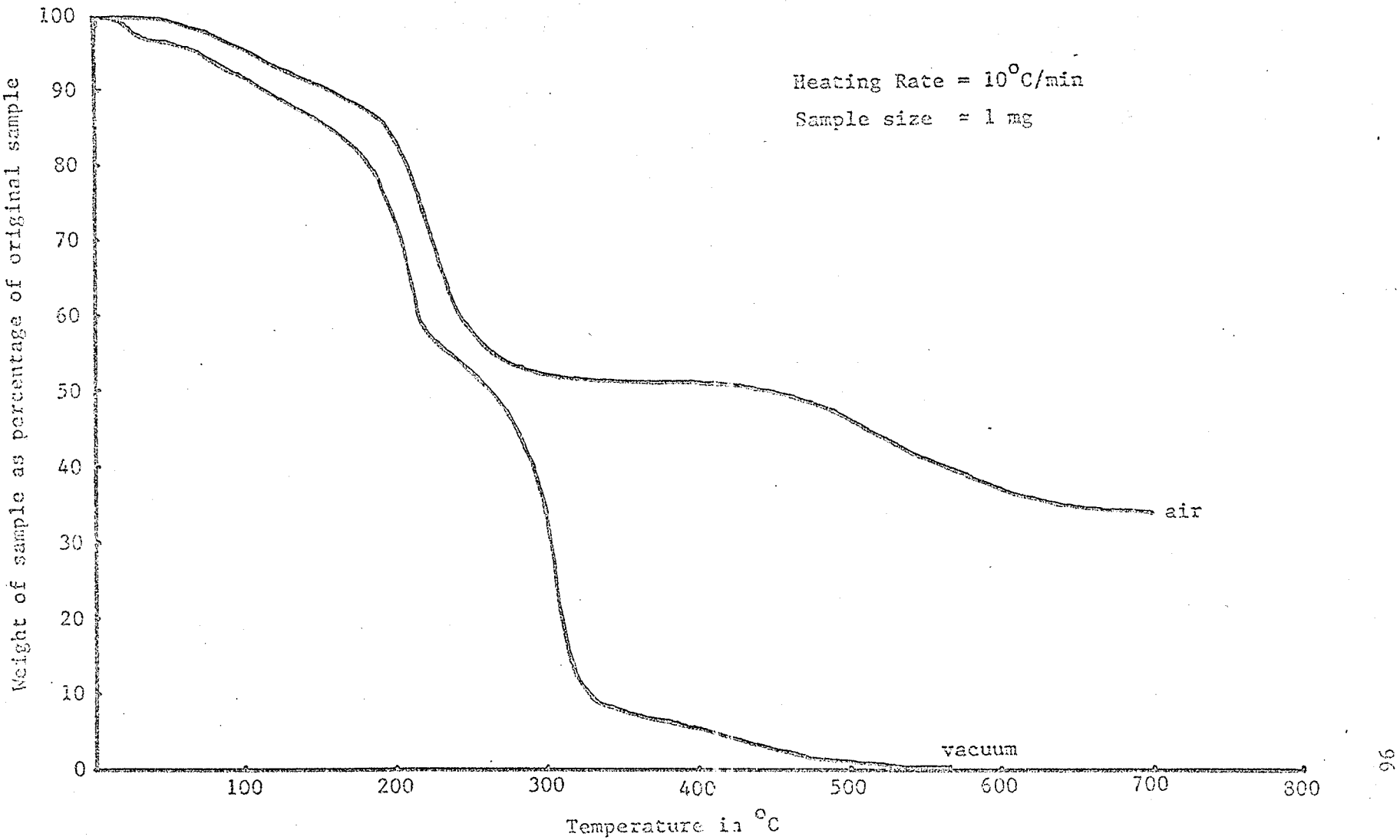

FIGURE XXXII Thermograms of Cupric Monochloroacetate

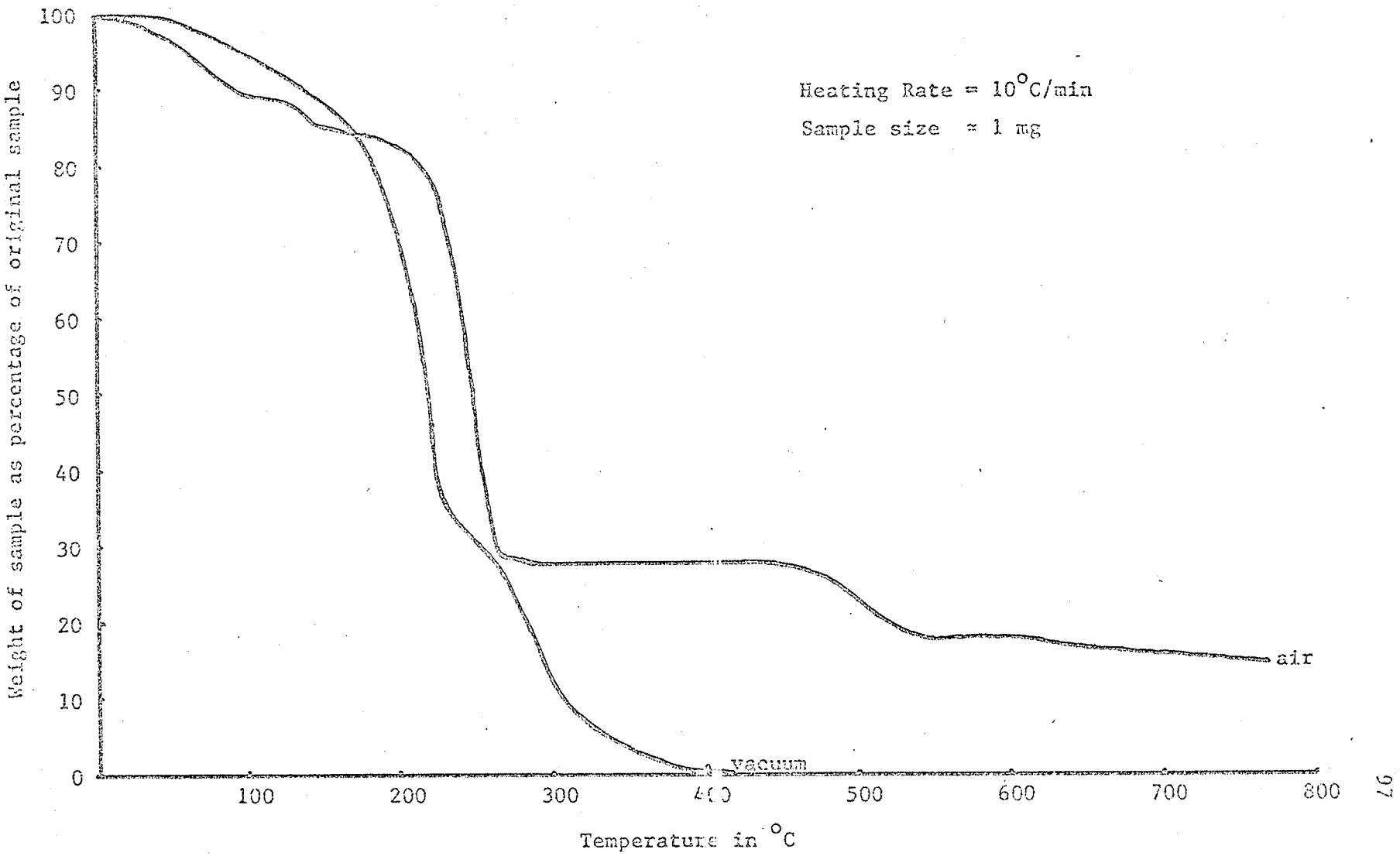

FIGURE XXXIII Thermograms of Cupric Dichloroacetate

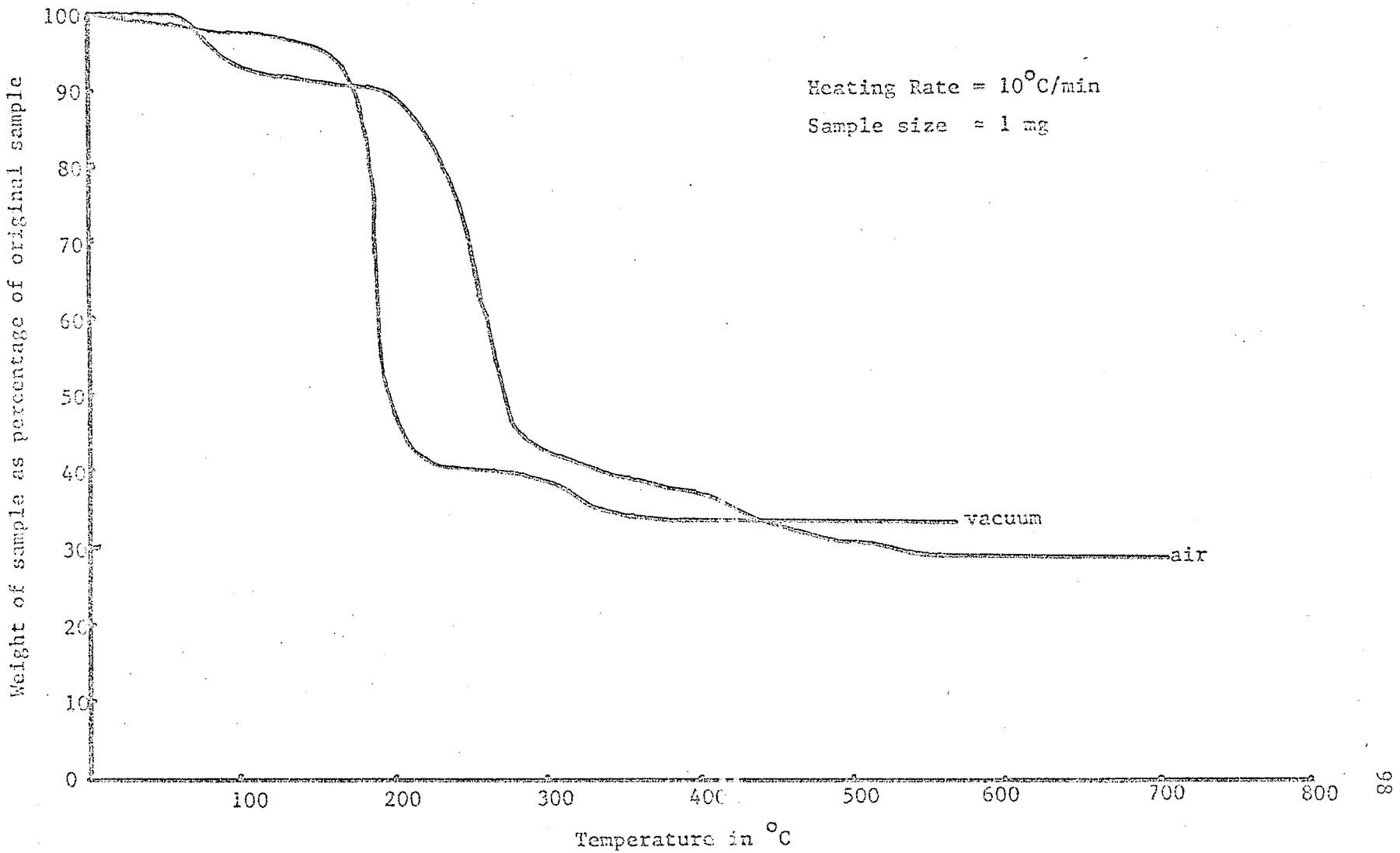

FIGURE XXXIV Thermograms of Cupric Phenylacetate

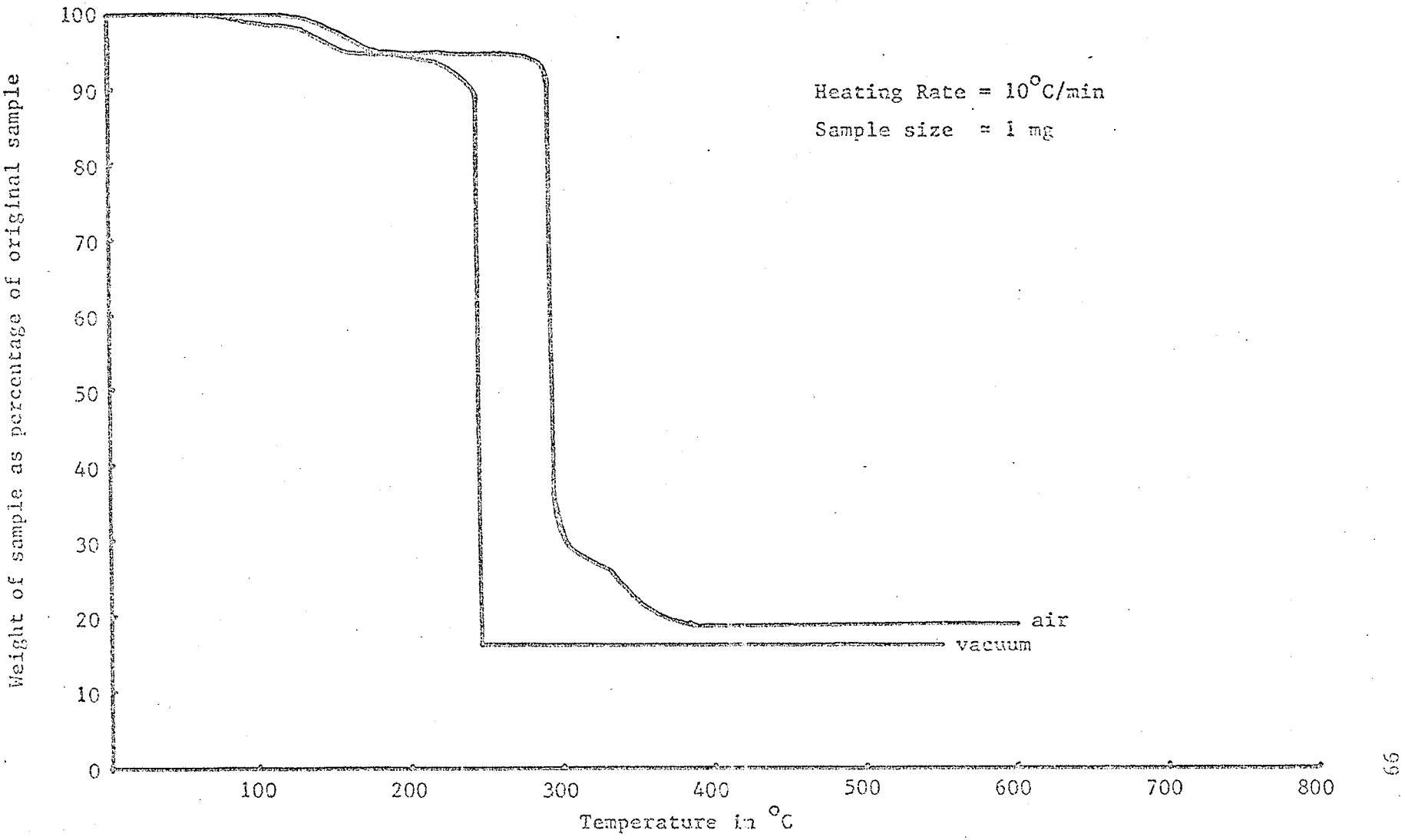

FIGURE XXXV Thermograms of Cupric o-Nitrobenzoate

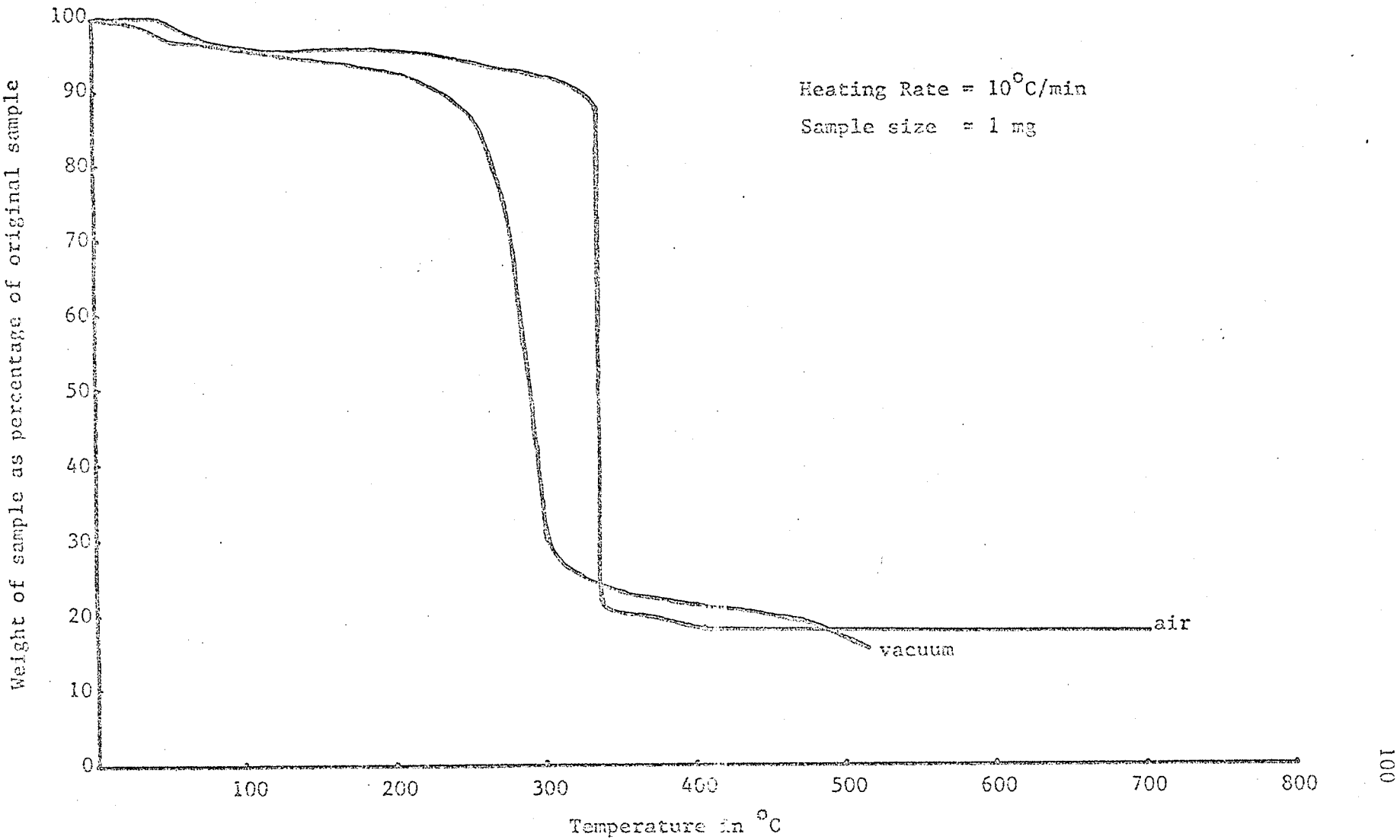

FIGURE XXXVI Thermograms of Cupric p-Nitrobenzoate

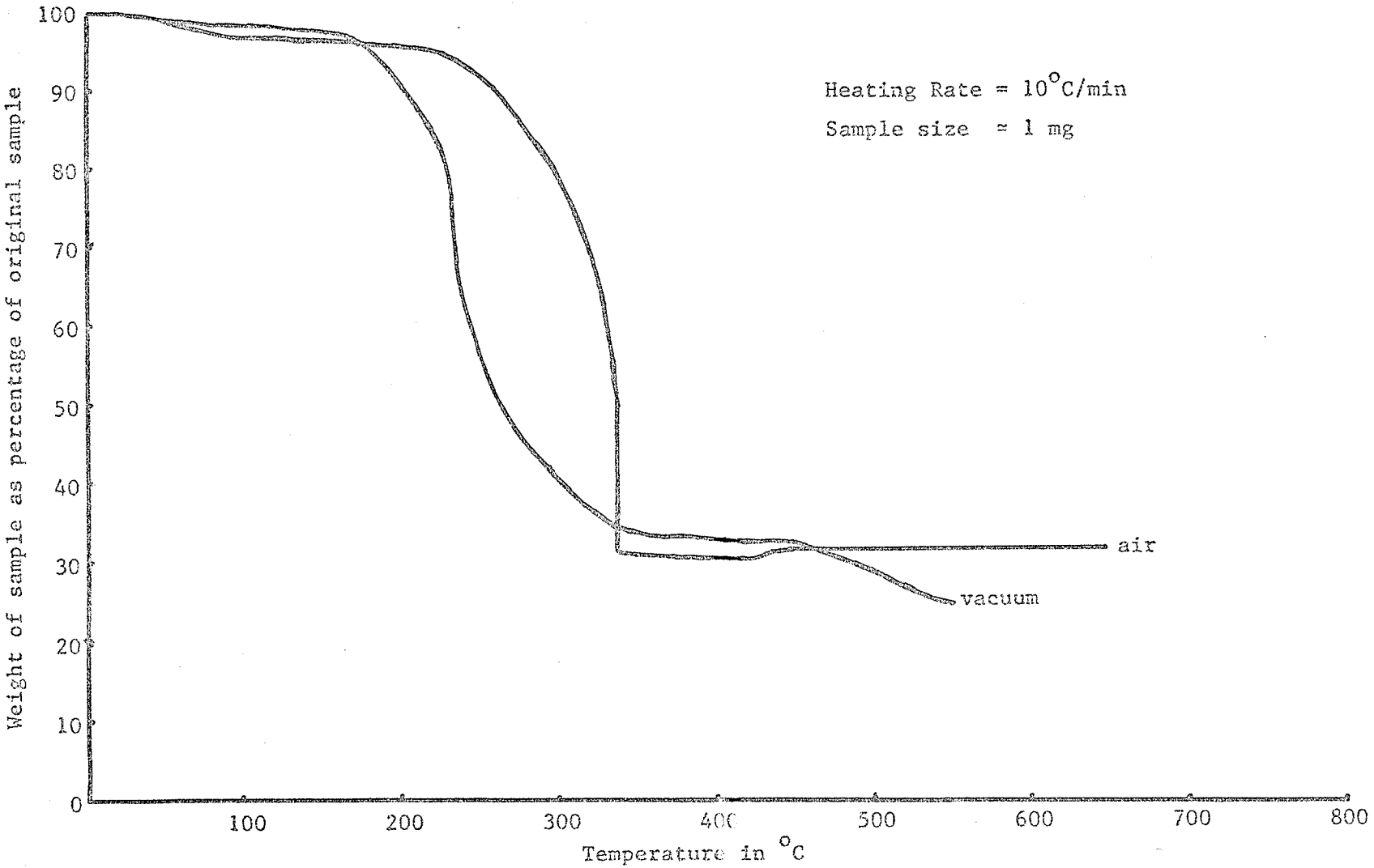

FIGURE XXXVII Thermograms of Cupric o-Fluorobenzoate

decomposition. Dehydration is followed by the fast loss of the organic ligands and the formation of the oxide in agreement with the observations of Charbonnier et al[10].

Figure XXXVII shows the thermograms of cupric o-fluorobenzoate. The thermogram in air agrees with that reported in the literature[10]. It was suggested that it gives cuprous salt as decomposition product similar to the cupric p-fluorobenzoate. However the thermogram in vacuum seems to behave differently from that of the p-fluorobenzoate. This indicates that the o-fluorobenzoate decomposes in a manner different from that of the para-substituted compound.

In general, as indicated from the thermograms, the cuprous carboxylate is not an intermediate species that the cupric salt must go through in the process of thermal decomposition. For comparison purposes the T.G.A. method shows that the cupric carboxylates decompose in a variety of ways and at different rates. However this method is incapable of producing conclusive predictions of the ways in which the decompositions can occur. Rationalizations, where possible, seem to be consistent with the mass spectrometric results.

PART FOUR

CONCLUSION

In the mass spectrometric and thermogravimetric study of the thermal decomposition of the twenty six cupric carboxylates, twelve of them (including trideuterated acetate) produce the cuprous salt as one of the decomposition products. It does not appear possible to postulate which cupric aromatic carboxylates produce the cuprous salt during the process of decomposition. On the other hand, for the alkyl and substituted-alkyl carboxylates, except for the formate, it seems that they all give the appropriate cuprous carboxylate among the decomposition products, unless other, more volatile, cuprous compounds, such as cuprous chloride, can be formed.

The formation of cuprous carboxylates does not seem to be confined to those salts from carboxylic acids with pK_a values which fall in a particular range. However, it seems that for the acids having higher pK_a values the cuprous compounds tend to be more stable.

The cuprous carboxylates are dimeric. A structure similar to that of the silver perfluorobutyrate is proposed. It is suggested that no metal-metal bond is expected between the two copper atoms.

In the mass spectra, two different fragmentation patterns are postulated for the cuprous carboxylates; one for the alkyl and the other for the aryl compounds. The thermal decomposition products of the cupric carboxylates are identified chiefly as the acid and the anhydride from the mass spectra.

In the thermograms, the cupric arylcarboxylates which have cuprous salts as decomposition products tend to show some indication of their presence, whereas the alkyl carboxylates have an apparently simple decomposition. The thermograms of the other carboxylates show various degrees of complexity. Further investigation to explain these thermograms can probably be achieved by direct connection of the thermobalance with the mass spectrometer via some sort of differential vacuum system.

APPENDIX

```
C     MATCHING THE METASTABLE PEAKS IN MASS SPECTRUM.  Z = spectrum no.,
C     N = no. of major peaks  The peaks are entered in ascending mass unit.
      REAL B,SUM
      INTEGER A,Z,Y
      DIMENSION A(100),B(100,100)
   10 READ (5,100,END=900) Z,N,(A(I),I=1,N)
  100 FORMAT (12I5)
      WRITE (6,200) Z
  200 FORMAT (////1H ,20X,I5//1H ,4X,' METASTABLE',12X,' PARENT',10X,'
     1DAUGHTER')
      I =0
  201 I=I+1
      J =I+1
      IF (J .GT. N) GO TO 203
  202 B(I,J) = FLOAT(A(I)*A(I))/A(J)
      IF (J .EQ. N) GO TO 203
      J = J+ 1
      GO TO 202
  203 IF (I .EQ. N) GO TO 300
      GO TO 201
  300 K = N - 1
      TMAX = 0.0
      DO 400 I=1,K
      Y = I + 1
      DO 400 J=Y,N
      IF (TMAX .LT. B(I,J)) GO TO 500
      GO TO 400
  500 TMAX = B(I,J)
      L = I
      M = J
  400 CONTINUE
      WRITE (6,700) TMAX,A(M),A(L)
  700 FORMAT (1H ,4X,F10.5,12X,I5,14X,I5)
      B(L,M) = 0.0
      SUM = 0.0
```

```
      DO 800 I=1,K
      Y = I + 1
      DO 800 J=Y,N
      SUM = SUM + B(I,J)
      IF (SUM .GT. 0.0) GO TO 300
  800 CONTINUE
      GO TO 10
  900 CALL EXIT
      END
```

BIBLIOGRAPHY

1. Angel,A., Scholar,D., and Harcourt,A.V.; J. Chem. Soc., 1385 (1902).

2. Van My, L. and Perinet, G.; B. S. Chim. Fr., 1379, (1965).

3. Edwards, D.A. and Hayward, R.N.; Can. J. Chem., 46, 3443, (1968).

4. Patil, K.C., Chandrashekar, G.V., George, M.V. and Rao, C.N.; Can. J. Chem., 46, 257, (1968).

5. Hill, J.A., Murphy, C.B. and Schacher, G.P.; Analyt. Chim. Acta, 24, 496, (1961).

6. Angel, A.; Trans. of Chem. Soc., 345, (1906).

7. Van My, L., Perinet, G. and Bianco, P.; B. S. Chim. Fr., 10, 3104, (1966).

8. Ibid.; B. S. Chim. Fr., 10, 3109, (1966).

9. Obier, M.F. and Dartiguenave, Y.; C. R. Acad. Ac. Paris, Serie C., 373, (1968).

10. Charbonnier, F., Gazet, J. and Gauthier, J.; C. R. Acad. Ac. Paris, Serie C., 373, (1968).

11. Sneed, M.C., Maynard, J.L. and Brasted, R.C.; Comprehensive Inor. Chem. II, p106, (Van Nostrand, New York, 1954).

12. Kato, M., Jonassen, H.B. and Fanning, J.C.; Chemical Review, 99, (1964).

13. Lewis, J. and Mabbs, F.; J. Chem. Soc., 3894, (1965).

14. Van Niekerk, J.N. and Schoening, F.R.L.; Acta Cryst., 6, 227, (1953).

15. Koizumi, H., Osaki, K. and Watanabe, T.; J. Phys. Soc. Japan, 18, 117, (1963).

16. Figgis, B.N. and Martin, R.L.; J. Chem. Soc., 3837, (1956).

17. Martin, R.L. and Waterman, H.; J. Chem. Soc., 2545, (1957).

18. Forster, L.S. and Ballhausen, C.J.; Acta Chem. Scandinavica, 16, 1385, (1962).

19. Boudreaux, E.A.; Inor. Chem., 4, 506, (1964).

20. Bleaney, B. and Bowers, K.D.; Proc. Roy. Soc., 214, 451, A, (1952).

21. Lewis, J. and Thompson, R.C.; Nature, Vol. 200, 468, (1963).

22. Lewis, J., Lin, Y.C. and Royston, L.K.; J. Chem. Soc., 6464, (1965).

23. Yamada, S., Nishikawa, H. and Miki, S.; Bul. Chem. Soc. Japan, 576, Vol 37, 4, (1964).

24. Yamada, S.; Quad. Chim.-Cons. Nat. Ricerche, 103, 3, (1966).

25. Ross, I.G.; Trans. Faraday Soc., 55, 1058, (1959).

26. Ross, I.G. and Yates, J.; Ibid., 55, 1064, (1959).

27. Ross, I.G., Tonnet, M.L. and Yamada, S.; Ibid., 60, 840, (1964).

28. Nakamoto, K.; Infrared Spectra of Inorganic and Co-ordination Compounds, (John Wiley, New York, 1963).

29. Thompson, R.C. and Yawney, D.B.W.; Can. J. Chem., Vol 43, 1240, (1965).

30. Warrier, A.V.R. and Narayanan, P.S.; Spectrochim. Acta, Vol. 23A, (1967).

31. Baille, M.J., Brown, D.H., Moss, K.C. and Sharp, D.W.A.; J. Chem. Soc. (A), 3110, (1968).

32. Agambar, C.A., Orrell, K.G.; J. Chem. Soc. (A), 898, (1969).

33. Herring, F.G. and Thompson, R.C.; Can. J. Chem., Vol. 47, 555, (1969) and references cited therein.

34. Reichert, C., Fung, D.K.C., Lin, D.C.K. and Westmore, J.B.; Chem. Comm., 1094, (1968).

35. Thomson, J.J.; Rays of Positive Electricity and Their Application to Chemical Analyses, (Longmans, Green & Co., London, 1913).

36. Beynon, J.H.; Mass Spectrometry and Its Application to Organic Chemistry, (Elsevier Pub. Co., Amsterdam, London, New York, Princeton, 1960).

37. Kiser, R.W.; Introduction to Mass Spectrometry and Its Applications, (Prentice-Hall Inc., Englewood Cliffs, N.J., 1965).

38. McDowell, C.A.; Mass Spectrometry, (McGraw-Hill Book Co. Inc., New York, San Francisco, Toronto, London, 1963).

39. McLafferty, F.W.; Interpretation of Mass Spectra, (W.A.Benjamin Inc., New York, Amsterdam, 1966).

40. Hipple, J.A., Fox, R.E. and Condon, E.U.; Phys. Rev., 69, 347, (1946).

41. Petrov, V.P. and Koptyug, V.A.; Chem. Abstract, Vol. 66, 108906B (1967).

42. Blakesleg, A.E. and Hoard, J.L.; J. Amer. Chem. Soc., 78, 3029, (1956).

43. Orgel, L.E.; J. Chem. Soc., 4186, (1958).

44. Cotton, F.A. and Wilkinson, G.; Advanced Inorganic Chemistry,2nd Ed., John Wiley and Sons, New York, (1966).

45. Honda, K.; Sci. Rept. Tohoku Univ., 4, 97, (1915).

46. Peltier, S. and Duval, C.; Anal. Chim. Acta., 1, 346, (1947).

47. Wendlandt, W.WM.; Thermal Methods of Analysis, (Interscience, John Wiley and Sons, New York, 1964).

48. Garn, P.D.; Thermoanalytical Methods of Investigation, (Academic Press, New York, 1965).

49. Newkirk, A.E.; Anal. Chem., 32, 1559, (1960).

50. Simons, E.L. and Newkirk; A.E., Talanta, 11, 549, (1964).

51. Duval, C.; Inorganic Thermogravimeteric Analysis, 2nd Ed., (Elsevier, Amsterdam, 1963).

52. Bamdas, B.M. and Shemyakin, M.M.; Chem. Abstract, Vol. 43, 125b, (1949).